FutureWater

SC 119480 UZB: Digitize to Decarbonize – Power Transmission Grid Enhancement Project

Climate Risk and Adaptation Assessment for Digitize to Decarbonize – Power Transmission Grid Enhancement Project – Uzbekistan

REPORT 243

CLIENT **Asian Development Bank**

AUTHORS **Sonu Khanal**
Tania Imran
Corjan Nolet

DATE **01 March 2023**

Climate Risk and Adaptation Assessment for Digitize to Decarbonize – Power Transmission Grid Enhancement Project – Uzbekistan

SC 119480 UZB: Digitize to Decarbonize – Power Transmission Grid Enhancement Project

Client
Asian Development Bank

Author
Sonu Khanal – Hydrologist and Climate Change Expert (s.khanal@futurewater.nl)

Date
01 March 2023

Executive Summary

The Asian Development Bank (ADB) is assisting the Government of Uzbekistan through the “Power Transmission Grid Enhancement Project” to improve the current status of the electric grid system considering future climate change. The project will support the low-carbon transition and green economy development agenda of the country. It aims to improve the power transmission network capacity and reliability in the northwest region of Uzbekistan, reduce transmission losses, and increase the operational efficiency of the power sector.

To inform the project feasibility study, a Climate Risk and Adaptation (CRA) assessment is carried out to assess the climate vulnerability of the 14 transmissions lines and four substations subject to reconstruction and modernization. A detailed CRA is conducted to assess historic trends in relevant climate-related variables and analyse climate projections in the region. Adaptation measures are identified based on this analysis that will help enhance the climate resilience of the proposed project interventions.

An analysis of the historical climate patterns and trends in the last 40 years (1981-2020) shows that the mean temperature has increased by 0.04 ºC per year on average across the project locations which span over 10 provinces in Uzbekistan. Trends in precipitation showed a consistent decrease of 0.73 mm/year on average, with the highest decline observed in the Surkhdarya region (-1.44 mm/year). However, the northeastern provinces of Uzbekistan i.e. Ferghana and Andizhan where the precipitation increased by 0.12 mm/year.

Similarly, a state-of-the-art downscaled multi-model ensemble (CMIP6-NASA-NEX) was used to analyze future climate projections under 2 SSP emissions scenarios and 3 future time horizons (2030, 2050 and 2070). Future trends in precipitation and temperature were obtained and analyzed to identify potential climate risks in the country. All climate models predicted a warmer future across the project locations, with most of the models predicting an increase of more than 4ºC for the 2070 horizon. For precipitation, the models were not in agreement as some projected a drier future whereas the others a slightly wetter one.

In terms of seasonality, the climate model ensemble projects a general consistent increase in mean temperatures for all months for all project locations. A greater increase in temperatures is predicted in the long-term future horizon and under the higher SSP 5 scenario. The GCM ensemble results show an increase in precipitation, especially in the winter season from October-May for all locations. On the other hand, the summer months’ (June-September) precipitation decreases in the future compared to the reference for all the time horizons and scenarios by 7%.

An analysis of the climate extreme indices indicates that the climate will be more extreme in the future for the project locations. While the extreme temperature changes remain fairly similar, the changes in the number of continuous dry days in the future are comparatively higher in magnitude in the Ferghana and Andizhan provinces. This may have serious implications for the heat wave and drought hazards in the future. The annual maximum 1-day precipitation is expected to increase by more than 50% for SSP2 and double for SSP5 by the end of century. The increase in occurrence and magnitude of such extreme events in the future may increase the likelihood of hazards, for instance erosion, floods, and sedimentation.

Next, the potential impacts were assessed to categorize relevant climate risks and identify priorities for adaptation. Through a combination of literature-based information, quantitative analysis, and expert judgement, the extent to which the key climate risks pose a threat to the project were assessed. Floods were identified as a medium to high climate risk in the project locations, exposing the electric grid

infrastructure to erosion, short-circuits and subsequent blackouts. Similarly, heatwaves and droughts were also classified as high climate risks, potentially causing higher losses through the transmission lines and extensive dust damage. With respect to dust storms and wind erosion, most of the project locations are at a medium risk and may suffer from structural instability in case of an extreme event. The risk of landslides and mudflows in the region were also analyzed and classified as medium, except in the eastern and southern parts of the country which are mountainous and hence at a higher risk. Given the increasing mean temperatures, wildfire was also investigated as a potential risk; however, the risk remains low in the project locations.

Based on the potential impacts, adaptation options were presented for each climate risk. The adaptation measures comprise of both engineering and non-engineering interventions. Among others, installation of monitoring systems such as supervisory control and data acquisition (SCADA) can significantly improve transmission operation reliability. Similarly, capacity building of the authority managing the national electric grid (JSC NEGU) can lead to effective management of risks and recovery. An analysis of the existing hydrometeorological network, covering the project locations, was also conducted which revealed that there is a dire need to install additional monitoring stations, particularly in the mountainous regions, for improved surveillance and development of data-driven adaptation interventions.

Lastly, GHG accounting was performed to determine the project's contribution towards assisting Uzbekistan actualize its second Nationally Determined Contribution (NDC) agenda which seeks to reduce its GHG emissions per unit of GDP by 35% (compared to the level in 2010), by the year 2030. The reduction in greenhouse gas emissions was estimated for the two proposed interventions as per the guidelines developed by ADB for GHG accounting. If the efficiency of the transmission lines is increased by 0.5%, there will be a reduction of 60,428 tCO_2 per year. Similarly, if 100 kW solar panels are installed on the rooftops of all four substations to provide power for the auxiliary services, the emissions would decrease by 409 tCO_2 per year.

Content

Tables

Figures

1 Introduction

1.1 Background

Uzbekistan is not only the most populous country in Central Asia but also the fastest-growing economy in the region. The economy has sustained a high growth rate, with a reported GDP of 7.4% for the year 2021[1]. Such rapid socioeconomic development calls for adequate, uninterrupted, and reliable power supply. However, with over 1,850 km of 500kV linemis, 6,200 km of 220kV lines and 15,300 km of 110kV lines, the power transmission system in Uzbekistan is currently facing challenges with respect to deteriorating infrastructure and power outages. Earlier this summer, the country suffered from occasional blackouts owing to high temperatures and increased demand. The power transmission grids, particularly those subject to direct sunlight, were adversely affected and to reduce the pressure on the national gird, the trains had been running slow on two lines of the Tashkent metro[2]. The impacts of climate change are growing fast in the region; with water scarcity, heat waves and increased number of high heat days (max temperature >39°C) becoming more frequent and intense[3].

To improve the national electric grid system of Uzbekistan, a joint-stock company (JSC) was established in March 2019 to further develop and reform the existing network system. The JSC-National Electric Grid Uzbekistan (JSC NEGU) falls under the jurisdiction of the Ministry of Energy and is responsible for the operation and development of the main electrical networks (as shown in Figure 1), as well as implementation and cooperation with internal and external electric power systems. At the moment, it consists of 14 regional backbone electric networks, 84 substations of 220-500 kV, a central relay protection, automatic service and functional branches[4].

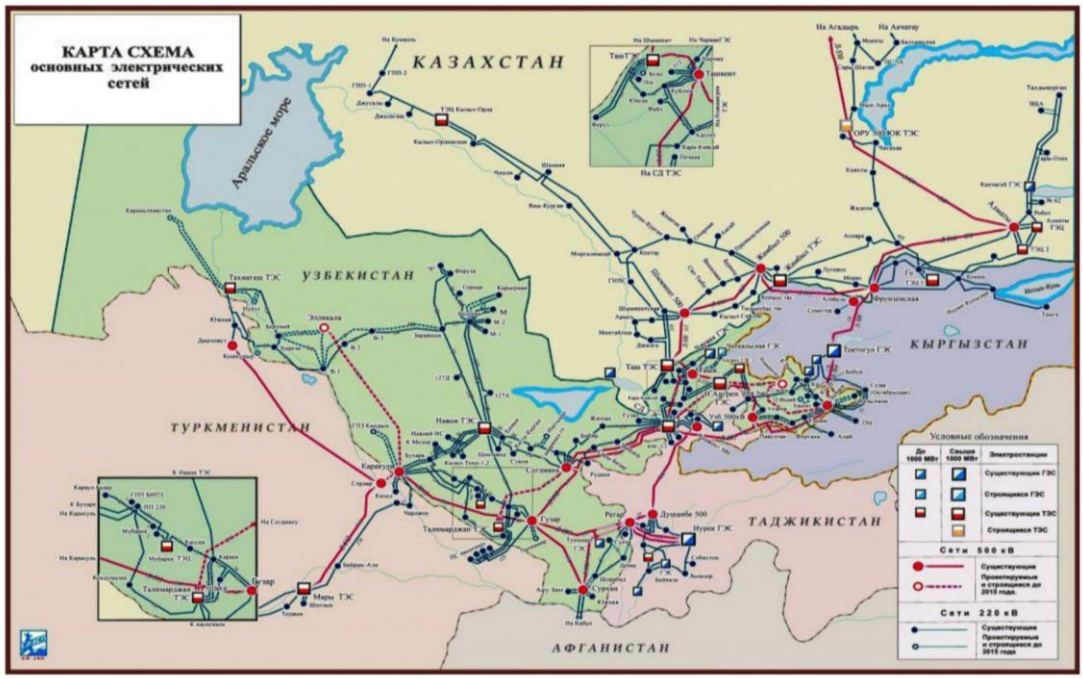

Figure 1. Map of main electrical network (Source: JSC NEGU).

[1] http://wdi.worldbank.org/table/WV.1
[2] https://eurasianet.org/uzbekistan-electricity-grid-strained-by-heat
[3] https://climateknowledgeportal.worldbank.org/country/uzbekistan/climate-data-projections
[4] https://www.uzbekistonmet.uz/en/lists/view/79

The power transmission network was mainly developed in the Soviet era, making the existing transmission lines and substations 30-50 years old. Replacement of any protection and monitoring equipment for the substations is a challenge since spare parts are no longer available. This has resulted in increased power outages, losses, and failure to meet the energy requirements. Additionally, compromised substations also impede the process of acquiring and delivering power from renewable power plants. In addition to a fragile and an aging electric grid infrastructure, the operational management practices are also obsolete. Hourly records measuring the load of transformers and transmission lines are maintained manually using analog instruments, thus making the process as well as the resulting database extremely vulnerable to errors and losses. Lack of use of modern technology makes the process of fault detection and repair time intensive.

In addition to a weakening power transmission network, Uzbekistan's energy sector is also currently struggling with a surge in electricity demands owing to the rapidly growing population. It is reported that since mid-half of 2010, the demand has grown by 4-5% per annum and will increase by 6-7% per annum till 2030. Therefore, there is an urgent need to upgrade the existing transmission infrastructure to fulfil the energy demands and ensure steady socioeconomic development in the country. Moreover, increased efficiency will lead to reduced carbon emissions and help Uzbekistan actualize its second Nationally Determined Contribution (NDC) agenda which seeks to reduce greenhouse gas emissions per unit of GDP by 35% (compared to the level in 2010), by the year 2030.

1.2 Project description

Considering the current status of the electric grid system and the growing impacts of climate change, the Asian Development Bank (ADB) is assisting the Government of Uzbekistan through the "Power Transmission Grid Enhancement Project". The project will support the low-carbon transition and green economy development agenda of the country. It aims to improve the power transmission network capacity and reliability in the northwest region of Uzbekistan, reduce transmission losses, and increase the operational efficiency of the power sector. With an overall goal to strengthen the existing power transmission system, the project has four expected outputs:

- **Output 1**: Rehabilitate and equip twelve transmission lines (Figure 2 and Table 1) in six regions (Bukhara, Fergana, Kashkadarya, Samakhand, Surkhandarya, and Tashkent) with climate-resilient technologies
- **Output 2**: Reconstruct and equip four 220kV substations (Faizabad, Obi-Khaet, Zafar and Zarafshan) and expand by 420 megavolt-amperes.
- **Output 3**: Streamline and enhance the corporate governance at JSC NEGU
- **Output 4**: Improve the project management capacity at JSC NEGU

The scope of the project also aligns with ADB's country partnership strategy for Uzbekistan (2019-2023) as well as its internal 2030 strategy which aims to alleviate poverty and inequalities, tackle climate change, build climate and disaster resilience, enhance environmental sustainability, and strengthen institutional capacity.

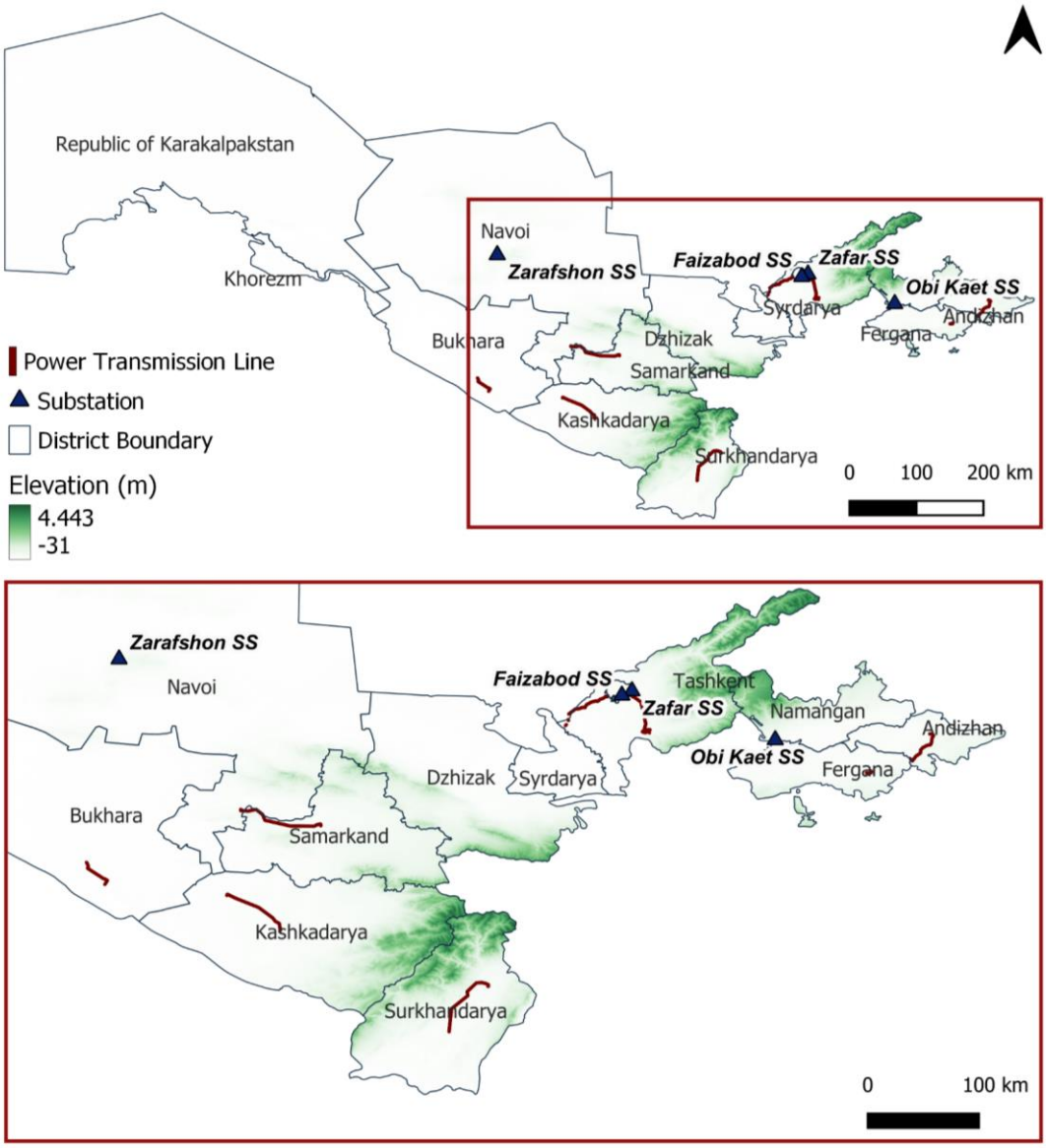

Figure 2. Target transmission lines and substations subject to improvements as part of the "Power Transmission Grid Enhancement Project" by ADB.

Table 1. Specifications of transmission lines and substations subject to improvements.

	No.	ID	Region	Voltage	Lengths (km)
Transmission Line	1	L-19-23	Tashkent	110 kV	14.53
	2	L-F-Ch	Tashkent	110 kV	8.00
	3	L-19-D	Tashkent	110 kV	11.36
	4	L-22-23	Tashkent	110 kV	23.90
	5	L-7-F-1,2	Ferghana	110 kV	6.56
	6	L-Ks-A	Tashkent	220 kV	15.40
	7	L-K-K	Kashkadarya	220 kV	37.50
	8	L-32-K	Kashkadarya	220 kV	27.70
	9	L-32-M	Kashkadarya	220 kV	5.00

	10	L-Hamza-1	Bukhara	220 kV	36.10
	11	L-D-Sh	Surkhandarya	220 kV	77.20
	12	L-H-K	Samarkand / Navoi	220 kV	81.50
	13	L-A-F	Tashkent	220 kV	55.08
	14	L-Yu-L	Andizhan	220 kV	42.96
Substation	I	Zafar	Tashkent	220kV	-
	II	Zarafshon	Navoi	220 kV	-
	III	Obi Khaet	Namangan	220 kV	-
	IV	Fayziobod	Tashkent	220 kV	-

To enhance the climate resilience of the electric grid infrastructure and inform the project design, a detailed climate risk and adaptation assessment (CRA) is performed. Insights from the CRA will be used to devise adaptation strategies and costs to promote climate financing. Through this project, ADB will be supporting Uzbekistan's Green Economy Transition Program and the revised Nationally Determined Contributions by investing in climate mitigation and adaptation measures. Moreover, an efficient and modern power transmission infrastructure will also serve as an incentive for the private sector involved in harnessing renewable energy resources to increase their production and subsequent supply to the national electric grid of Uzbekistan.

1.3 Scope of work

The project aims to modernize the current power transmission infrastructure and strengthen the institutional capacity of JSC NEGU to efficiently operate the network. In addition to addressing the aging transmission grid infrastructure issues and minimizing the associated power losses, the project also accounts for current and future impacts of climate change on the energy sector.

To ensure that the proposed project interventions are climate resilient, an in-depth assessment of climate risks is needed. A detailed climate risk and adaptation assessment (CRA) is carried out to identify and quantify the risks posed by climate change. Downscaled Coupled Model Intercomparison Project Phase 6 (CMIP6) ensembles will be used, along with other relevant hazards and local information, to develop the CRA. The results from this CRA will be used to identify adaptation measures and provide initial cost estimations to promote climate financing in the energy sector. The existing meteorological monitoring network is reviewed as part of the assignment, so the project can potentially integrate a component which aims at improving the monitoring and surveillance in the project areas.

Lastly, reduction in GHG emissions from the upgraded transmission lines and substations are quantified to secure climate financing and highlight the potential impact of the project with respect to Uzbekistan's revised NDC ambition.

2 Methodology

2.1 Climate risk assessment guidelines

Since 2014, ADB requires that all investment projects consider climate and disaster risk and incorporate adaptation measures to make the projects more climate resilient. This is consistent with ADB's commitment to scale up support for adaptation and climate resilience in project design and implementation, articulated in the Midterm Review of Strategy 2020: Meeting the Challenges of a Transforming Asia and Pacific (ADB, 2014a), in the Climate Change Operational Framework 2017–2030: Enhancing Actions for Low Greenhouse Gas Emissions and Climate-Resilient Development (ADB, 2017), and in the Climate Risk Management in ADB Projects guidelines (2014).

Climate risk management (CRM) is a mandatory part of project development. Climate risk screening is applied to all ADB investments, with a more detailed assessment undertaken for projects that are assessed to be at medium or high risk. The principal objective of a Climate Risk and Adaptation (CRA) assessment is to identify those components of the project that may be at risk of failure, damage and/or deterioration, reduction, interruption, and/or decreased reliability of service delivery from natural hazards, extreme climatic events or significant changes to baseline climate design values (ADB, 2011, 2014 and 2017). Adaptation measures consistent with the risk assessment serve to improve the resilience of the infrastructure to the impacts of climate change and geo-physical hazards, to protect communities and provide a safeguard so that infrastructure services are available when they are needed most (Figure 3). As part of this process, the nature and relative levels of risk are evaluated and determined to establish appropriate actions for each proposed investment to help minimize climate change associated risk.

Earlier the terminology "Climate Risk and Vulnerability Assessment (CRVA)" was used. However, since vulnerability is part of risk, ADB now recommends using the term "Climate Risk and Adaptation Assessment (CRA)". The CRA process embodies the recognition that many of the future impacts of climate change are fundamentally uncertain and that project risk management procedures must be robust to a range of uncertainty. The CRA therefore includes a technical and economic appraisal of adaptation options for the project design.

ADB has developed specific guidelines regarding CRAs. These guidelines mentioned that the main characteristics of a CRA are (i) to characterize climate risks to a project by identifying both the nature and likely magnitude of climate change impacts on the project, and the specific features of the project that make it vulnerable to these impacts. (ii) To identify the underlying causes of a system's vulnerability to climate change, and (iii) to ensure that adaptation measures are locally beneficial, sustainable, and economically efficient.

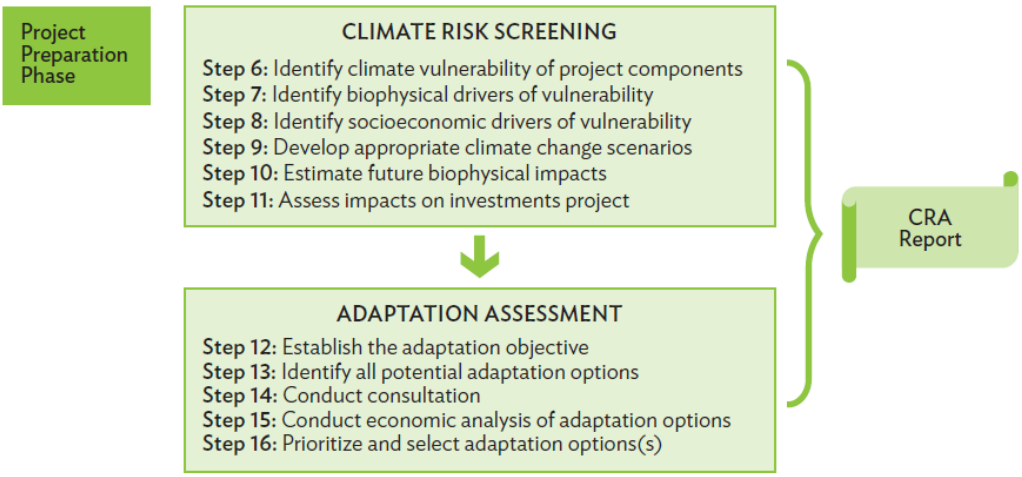

Figure 3. Climate Risk and Adaptation Assessment components (Source: ADB, 2015).

CRAs use a variety of definitions relating to risk and climate change. In this study the following definitions are used (adapted from IPCC, 2014):

- **Hazard:** A process, phenomenon or human activity that may cause loss of life, injury or other health impacts, property damage, social and economic disruption or environmental degradation[1]
- **Exposure:** The presence of people, livelihoods, species or ecosystems, environmental functions, services, and resources, infrastructure, or economic, social, or cultural assets in places and settings that could be adversely affected by climate change and variability.
- **Sensitivity:** The degree to which a system, asset, or species may be affected, either adversely or beneficially, when exposed to climate change and variability.
- **Potential impact:** The potential effects of hazards on human or natural assets and systems. These potential effects, which are determined by both exposure and sensitivity, may be beneficial or harmful.
- **Adaptive capacity:** The ability of systems, institutions, humans, and other organisms to adjust to potential damage, to take advantage of opportunities, or to respond to consequences of hazards.
- **Vulnerability:** The extent to which a system is susceptible to, or unable to cope with, adverse effects of climate change, including climate variability and extremes. It depends not only on a system's exposure and sensitivity but also on its adaptive capacity.
- **Likelihood:** A general concept relating to the chance of an event occurring. Generally expressed as a probability or frequency.
- **Confidence:** A general concept relating to the agreement among the different data and model sources, and the available evidence.
- **Risk:** A combination of the chance or probability of an event occurring, and the impact or consequence associated with that event if it occurs.

The risks originating from climate hazards to individual project activities or outputs can be derived based on the AR6 IPCC risk framework formulation, which considers risk as a combination of hazard (H), exposure (E), and vulnerability (V):

$$R = f(H, E, V)$$

Vulnerability, as earlier defined in the definitions, is a combination of the sensitivity of a project activity to a climate hazard, and the adaptative capacity of the activity (or the project or project context as a

[1] United Nations General Assembly. 2016. Report of the open-ended intergovernmental expert working group on indicators and terminology relating to disaster risk reduction. New York.

whole). Climate risk scores can be calculated quantitatively in case accurate spatial data is available on these risk components. While quantitative hazard data is typically available (for historic conditions based on observations, for future conditions based on model projections), data on sensitivity and adaptive capacity is often more qualitative. In that case, an expert-based judgement on the risk score for the project activities is recommendable.

For this CRA, the risk inputs (exposure to hazard, vulnerability) and the outputs (risk) are classified using a simple qualitative rating scheme comprising four classes, as shown in Table 2.

Table 2. Qualitative classes used to rank hazard.

Classes	Rating	Colour
No data	**0**	
Low	**1**	
Moderate	**2**	
High	**3**	

2.2 Approach to CRA

The approach towards the development of the CRA is described in this section, while the specific details regarding methodologies and results are presented in the subsequent chapters. Overall, the CRA will consist of the following steps:

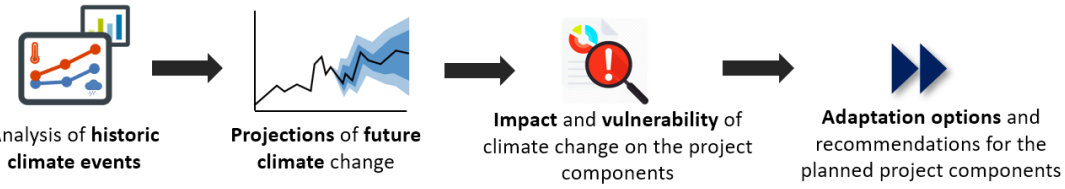

Figure 4. Steps to develop a climate risk and adaptation assessment.

2.2.1 Analysis of historic climate events

A credible and acceptable CRA assessment starts with analyzing historic observations of climate-related events and performing trend analysis. Obviously, trends, or the absence of trends, do not imply that future changes will follow those historic trends. Any statistical trend analysis should be accompanied by an understanding of the underlying physical processes. Analysis of historic climate events should go beyond looking at weather parameters (e.g., temperature and precipitation) and should include parameters that might have been influenced by historic weather conditions. Given the climate risks and vulnerabilities associated to components of the energy sector in general and specific to this project (energy transmission in the desert and mountains), the following long-term climate change processes and hazards were prioritized:

1. Extreme precipitation, related to extreme runoff and flooding events including flash floods, and landslide, erosion.
2. Extreme temperature, related to wildfires, snow and glacier melt runoff floods.
3. Drought hazards
4. Heatwave hazards
5. Wind-related hazards

Climate change-related hazards which are not included as they are not considered relevant for the project area are: cyclonic activities, sea level rise, and are not included in this report as the risk level is insignificant for the scope of this report[1].

2.2.2 Projections of future climates

Projections of future climates are provided by GCMs (Global Circulation Models). An important source of the climate projections to date is the results from the Coupled Model Intercomparison Project Phase 6 (CMIP) activities. CMIP6 has led to a standard set of model simulations and a (more or less) uniform output. Since the downscaling and local adjustment of GCMs are needed, NASA has developed the so-called NEX-GDDP (NASA Earth Exchange Global Daily Downscaled Projections) (Thrasher et al., 2022). The dataset is provided to assist in conducting studies of climate change impacts at local to regional scales and to enhance public understanding of possible future global climate patterns at the spatial scale of individual towns, cities, and watersheds.

The NASA-NEX-GDDP consists of 35 GCM outputs for two SSPs (2 and 5) for a historic period (1950-2014) and the future (2015-2100). For the CRA these data are used for two purposes. First, the projections are analyzed using a set of indicators ranging from more direct ones (e.g., change in temperature) to more meaningful integrated and advanced indicators (e.g., monthly maximum consecutive 5-day precipitation). Second, the NASA-NEX-GDDP is used in the bottom-up approach of the impact and vulnerability assessment. As described later in this report, the projections of future climate vary strongly per climate model, forming one important dimension of future climate uncertainty. It is key to consider this uncertainty by including an ensemble of climate models in the analysis. Based on the range (uncertainty) in the projections, a confidence threshold can be used to benchmark infrastructural developments in the context of future climate change.

2.2.3 Impact and vulnerability of climate change

A standardized approach to climate change impact and vulnerability assessment does not exist. There is however a clear trend in CRAs to move from climate projections (GCM) focus to a vulnerability-oriented approach. This change started by the often-non-consistent projections of GCMs (especially in precipitation) and at the same time the desire to put stakeholders' perspectives back into the analysis. This distinction between climate scenario-driven impact assessment approaches is often referred to as "top-down", while the vulnerability-oriented approach is referred to as "bottom-up." The ADB guidelines are less restrictive and recognize that both approaches are complementary and can even be conducted in parallel. In this CRA we combine the approaches and present the full scope of possible futures in terms of climate change, but for the final chapters on vulnerability and adaptation options, we take the perspective from the project design to come up with actionable recommendations.

2.2.4 Adaptation options and recommendations for design

The identification of adaptation options requires the consideration of project specifics and needs, project socio-economic context, and should cover both "hard" measures, for example modifications in the design that make an infrastructure less sensitive to a hazard, or "soft" measures, which relate to capacity building, institutional strengthening, etc. Estimates of the adaptation cost need to be provided, which can be done in relative terms if the project is yet in a concept phase, and in absolute terms if the project is in a feasibility or design phase.

For this project, some potential climate adaptation options are outlined. These options are based on the detailed risk assessment and the information so far available on the project. When the project is further designed, a more specific list of recommendations for adaptation can be prepared.

[1] https://thinkhazard.org/en/report/261-uzbekistan/CY

ADB has developed some specific guidelines regarding CRAs that are used as source:

- Climate risk management in ADB projects (ADB, 2014)
- Climate Risk and Adaptation in the Electric Power Sector (ADB, 2012)
- Guidelines for Climate Proofing Investment in the Energy Sector (ADB, 2013)
- Guidelines for Climate Proofing Investment in the Transport Sector: Road Infrastructure Projects
- Guidelines for Climate Proofing Investment in the Water Sector: Water Supply and Sanitation (ADB, 2016)

3 Historic Climate Trends

The first step in developing a detailed Climate Risk and Adaptation assessment (CRA) is to analyze historic observations of climate and to perform trend analyses. This can reveal whether trends in climate variables can already be observed based on historic data. Obviously, trends, or the absence of trends, do not imply that future changes will follow historic patterns. Any statistical trend analysis should be accompanied by an understanding of the underlying physical processes and future projections using GCMs.

3.1 Dataset used

Reanalysis of past weather (model) data provides a clear picture of past weather. Through a variety of methods of observations from various instruments (in situ, remote sensing, models) are assimilated onto a regularly spaced grid of data. Placing all instrument observations onto a regularly spaced grid makes comparing the actual observations with other gridded datasets easier. In addition to putting observations onto a grid, reanalysis also holds the gridding model constant keeping the historical record uninfluenced by artificial factors. Reanalysis helps ensure a level playing field for all instruments throughout the historical record.

ERA5 Reanalysis Data

ERA5 is the fifth generation European Centre for Medium-Range Weather Forecasts (ECMWF) reanalysis for the global climate and weather for the past 4 to 7 decades. Currently data is available from 1951 until near-present. Reanalysis combines observations from different sources into globally complete fields using the laws of physics with the method of data assimilation (4D-Var in the case of ERA5). ERA5 provides hourly estimates for many atmospheric, ocean-wave and land-surface quantities and fluxes.

ERA5-land is a reanalysis dataset at an enhanced resolution compared to ERA5. ERA5-land has been produced by replaying the land component of the ECMWF ERA5 climate reanalysis. Currently data is available from 1981 until near-present. Reanalysis combines model data with observations from across the world into a globally complete and consistent dataset using the laws of physics. Reanalysis produces data that goes several decades back in time, providing a uniform and accurate description of the climate of the past.

Source: ECMWF

To this end, the ERA5-land reanalysis product from the ECMWF is used to analyze historical trends in temperature and precipitation, and derived indicators, for the project area. This product is used as it provides a global, spatially gridded time series of several climate variables at resolutions of 9km and sub-daily (3hr) timescales. The dataset is fully operational (updated every month) and runs from 1981 to the near present. From this dataset, spatially averaged time series of precipitation and temperature are extracted for the project area at daily, weekly, and yearly timescales for the entire period that the dataset covers. This allows the analysis of annual and seasonal trends in historical climate alongside extremes.

To understand the historical climate patterns and trends, the project infrastructure is clustered into 5 regions (see Figure 5 and Table 3). Since Uzbekistan has a high variability in climate conditions, we chose to use 5 boxes rather than the whole country for the historical climate patterns. The historical data is aggregated for the region covered by the boxes and analyzed in the following sections. To make sure the plots are not repetitive, we only show the trends and patterns for the boxes if they are different from each other.

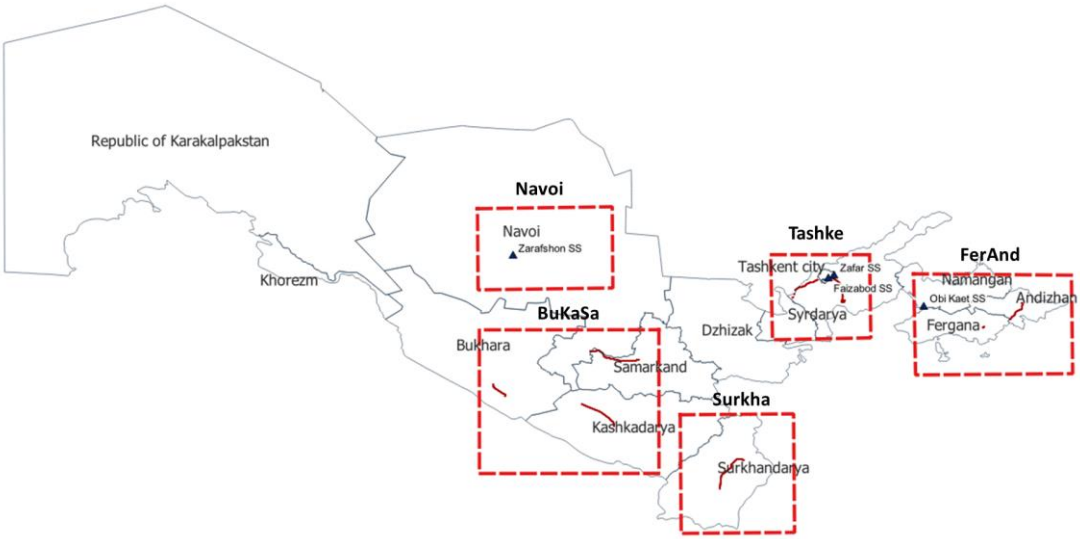

Figure 5. The distribution of the transmission line and the cluster.

Table 3. Description of the boxes and the project components.

Name ID of the boxes	Regions	Project components	Type of infrastructure
FerAnd	Fergana, Andizhan	L_Yu_L_MM (Andizhan) L-7-F-1 (Fergana) Obi Kaet SS (Namangan)	Transmission line Transmission line Sub-station
Surkha	Surkhandarya	L_D_W (Surkhandarya)	Transmission line
BuSaKa	Bukhara, Samarkand, Kashkadarya	L-Hamza (Bukhara) L-H-K (Samarkand) L-32-K (Kashkadarya) L-32-M (Kashkadarya) L_K_K_MM (Kashkadarya)	Transmission line Transmission line Transmission line Transmission line Transmission line
Tasken	Tashkent	L-A-F (Tashkent) L_Kc_A_MM (Tashkent) L-19-D (Tashkent) L-19-23 (Tashkent) L-22-23 (Tashkent) L-F-CH (Tashkent) Zafar SS (Tashkent) Faizabod SS (Tashkent)	Transmission line Transmission line Transmission line Transmission line Transmission line Transmission line Sub-station Sub-station
Navoi	Navoi	Zarafshon SS (Navoi)	Sub-station

Note: - The box names are 6 characters long, except for the Navoi. If the boxes include two or more regions, then the first few characters are used to name the box.

3.2 Analysis

3.2.1 Climate summary

The physical environment of Uzbekistan is diverse, ranging from the flat, desert topography that comprises almost 80% of the country's territory to mountain peaks in the east reaching about 4,500 meters above sea level. Uzbekistan has a generally arid and continental dry climate with long, warm to hot summers and moderate to cold winters. The country is prone to large fluctuations in temperature, both seasonally and from day to day (WB & ADB, 2020).

The country can be broadly divided into two climatic zones: (a) a desert and steppe climate in the western two-thirds of the country and (b) a temperate climate characterized by dry summers and humid winters in the eastern areas. The desert plains, which includes the province of Bukhara, receive only around 80-200 millimeters (mm) of precipitation annually, while the foothills (Samarkand province) can get as much as 300-400 mm and mountainous regions up to 600-800 mm per year (Figure 6). Due to these prevailing climate conditions, agricultural output is almost fully dependent on irrigation. The main sources of water are transboundary rivers; Amu Darya and Syr Darya.

Uzbekistan receives 52% of the total water available in the region, 92% of which is consumed by the agricultural sector (FutureWater, 2020). Rainfall occurs mostly in late autumn through early spring, dropping off significantly during the summer months. The average monthly temperature for the country is highest in July, at 27°C, and lowest in January, at -3°C. However, temperature ranges vary across the country (Figure 6). Western areas of the country experience relatively colder winter temperatures, whereas temperatures are highest in the south, near the borders with Turkmenistan and Afghanistan (WB & ADB, 2020). Uzbekistan's desert regions can reach maximum temperatures of 45 – 49°C, while minimum temperatures in the southern parts of the country can drop as low as -25°C.

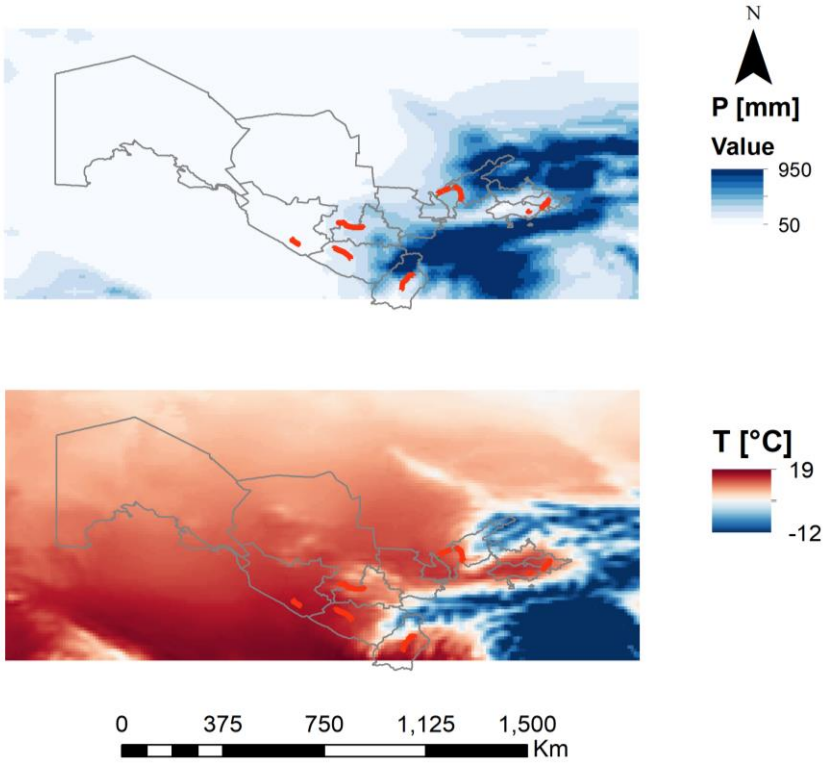

Figure 6. Mean annual precipitation (top) and temperature (bottom) for 1981–2020 across Uzbekistan (Source: own elaboration based on ERA5 dataset).

3.2.2 Temperature and precipitation trends

Historical temperature shows that the average annual temperature is lowest (8.5°C) for box FerAnd which includes parts of eastern regions such as Andizhan, Fergana and Namangan and highest (16.5°C) for box BuSaKa which includes the southern regions such as Bukhara, Samarkand and Kashkadarya (see Figure 7 and Figure A1 to Figure A4). Extreme variations in temperature are evident as average daily temperatures ranges from around -18 to 29 ºC for box FerAnd, -18 to 35 ºC for box Tasken, -15 to 31.5 ºC for box Surkha, -16.5 to 38 ºC for box BuSaKa and -20 to 15ºC for box Navoi over 1981–2020. Analysis of temperature data shows that the mean temperature has increased approximately to about 1.2 ºC for box FerAnd and box BuSaKa, 1.6 ºC for box Surkha and Navoi and 2 ºC for box Tasken in 40 years in the period 1981–2020 (see Figure 7 and Figure A1 to Figure A4). This supports the fact that the temperature extremes have increased in recent years and may have significant impacts on energy loss from the distribution network.

Historical ERA5 precipitation reveals that the average total annual precipitation exhibits spatial and temporal variability. Western regions receive less than 100 millimeters (mm) of precipitation per year, whereas parts of the east and south-east around the high mountains forming part of the Tien-Shan and Gissar-Alai Ranges can receive up to 800–900 mm per year (Figure 6). The annual average precipitation ranges from 600-1000 mm (mean around 770 mm) for box FerAnd, 350-710 mm (mean around 500 mm) for box Tasken, 430-850 mm (mean around 640 mm) for box Surkha,150-340 mm (mean around 255 mm) for box BuSaKa and 90-260mm (mean around 150mm) for Navoi (Figure 8 and Figure A5 to Figure A7). The precipitation consistently decreases in all the region except for the FerAnd box where it slightly increases at the rate of +0.12 mm per year. The 10-daily maximum precipitation for individual years, which is an indicator of extreme precipitation, does not indicate a clear increasing trend (Figure 8 and Figure A5 to Figure A7).

There is a large annual precipitation variability in the region. However, the exact figures may have some uncertainty due to possible biases in the precipitation data of ERA5 compared to stations over High Mountain Asia (Khanal et al., 2021). The true amounts of precipitation over the High Mountains of Asia are highly uncertain in general (Immerzeel et al., 2015). Rain gauges are usually situated in the valleys because of accessibility, whereas most of the precipitation falls at high altitudes due to orographic effects. Besides, precipitation gauges usually under catch snowfall. Remote sensing precipitation products on the other hand underestimate snowfalls. Work analyzing glacier mass balances and observed discharge in the upper Indus in the western Himalayas and Karakoram indicates that station-based precipitation products may underestimate the total amount of precipitation by up to 50% (Immerzeel et al., 2015; Immerzeel et al., 2012). The use of a numerical weather model-based reanalysis product, like ERA5, which takes the orographic effect into account, could provide better alternative (Khanal et al., 2022).

Again, the boxes show variable signs and trends in precipitation. A trend (~1mm per year) of increasing total annual rainfall is evident for the historical period for box FerAnd which covers the mountains in the East, but with significant interannual variability (Table 4). In contrast, the precipitation decreases (~-1mm per year) for box BuSaKa which covers the dry central and southern part of Uzbekistan.

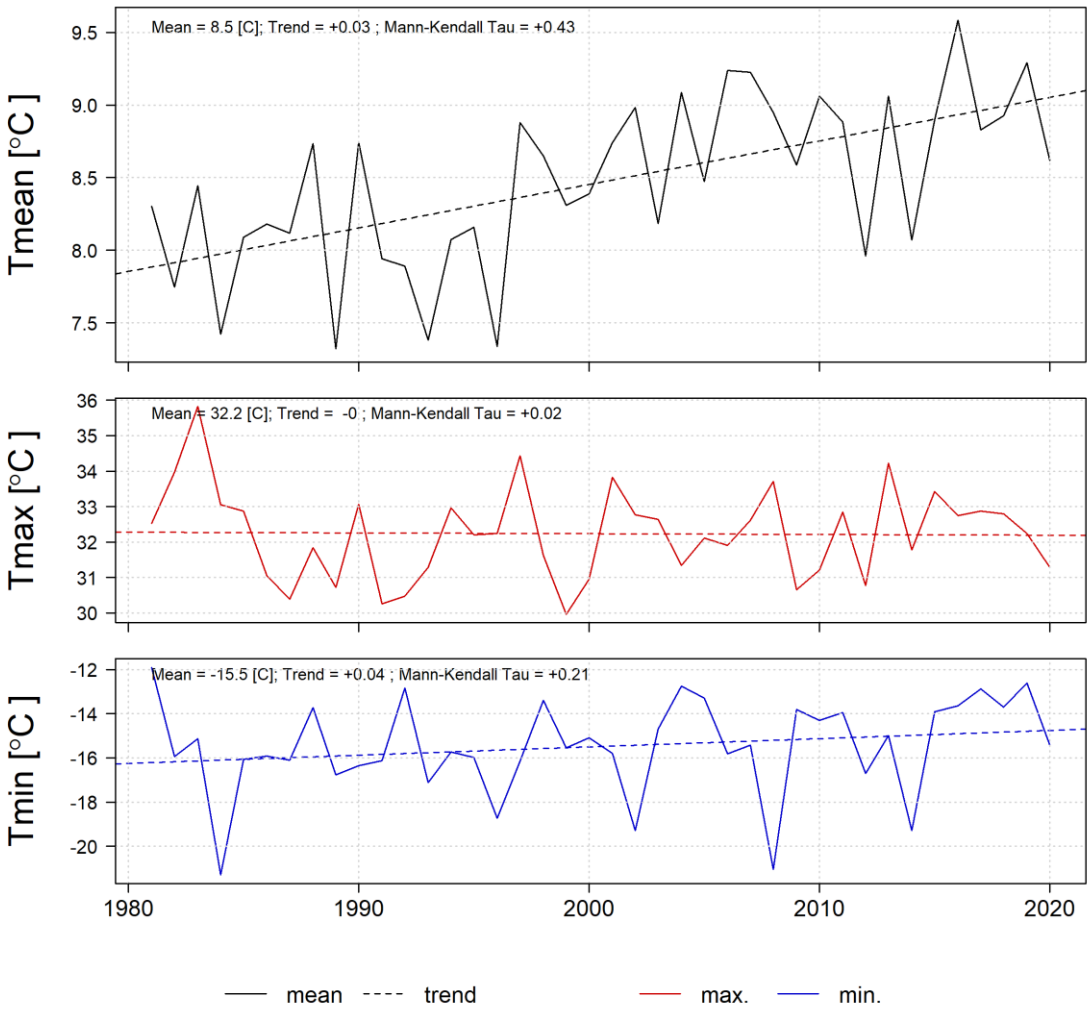

Figure 7. Average, maximum and minimum yearly temperatures from ERA-5 dataset with trendline for box FerAnd.

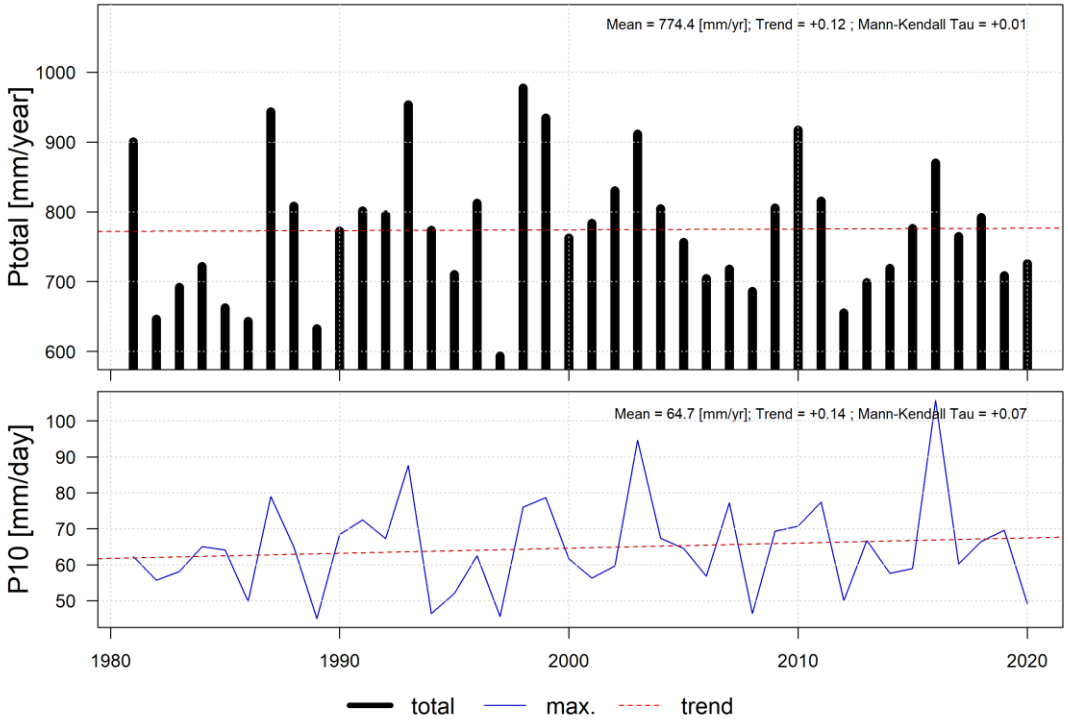

Figure 8. Total yearly and maximum 10-day precipitation with a trendline for box FerAnd.

As shown in Figure 8, Mann Kendall Tau value indicates the strength of the monotonic trend of increase or decrease in a time series, with a value of 1 indicating a strong significant trend and -1 indicating no trend.

3.2.3 Seasonality

A clear seasonality is evident, with high average monthly temperatures (around 20ºC for box FerAnd and around 30ºC for box BuSaKa) prevailing during April – September (Figure 9 and Figure A9). Most of the rainfall occurs during the winter period in December, January, February, and March. The interannual variation, high precipitation in the winter season and low precipitation in the summer season (Figure 10 and Figure A10).

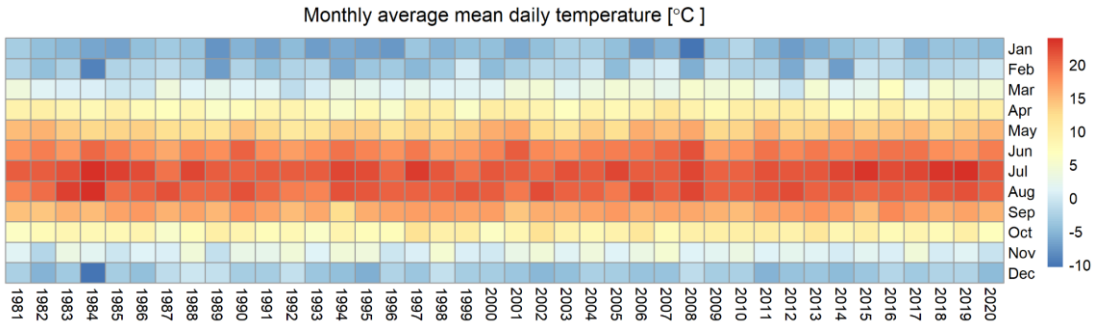

Figure 9. Seasonality in temperature from ERA-5 dataset for box FerAnd.

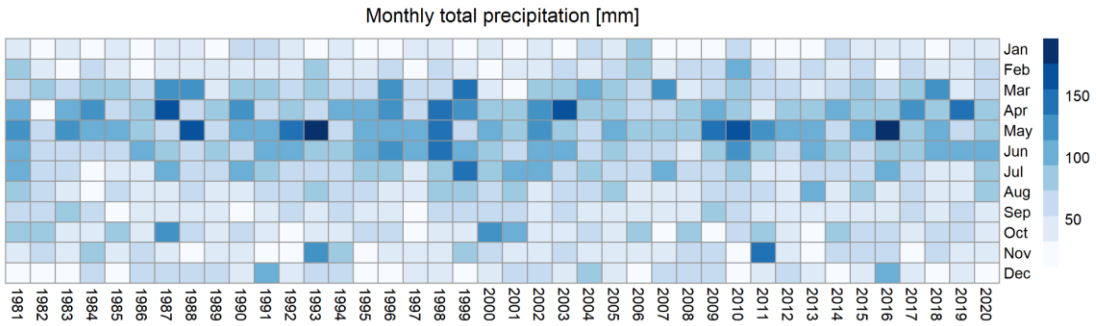

Figure 10. Seasonality of precipitation from ERA-5 dataset for box FerAnd.

3.3 Summary tables

Summary tables of the mean temperature and precipitation, including trends, are presented in Table 4**.**

Table 4. Summary tables for the box selected.

Box	Precipitation		Temperature	
	Mean (mm)	Trend (mm/yr)	Mean (°C)	Trend (°C/yr)
FerAnd	775	+0.12	8.5	+0.03
Tasken	500	-0.30	13.7	+0.05
Surkha	621	-1.44	12.4	+0.04
BuSaKa	239	-0.49	16.5	+0.04
Navoi	150	-0.65	14.7	+0.04

4 Future Climate Projections

4.1 Methodology

4.1.1 Climate Model Ensemble

For this CRA, the NEX-GDDP-CMIP6 (Thrasher et al., 2022) data is used to analyze future climate trends. This dataset contains extended sets of variables and is used to provide an analysis of trends in terms of temperature and precipitation, and derived climate change indicators. This product is used as it provides spatially gridded time series including temperature and precipitation derived from an ensemble of 35 General Circulation Models with global coverage (see Table 5 for descriptions of models and units). The data is available at downscaled resolutions of ~25 km and daily time series, covering “historical” (1950 – 2014) and “future” (2015 – 2100) periods and varying emissions scenarios or across two of the four "Tier 1" greenhouse gas emissions scenarios known as Shared Socioeconomic Pathways (SSPs), which are sufficient for the scale of the project.

From this dataset, spatially averaged time series of precipitation and temperature are extracted for the project area at daily, weekly, and yearly timescales for the entire period that the dataset covers. This allows for the analysis of annual and seasonal trends in the future for climatic means and extremes.

4.1.2 Scenarios and future horizons

Two SSP scenarios (SSP2-4.5 and SSP5-8.5) are analyzed to provide a range of future climate projections. SSP2-4.5 represents a “stabilisation scenario”, in which greenhouse gas emissions peak around 2040 and are then reduced. Although often used as ‘business as usual’, the SSP5-8.5 is above the business-as-usual emission scenarios and designed as a worst-case scenario. We include this scenario as an upper limit to the possible future climate. These scenarios are selected as they represent an envelope of likely climate changes and hence cover a plausible range of possible future changes in temperature and precipitation relating to project implementation.

Alongside the two SSP scenarios, projections are evaluated at the following time horizons:

- Reference period [2005]: 1995 – 2014
- Short (T1) [2030]: 2020 – 2039
- Mid-future (T2) [2050]: 2040 – 2059
- Distant-future (T3) [2070]: 2060 – 2079

These periods were selected for the project as they are relevant to the lifetime of the project infrastructure, and therefore cover a realistic range of climate changes that are likely to affect project functioning. A 20-year window was selected as appropriate for deriving average climate changes, effectively considering interannual variations in temperature and precipitation, and robust comparison (see Table 6).

The lifetime of energy transmission projects is typically in the order of **60 years**.[1] This means that also the distant-future horizon (T3) can be considered relevant for this CRA.

[1] Salazar and Mendoza. 2008. Life prediction of electrical power transmission towers. Proceedings of the 9th Biennial ASME Conference on Engineering Systems Design and Analysis ESDA08.

Table 5. Climate models included in NASA-NEX dataset.

Model	hurs	huss	pr	rlds	rsds	sfcWind	tas	tasmax	tasmin
unit	%	kg/kg	mm/day	W/m^2	W/m2	m/s	degC	degC	degC
ACCESS-CM2									
ACCESS-ESM1-5									
BCC-CSM2-MR									
CanESM5									
CESM2									
CESM2-WACCM									
CMCC-CM2-SR5									
CMCC-ESM2									
CNRM-CM6-1									
CNRM-ESM2-1									
EC-Earth3									
EC-Earth3-Veg-LR									
FGOALS-g3									
GFDL-CM4 (gr1)									
GFDL-CM4 (gr2)									
GFDL-ESM4									
GISS-E2-1-G									
HadGEM3-GC31-LL	360	360	360	360	360	360	360	360	360
HadGEM3-GC31-MM	360	360	360	360	360	360	360	360	360
IITM-ESM	2099	2099	2099	2099	2099	2099	2099		
INM-CM4-8									
INM-CM5-0									
IPSL-CM6A-LR									
KACE-1-0-G	360	360	360	360	360	360	360	360	360
KIOST-ESM	2058								
MIROC-ES2L									
MIROC6									
MPI-ESM1-2-HR									
MPI-ESM1-2-LR									
MRI-ESM2-0									
NESM3									
NorESM2-LM									
NorESM2-MM									
TaiESM1									
UKESM1-0-LL	360	360	360	360	360	360	360	360	360

Green	historical, SSP245, SSP585 available	360	360 days / year available
yellow	historical & one SSP available;	2099	Timeseries until 2099
Red	No data available	2058	Year 2058 not avaialable

Table 6. Summary of RCP scenarios and future time horizons used in this CRA.

RCP Scenarios	Time horizons	Model projections
Historical	2005 (1995 – 2014)	35
SSP2-45	2030 (2020-2039) T1	35
	2050 (2040-2059) T2	35
	2080 (2070-2089) T3	35
SSP5-85	2030 (2020-2039) T1	35
	2050 (2040-2059) T2	35
	2080 (2070-2089) T3	35

4.1.3 Climate Extremes Indices

To determine future trends in extreme climate events, CLIMDEX[1] indicators are used. These represent a standardized, peer-reviewed way of representing extremes in climate data and are widely used in climate analyses. They are derived from daily temperature and precipitation data. These are produced through processing the NASA-NEX dataset with Climate Data Operator (CDO) software. This takes as input spatially gridded daily time series and returns yearly series of CLIMDEX indices. This process is useful as it effectively reduces the amount of data analysis needed whilst retaining the ability to represent extremes within data in a comparable way.

To this end, the indices described here are considered the most relevant out of the 27 available. The Rx1day (annual maximum 1-day precipitation) and Rx5day (annual maximum 5-day precipitation) indexes are representative of future trends in extreme precipitation and therefore likely to be a good measure of potential impacts related to flooding, slope instability, water-induced erosion, mudflow and extreme snowfall on project components (see Table 7). CDD (consecutive dry days) is important as it provides a useful indication of trends in meteorological drought, which may impact energy transmission via distribution lines. TX_X (annual maximum of daily maximum temperature), good predictor of extreme temperature, which may have negative effects on project components through extreme heat events, dust storms, snow and glacier melt related flooding events.

Table 7. CLIMDEX Precipitation Indices used in the project.

Index name	Description	Unit
RX1 day	Annual maximum 1-day precipitation	mm
RX5 day	Annual maximum 5-day precipitation sums	mm
CDD	Annual maximum consecutive dry days: annual maximum length of dry spells, sequences of days where daily precipitation is less than 1mm per day.	days
TXx	Annual maximum of daily maximum temperature	Celsius

4.2 Climate projections for the project area

4.2.1 Average trends in temperature and precipitation

In terms of average climate trends, the climate model ensemble predicts a clear increase in mean temperature for the FerAnd in the future for all time horizons (Figure 11). It is also clear that under the higher SSP5 scenario, a larger increase in temperature is expected compared to the SSP2 scenario for the boxes (Figure 11 and Figure A11-Figure A14). For the short-term (T1), changes in temperature around 0.8-1°C are predicted by the climate model ensemble, for the mid and long-term horizon T2 and T3 this increases to around 1.6-2.3°C and 2.4-4°C for the FerAnd box (see Table 8 and Table 9). Changes of similar order of magnitude are projected for the other boxes (Table A1-Table A8).

The future trend for precipitation is less clear but, overall, the climate model ensemble projects a slight increase in mean precipitation for all the boxes till the end of the century (Figure 12 and Figure A15-Figure A18). A large spread in model predictions is evident, with some models predicting (much) higher future increases in precipitation than others. For the short-term horizon (T1), changes in precipitation in the range of around 5-6% are projected by the climate model ensemble, for the mid and long-term horizon (T2), this increases to around 10–13% and 12–19%, with a larger spread in model projections and higher divergence between emissions pathway SSP2 and SSP5 for the FerAnd box (Figure 12 and Figure A15-

[1] https://www.climdex.org/learn/

Figure A18). Changes of similar order of magnitude are projected for the other boxes (Table A1-Table A8).

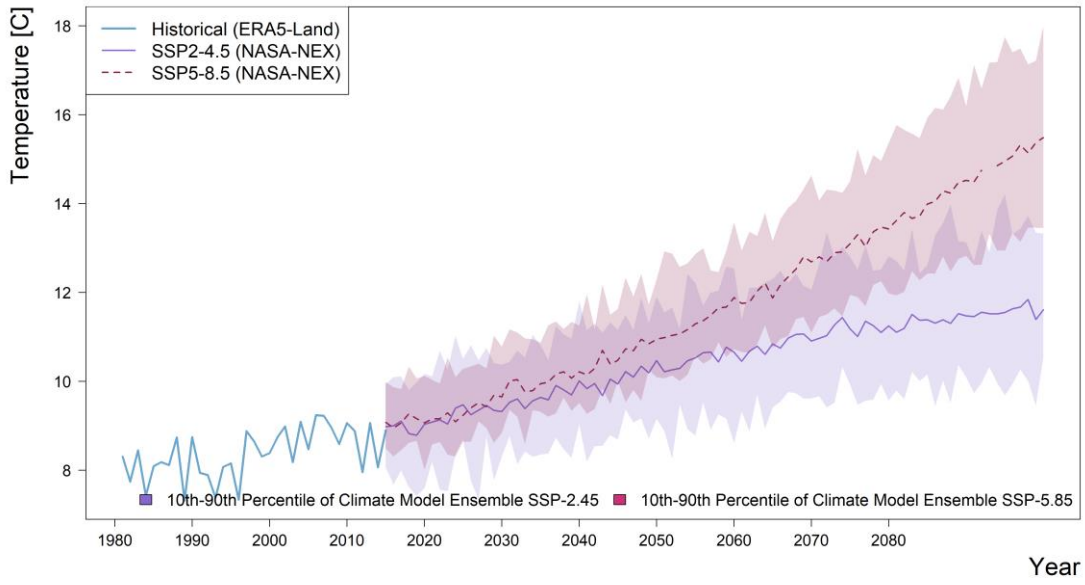

Figure 11. Time series of mean yearly ERA5 temperature for the box FerAnd for the historical period (1981-2020), and NASA NEX (per model bias corrected) for the future period. Shaded areas show the 10th and 90th percentiles in the spread of model predictions.

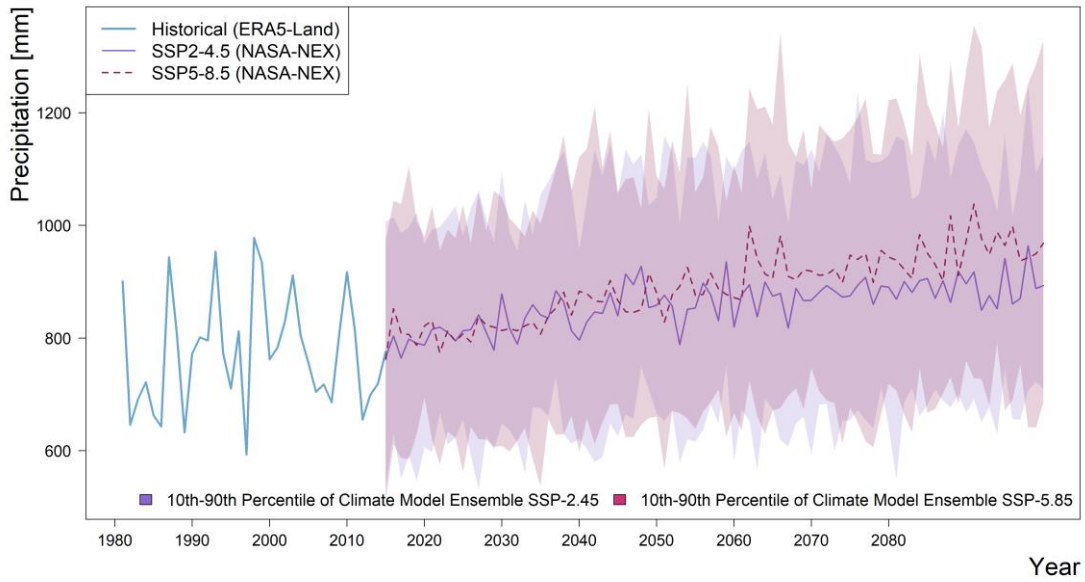

Figure 12. Time series of the yearly ERA5 precipitation for the box FerAnd for the historical period (1981-2020), and NASA NEX (per model bias corrected) for the future period. Shaded areas show the 10th and 90th percentiles in the spread of model predictions.

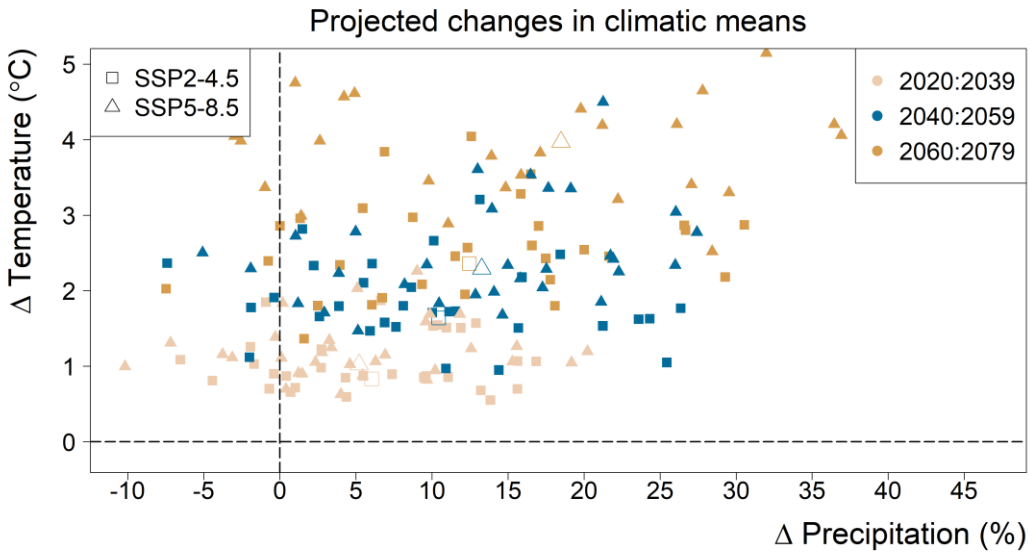

Figure 13. Average temperature and precipitation changes for the box FerAnd region. These indicate the difference (Δ) between historical (1995-2014) and future (2020-2039; 2040:2059; 2060:2079) time horizons for the two SSP scenarios.

4.2.2 Seasonality

In terms of seasonality, the climate model ensemble projects a general consistent increase in mean temperatures for all months for all boxes (Figure 14 and Figure A19-Figure A22). A greater increase in temperatures is predicted in the long-term future (T3) timescale and under the higher SSP 5 scenario. The GCM ensemble results suggest an increase in precipitation specially in the winter season from October-May for all the boxes (Figure 33 and Figure A23-Figure A26). This trend is more extreme under the SSP 5 scenario compared to SSP2. Interestingly, the summer months (June-September) precipitation decreases in the future compared to the reference for all the time horizons and scenarios.

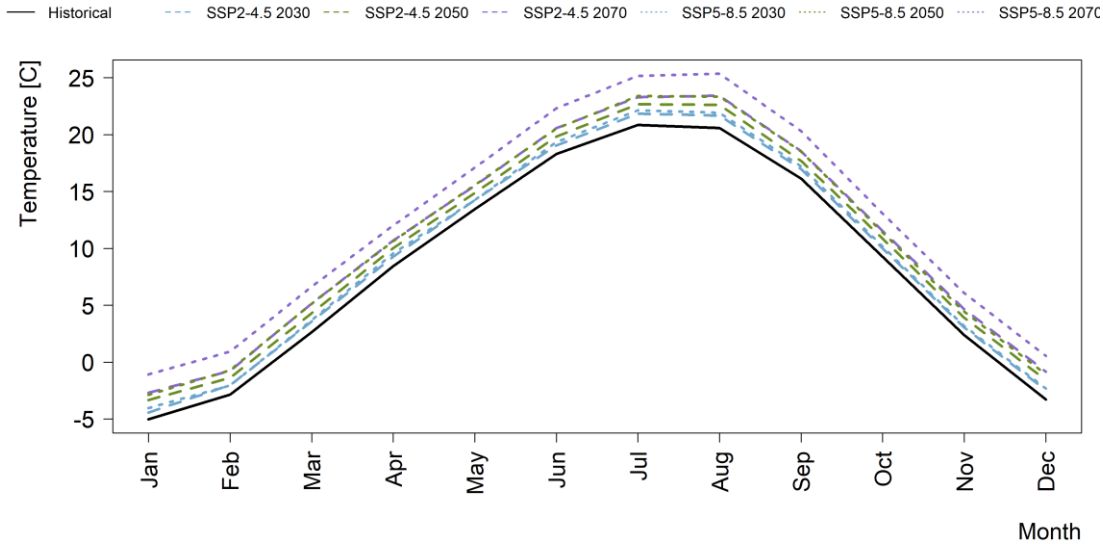

Figure 14. Average monthly temperature for historical (1995-2014) and future (time horizons under the two SSP scenarios for the box FerAnd.

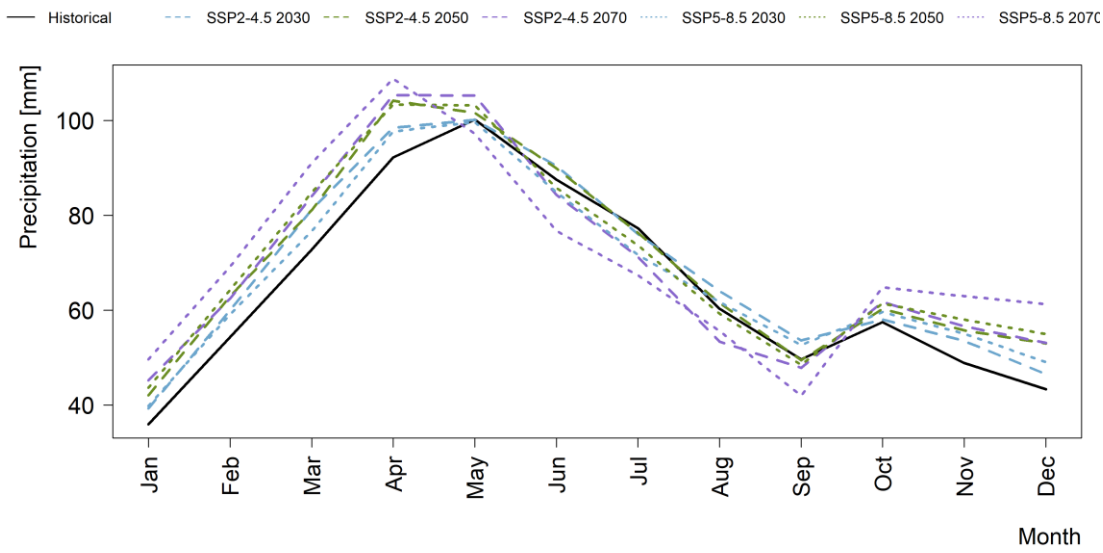

Figure 15. Average monthly precipitation for historical (1995-2014) and future time horizons under the two SSP scenarios for the box FerAnd.

4.2.3 Trends in Climate Extremes

Temperature-related extremes

When extreme trends are considered, a large level of variation is evident in climate model projections. The uncertainty is higher in prediction the extreme trends due to the stochastic nature of these events. The annual daily maximum temperature is expected to increase in the future (Figure 17 and Figure A27-Figure A30). The climate model ensemble does, however, show a clear trend of increasing extreme temperatures under both SSP scenarios and time horizons, suggesting an increase in the likelihood of heatwaves and wildfires in all the boxes.

These processes are certain to affect seasonal water storage and seasonal patterns of discharge, particularly in the high elevation sections of river basins where snow and glacier contribution is dominant. The consecutive dry days (CDD) will increase in future for all the boxes across all the time horizons and scenarios (Figure 18 and Figure A31-Figure A34). The mean CDD for SSP 5 scenario is higher compared to the SSP 2 scenarios. This increase may have implications on the drought in the future.

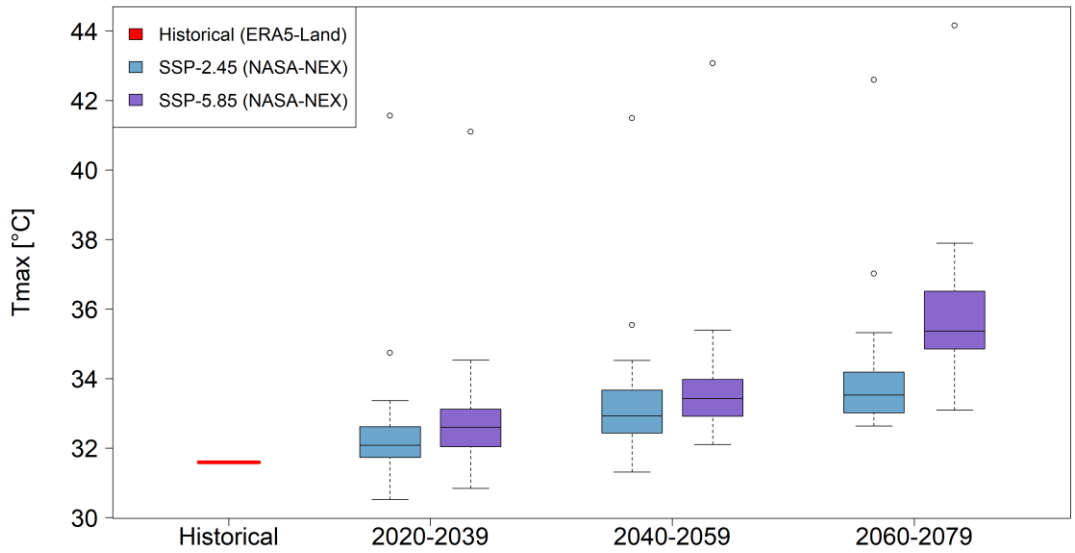

Figure 16. Boxplots indicating the spread in climate model predictions of maximum daily temperature per year (TXx) for the historical (1995-2014) and future time horizons under the two SSP scenarios for the box FerAnd.

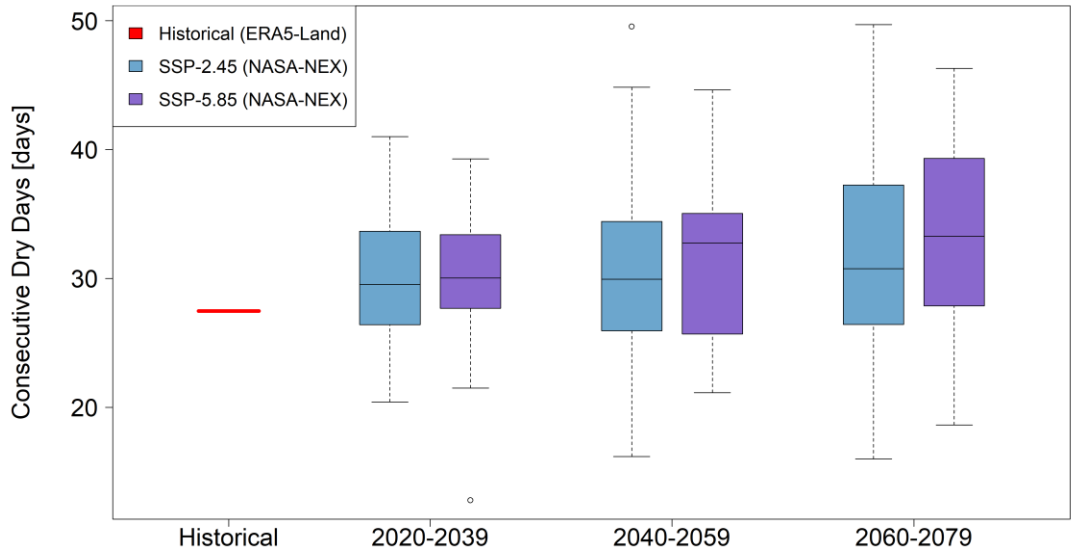

Figure 17. Boxplots indicating the spread in climate model predictions of average consecutive dry days per year (CDD) for the historical (1995-2014) and future time horizons under the two SSP scenarios for the box FerAnd.

Precipitation-related extremes

The climate model ensemble shows a clear trend of increasing extreme 1-day precipitation events under both SSP scenarios and time horizons for all the boxes, suggesting an increase in intense precipitation associated hazards (flash flooding and soil erosion) in the future for the project area (Figure 18 and Figure A35-Figure A38). Similarly, the consecutive 5-day episodes of precipitation increases in the future for all boxes implying that associated hazards such as river floods, landslide and mudflow may increase in the future (Figure 19 and Figure A39-Figure A42).

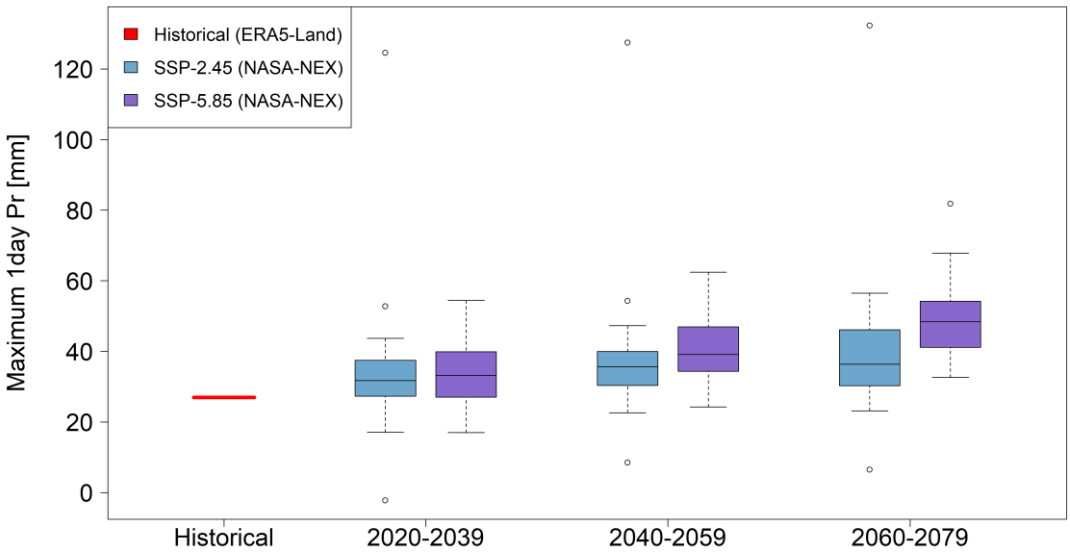

Figure 18. Boxplots indicating the spread in climate model predictions of yearly maximum 1-day precipitation sum (Rx1day, in mm/day) for the historical and future time periods under two SSP scenarios for the box FerAnd.

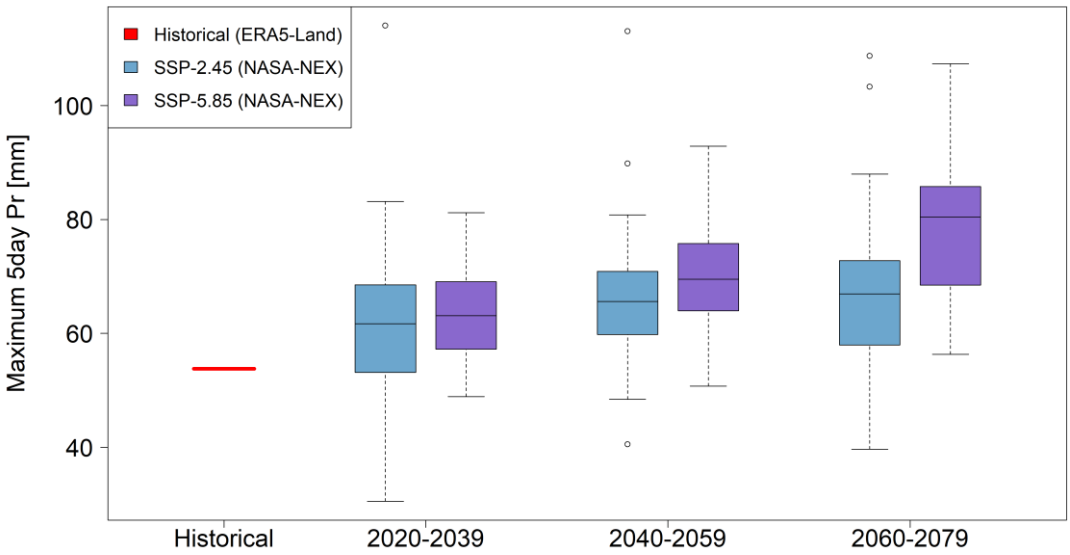

Figure 19. Boxplots indicating the spread in climate model predictions of yearly maximum 5-day precipitation sum (Rx5day, in mm/day) for the historical and future time periods under two SSP scenarios for the box FerAnd.

4.3 Summary tables

The combination of 35 GCMs, two SSPs and three time-horizons leads to a total of 210 (35 x 2 x 3) projections for the future. Table 8 and Table 9 shows detailed results for all projections of changes in mean annual temperature and total annual precipitation for the box FerAnd. Delta values (% change for precipitation and °C for temperature) indicate the difference between historical and future (T1, T2 and T3) time horizons for the two SSP scenarios (for other boxes check Table A1-Table A8). These tables show consistency between GCMs in terms of projecting a warmer future climate in the project area (especially for the longer-term horizon) but indicate the large uncertainty in the future precipitation.

The main statistics (median, 25th percentile and 75th percentile) of the changes in precipitation and temperature, respectively. It also includes the number of GCMs that are showing a positive versus negative change for precipitation, and number of GCMs that are predicting a change above 2ºC and 4ºC. In summary, all GCMs predict a hotter future, with most predictions lying between 2 and 4ºC. All climate models predicted a hotter future for all the clusters, with most of the models predicting an increase of more than 4ºC for the 2070 horizon (Table 9 and Table A1-Table A8). There is no clear consensus in precipitation predictions, but a slight majority of GCMs predict a wetter future for the SSP scenario. Considering the 75th percentile value of the projections as a benchmark for robust climate change adaptation, the statement can be made that wetter conditions should be anticipated in the future for all the boxes in the project area.

Similarly, Table 10 are Table 11 show that the extremes are going to exacerbate in future. While the extreme temperature changes remain fairly similar for all the boxes, the CDD changes in future are higher in magnitude for box FerAnd compared to the other boxes. This may have serious implications for the heat wave and drought hazards in the future. The RX1 is expected to increase by more than 50% for SSP2 and double for SSP5 by the end of century. The increase in occurrence and magnitude of such extreme events in the future may increase the likelihood of hazards, for instance erosion, floods, and sedimentation.

Table 8. Summary table showing statistics regarding spread in CMIP6 ensemble predictions for future changes in mean annual precipitation for the FerAnd box.

Scenarios	Average (%)	25th Perc. (%)	75th Perc. (%)	GCMs Dryer	GCMs Wetter
2030_SSP245	6%	0%	12%	9	25
2050_SSP245	10%	4%	16%	3	31
2070_SSP245	12%	6%	6%	3	31
2030_SSP585	5%	1%	1%	7	28
2050_SSP585	13%	5%	5%	4	31
2070_SSP585	19%	8%	28%	3	32

Table 9. Summary table showing statistics regarding spread in CMIP6 ensemble predictions for future changes in mean temperature for the FerAnd box.

Scenarios	Average (%)	25th Perc. (%)	75th Perc. (%)	GCMs >2°C	GCMs >4°C
2030_SSP245	+0.8	+0.8	+1.2	0	0
2050_SSP245	+1.6	+1.5	+2.1	10	0
2070_SSP245	+2.4	+2.4	+2.3	25	25
2030_SSP585	+1.0	+1.0	+1.0	1	1
2050_SSP585	+2.3	+2.3	+2.3	23	23
2070_SSP585	+4.0	+4.0	+4.0	31	31

Table 10. Summary table (mean values) for the historical extremes.

Regions	Rx1day (mm)	Rx5day (mm)	CDD (days)	TXx (°C)
FerAnd	25.4	50.1	30.0	32.4
BuSaKa	18.3	28.0	115.9	42.5
Navoi	14.0	19.0	105.4	42.5
Surkha	24.5	47.6	77.0	36.0
Tasken	23.4	41.1	56.7	39.3

Table 11. Percentage change in climate extremes for the SSP scenarios and time horizons compared to the historical extremes

Horizon	Scenarios	Box	Rx1day (%)	Rx5day (%)	CDD (%)	TXX (%)
T1	SSP2	FerAnd	29	16	7	3
		BuSaKa	42	31	1	3
		Navoi	47	38	1	3
		Surkha	28	14	1	4
		Tasken	40	20	0	3
	SSP5	FerAnd	27	19	8	4
		BuSaKa	39	27	0	4
		Navoi	31	28	1	4
		Surkha	25	11	1	5
		Tasken	35	22	-1	4
T2	SSP2	FerAnd	42	25	8	5
		BuSaKa	55	41	0	6
		Navoi	69	60	0	6
		Surkha	42	20	1	6
		Tasken	54	27	1	6
	SSP5	FerAnd	54	31	12	7
		BuSaKa	65	44	1	7
		Navoi	81	57	1	7
		Surkha	53	21	2	8
		Tasken	66	32	4	7
T3	SSP2	FerAnd	51	28	13	8
		BuSaKa	66	46	0	7
		Navoi	93	76	-1	7
		Surkha	45	22	2	8
		Tasken	71	33	4	7
	SSP5	FerAnd	87	49	20	13
		BuSaKa	103	70	2	11
		Navoi	121	94	3	11
		Surkha	82	38	4	13
		Tasken	101	55	9	12

Table 12. Average percentage change in climate extreme across all the scenarios and time horizons compared to the historical extremes (i.e., summary of Table 11).

	Rx1day	Rx5day	CDD	TXX
Related hazard	Floods, landslides, erosion, mudflows		Droughts, dust storms, wildfire	Heatwaves, dust storms, wildfire
FerAnd	48.3	28.1	11.4	6.6
BuSaKa	61.5	43.1	0.6	6.5
Navoi	73.6	59.0	0.9	6.5
Surkha	45.6	20.9	1.8	7.4
Tasken	61.2	31.5	2.9	6.5

5 Climate Risks and Vulnerabilities

Uzbekistan is becoming increasingly vulnerable to the impacts of climate change. Frequent and intense floods, heatwaves, droughts, and dust storms continue to threaten the accelerating socioeconomic development in the country. An efficient, adequate, and uninterrupted power supply is critical to sustain and improve Uzbekistan's growing economy; however, the aging electric grid infrastructure is now experiencing significant power losses, especially under climate change. Additionally, the rapidly increasing population has also put immense pressure on the existing infrastructure to meet the swelling energy demands. Therefore, it is crucial to not only enhance the capacity and efficiency of the existing system through modern engineering solutions but also gain a clear understanding of how the electric power system is vulnerable to the different impacts of climate change. An improved understanding of climate risks will lead to the identification and implementation of the most effectual mitigation and adaptation measures. This chapter identifies the sensitivities and vulnerability of the electric grid infrastructure to different climate risks and assesses the risk levels.

5.1 Sensitivity to project-relevant hazards

Power transmission systems are sensitive to climate factors in various ways. How climate change and increased severity and occurrence of climate-related hazards will impact the project will depend on how sensitive the infrastructural components are to climate variables. The sensitivity to project-relevant hazards is summarized in Table 13.

Table 13. Sensitivity to climate hazards of the main project components.

Hazard	Output 1: Transmission Lines	Output 2: Substations
Floods	Heavy rains and flooding can undermine tower structures through erosion Flooding can damage underground cables and infrastructure as moisture comes into contact with the equipment and leads to short circuiting	Floods can damage the structures (civil, mechanical, and electrical) by erosion and when water comes into contact with electrical control systems causing short circuits
Droughts and Heatwaves	Droughts can increase dust damage[1] High temperatures can damage control systems through loss of information and communications technology service or reduce quality of service Operating at or exceeding the maximum electricity carrying capacity of the lines due to	Increased strain on substations due to high demands during warm periods High temperatures can impair operation of substations Drought can increase dust damage

[1] Achakulwisut P, Anenberg SC, Neumann JE, Penn SL, Weiss N, Crimmins A, Fann N, Martinich J, Roman H, Mickley LJ. Effects of Increasing Aridity on Ambient Dust and Public Health in the U.S. Southwest Under Climate Change. Geohealth. 2019;3(5):127-144. doi: 10.1029/2019GH000187. PMID: 31276080; PMCID: PMC6605068.

	increased demand in warm periods can damage the equipment Increases in temperature can reduce the current rating of the transmission lines and increase their chances of sagging	
Dust storms and Wind Erosion	Strong winds can weaken the foundation of pole mounted transmission and distribution lines Dust storms can cause corrosion and transmission losses from overhead power lines Dust settling on transmission lines can cause sparks leading to potential fire eruptions	Dust storms and high-speed winds can cause damage (corrosion etc.) to the infrastructure
Landslides and mudflows	Landslides and mudflows can damage the foundations of overhead transmission poles	Landslides and mudflows can damage the substation infrastructure
Wildfire	Wildfires directly damage transmission lines and lead to power outages	Wildfires can damage different components within the substation, particularly the sensitive electrical circuits

5.2 Adaptive capacity

The socio-economic context of the project influences the project´s capacity to cope with climate hazards and climate change. For this multi-regional energy project, this context is predominantly influenced by national-level adaptation planning, and the national socio-economic resilience level.

According to the national-level Notre Dame Global Adaptation Index (ND-GAIN)[1], which indicates a country's climate vulnerability with respect to its readiness for enhanced resilience, Uzbekistan has a score of 49.4 and an overall country index rank of 83 (100 being the best). This shows that the country is well positioned to tackle the impacts of climate change, even though adaptation will be a challenge.

Figure 20 shows the temporal variation in vulnerability and readiness over the last 25 years. Vulnerability considers six major sectors i.e., food, water, health, ecosystem service, human habitat, and infrastructure while readiness is assessed according to economic, governance and social readiness.

[1] https://gain-new.crc.nd.edu/country/uzbekistan

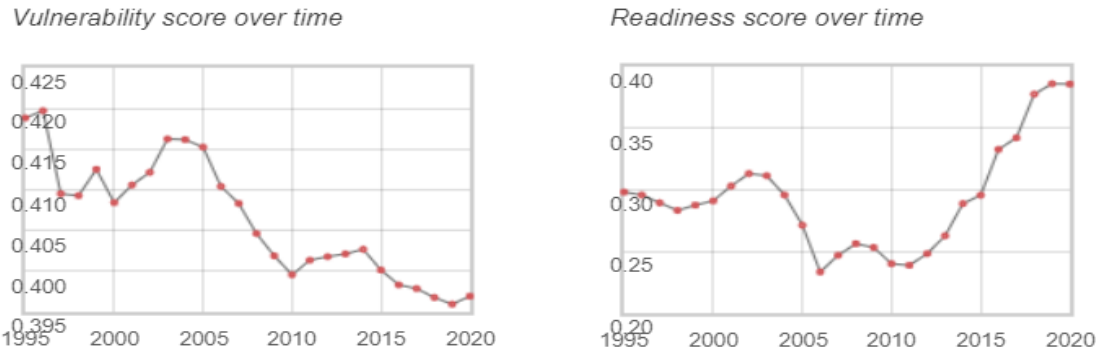

Figure 20. Temporal variation in Uzbekistan's vulnerability and readiness scores (1995 - 2020) (Source: GAIN-ND, University of Notre Dame).

Based on the ND-GAIN Index and the temporal changes in vulnerability and readiness scores, Uzbekistan has gained climate resilience over the years and has the potential to further enhance it. Figure 21 depicts the shift in Uzbekistan's position with respect to other countries on the vulnerability-readiness matrix (2010 vs 2020). The country has accelerated its efforts towards promoting climate mitigation and adaptation measures across all its sectoral strategies such as the National Development Goals, Green Economy Strategy, and Concept for the Development of Electric Power Industry. In its updated NDC, Uzbekistan has increased its commitments by more than 300 percent. The agenda includes increasing the share of renewable energy sources to 25 percent of total power generation, reduce the energy intensity of GDP by half, and double the energy-efficiency indicator relative to the level of 2018 – among others.

Figure 21. Shift in Uzbekistan's adaptive capacity in relation to other countries (2010 - 2020) (Source: GAIN-ND, University of Notre Dame).

With ADB's support, the country is committed to reforming its energy sector and transitioning into a green economy by 2030. Through Output 1 and 2 of the project, the growing issue of energy losses and frequent blackouts will be tackled while Output 3 and 4 will strengthen the technical and managerial capacity of JSC-NEGU to ensure smooth operations. As adaptation priorities are already reflected in almost all current and future socioeconomic development plans, Uzbekistan appears to be on track with effectual and timely implementation of these measures.

5.3 Climate risks

Due to variations in elevation, land use, and hydrology across the country, different regions of Uzbekistan are more or less exposed to the different climate hazards. Earlier this year in April, the country suffered

from extreme floods and mudflows after torrential rain – making it the worst flood event in 80 years. The floods were followed by extreme heatwaves in July where temperatures rose to 42.6°C[1]. There were occasional blackouts due to a surge in energy demand because of increased air conditioning and refrigeration needs. Such events are only going to become more frequent in the future; therefore, mapping hazards is crucial to minimize losses and ensure climate proof infrastructure development.

5.3.1 Flooding

Overall, there is a medium to high flood hazard across the country except for the north and southeastern regions which show medium to high hazard (Figure 22). Three major flooding events have occurred in the last two decades. In 2005, a flash flood hit Boymurod (Kanimekh) and Qoshgudug (Nurata), affecting over 1,500 people. In 2020, a massive flood hit the Syrdarya region impacting more than 70,000 people[2]. Similarly, in April 2022, deadly floods and mudslides hit Samarkand region along with parts of Navoi and Qashqadarya regions. This disaster resulted in the death of four people, damaged over 260 farms and buildings, and left many displaced[3].

The study based on global climate and hydrological model's (0.5° x 0.5° grid) reveals that eastern part of Uzbekistan is exposed to floods compared to other regions (Figure 23Figure 22Figure 23)[4]. However, the models used for the global simulations were not tailored to the specifics of Uzbekistan (Lange et al., 2020). The glaciers and vegetation-related processes were strongly simplified in the global scale models so the exposure may increase in the future. Another global study estimated that more than 300 thousand people (Figure 24) will be affected by the floods in the future for Uzbekistan (Ward et al., 2020). The total flood losses will increase from 850 million USD to about 20 trillion USD by 2080.

Considering the projected increases in extreme rainfall events, the present hazard level most likely will increase in the future and thus it is essential to design projects in these areas to be robust to river flood hazard in the long-term.

[1] www.hydromet.uz

[2] Darthmouth Flood Observatory, https://floodobservatory.colorado.edu/Archives/index.html

[3] Ministry of Emergency Situations, https://floodlist.com/asia/uzbekistan-floods-april-2022

[4] https://www.isipedia.org/report/will-climate-change-increase-the-exposure-to-river-flooding/uzb/

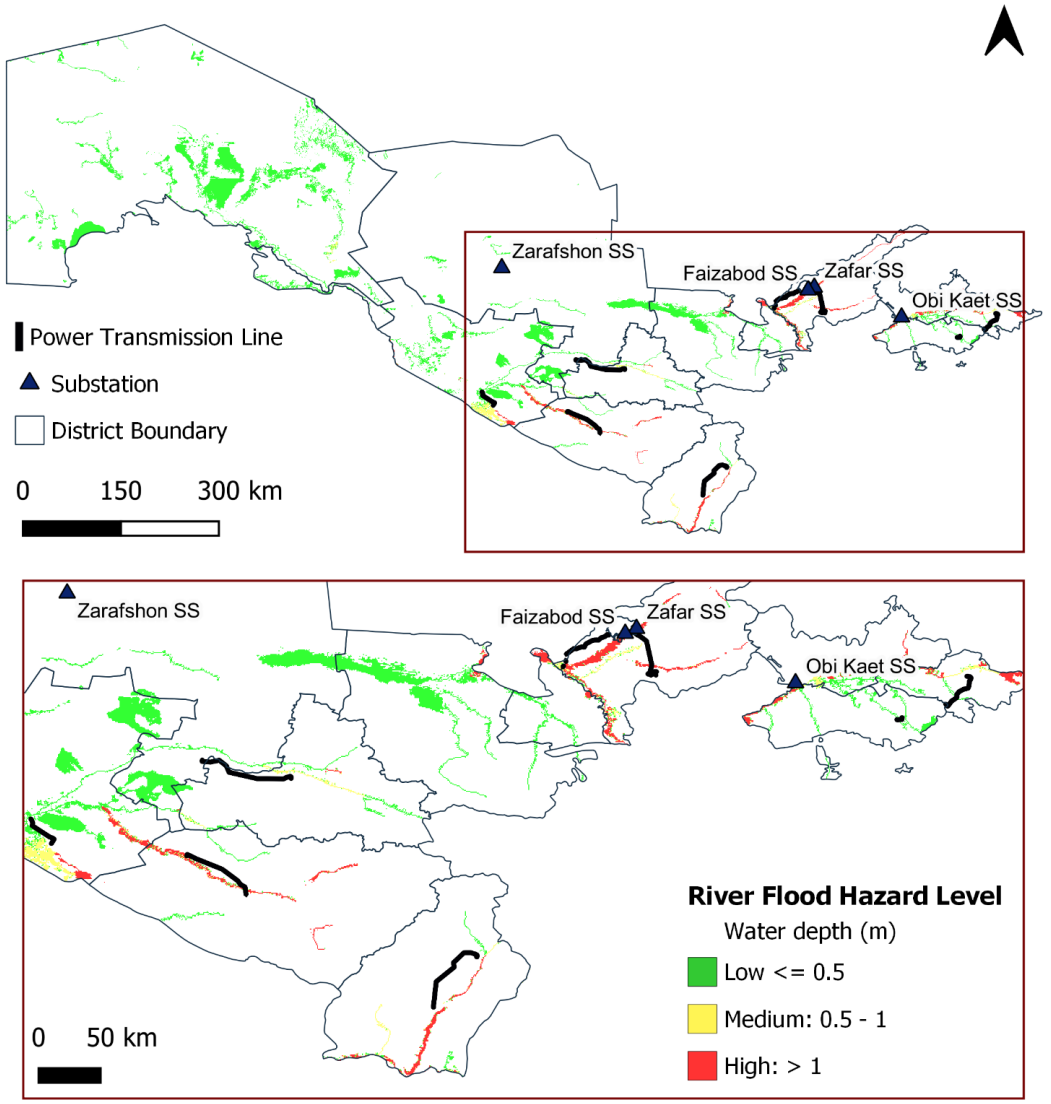

Figure 22. Flood hazard across Uzbekistan (Source: WRI Global Flood Model. Return Period 10, 100, 1000 years - water depth).

Based on Figure 22, most of the transmission lines and two substations (Faizabod and Zafar) subject to improvements lie near the high flood hazard zones in Tashkent and Kashkadarya region. Extra measures need to be in place to decrease the vulnerability of this infrastructure.

The increase in precipitation in the future will have a significant impact on the floods in the region (see section 4.2). It is likely that flood-related hazards will increase for the regions in the east compared to the west of Uzbekistan in the future. The clusters FerAnd and Tasken will be higher compared to the other regions. Thus, the additional risk due to climate change for floods related hazards is estimated to be **medium to high**.

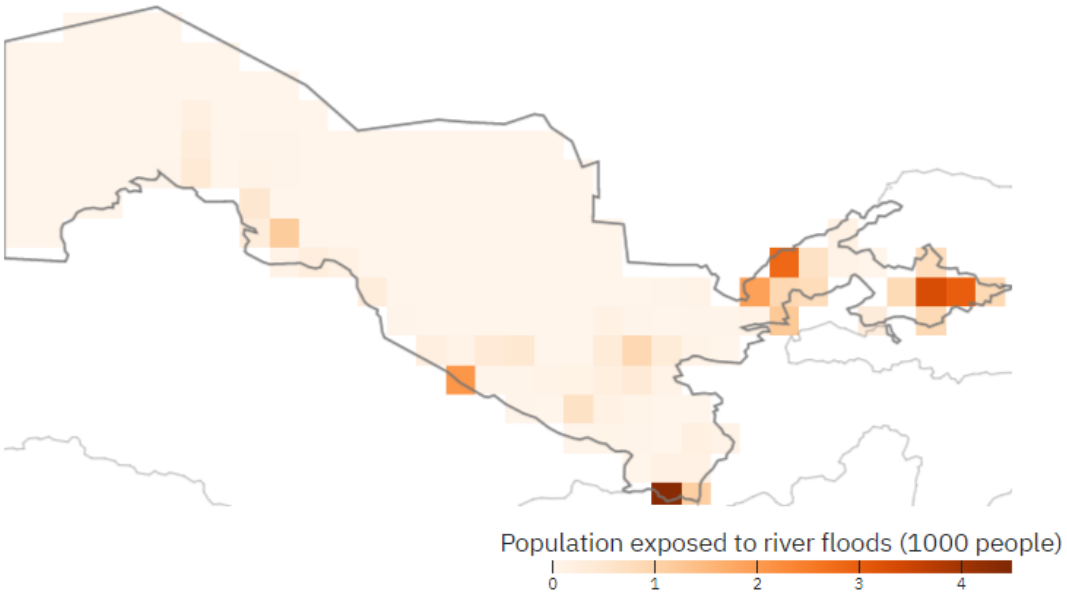

Figure 23. Population exposure to river flooding at 2°C global warming varies within Uzbekistan[1].

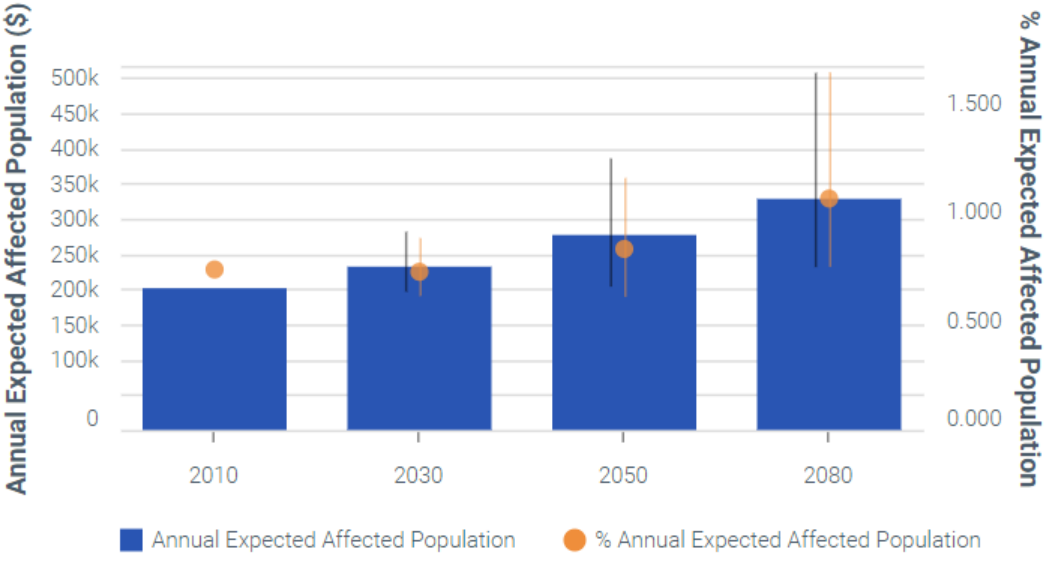

Figure 24. The expected annual damage to be incurred and the relative amount of damage for the Uzbekistan in the future. Error bars are bound by the minimum and maximum damage estimates from the different climate models[2].

5.3.2 Droughts and Heatwaves

The intensity and frequency of droughts and heatwaves is increasing in the country, with extreme heat levels being reported in Samarkand region. In 2021, the Centre of Hydrometeorological Service of Uzbekistan (UZHYDROMET) identified early June as the hottest early summer since the end of the 19th century, with air temperatures 7-10°C higher than the climatic norm. Temperatures in Tashkent, during this period, rose to 42.6°C, which exceeded the peak values observed in the 19th and 20th century.

[1] https://www.isipedia.org/report/will-climate-change-increase-the-exposure-to-river-flooding/uzb/
[2] https://www.wri.org/applications/aqueduct/floods/#/risk

Given its geographic location and terrain, majority of the country is already classified as semi-arid to arid. The rising temperatures have increased Uzbekistan's vulnerability to droughts. In 2000, an extreme drought event caused significant economic damages equivalent to USD 79,000, affecting more than 600,000 people over an area of 860 km^2.

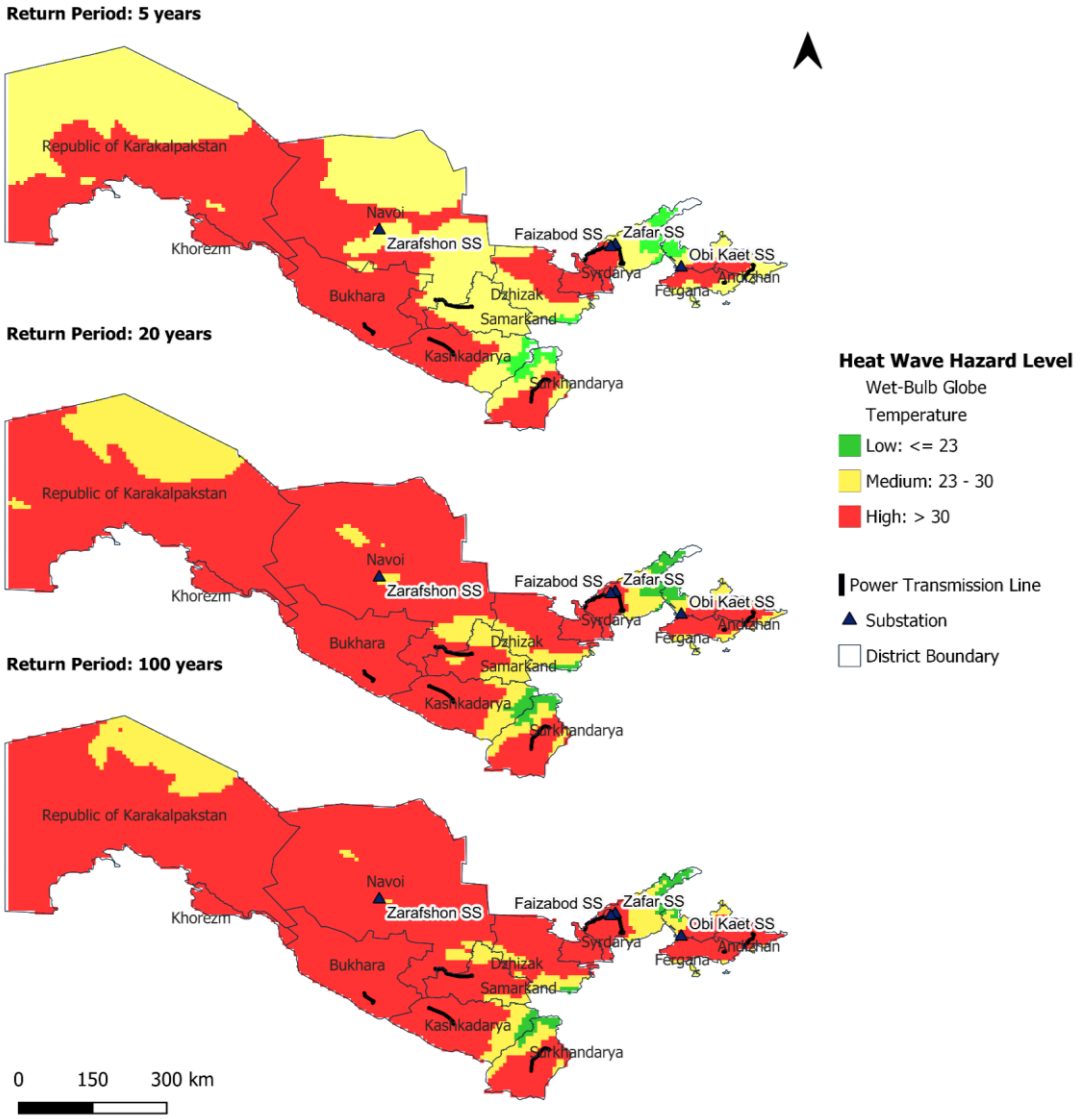

Figure 25. Heat wave hazard across Uzbekistan (Source: VITO Global Heat Model, 5, 20, 50 years RP hazard Map).

Figure 25 shows the heat wave hazard across the country. The location of the transmission lines and substations coincides with the extent of high hazard zones for all three return periods, thus making the infrastructure vulnerable to the adverse impacts of heatwaves. Moreover, alarming increase in average and extreme temperature related indices (see section 4.2 and Table 12) will further exacerbate the frequency and intensity drought and heatwaves in the future. Thus, the climate risk due to droughts and heat wave is estimated to be **high**.

5.3.3 Dust storms and wind erosion

Increasing desertification because of aridity and land degradation has amplified the number of dust storm events in Uzbekistan. Water shortages and increasing aridity caused by climatic changes coupled with

land degradation problems have aggravated the desertification processes. As a result, a desert expanding over 60,000 km^2, has formed at the bottom of the former Aal Sea and is now an additional source of sand and dust storms in the country[1]. As a major consequence, this has resulted in an increased number of dust storm events.

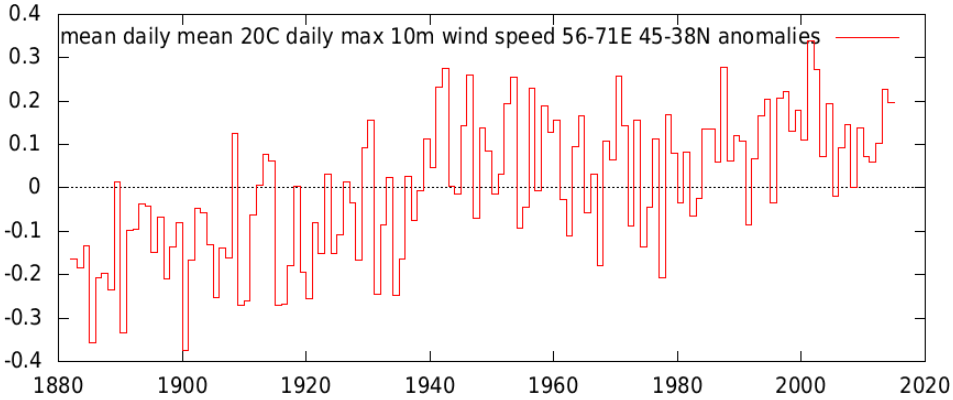

Figure 26. Wind speed anomaly for Uzbekistan (1880-2014) (Source: NOAA-CIRES).

The western part of Uzbekistan is susceptible to dust storms, as Figure 27 illustrates. The map shows the wind erosion risk for Uzbekistan, based on the erosivity of the wind and erodibility of the surface. Erosivity is expressed by max wind speeds at 10m heights measured[2], while erodibility is expressed as a combination of land cover[3] and soil type[4] (and texture). The expected substantial increase in air temperatures across Uzbekistan, is expected to lead to more prolonged periods of drought conditions. This is likely to contribute to increased aridity and desertification in the country, which may also increase the occurrence of dust storms.

For the most part the investigated transmission lines and substations lie within a low wind erosion hazard zone, as per Figure 27, but energy distribution infrastructure in Bukhara and Kashkadarya provinces are exposed to locally high wind erosion / dust storm risks. The increased hazard level may adversely affect energy transmission performance, as dust storms are known to cause corrosion and transmission losses from overhead power lines and can cause damage to pole mounted transformers and energy distribution systems. More powerful dust storms due to stronger wind may also develop, causing damage to overhead transmission lines and poles. Finally, dust particles hitting power lines can cause sparks, so dust storms could potentially start wildfires which may damage the energy network and cause power outages. These dust storms are not only harming human health but also damaging development infrastructure.

Based on the trends observed in the wind speed anomalies in Uzbekistan (Figure 26) and increase in temperature related extremes in the future, more frequent and intense dust storms are likely to follow in the future (see section 4.2 and Table 12). Overall, the climate risk for dust storms and wind-related erosion is **medium to high**.

[1] https://kun.uz/en/news/2022/02/05/sand-and-dust-storms-of-aralkum-yearly-carry-out-up-to-75-million-tons-of-sand-dust-and-salt
[2] Abatzoglou, J.T., S.Z. Dobrowski, S.A. Parks, K.C. Hegewisch, 2018, Terraclimate, a high-resolution global dataset of monthly climate and climatic water balance from 1958-2015, Scientific Data 5:170191, doi:10.1038/sdata.2017.191
[3] Buchhorn, M. ; Lesiv, M. ; Tsendbazar, N. - E. ; Herold, M. ; Bertels, L. ; Smets, B. Copernicus Global Land Cover Layers-Collection 2. Remote Sensing 2020, 12Volume 108, 1044. doi:10.3390/rs12061044
[4] Tomislav Hengl. (2018). Soil texture classes (USDA system) for 6 soil depths (0, 10, 30, 60, 100 and 200 cm) at 250 m (Version v02) [Data set]. Zenodo. 10.5281/zenodo.1475451

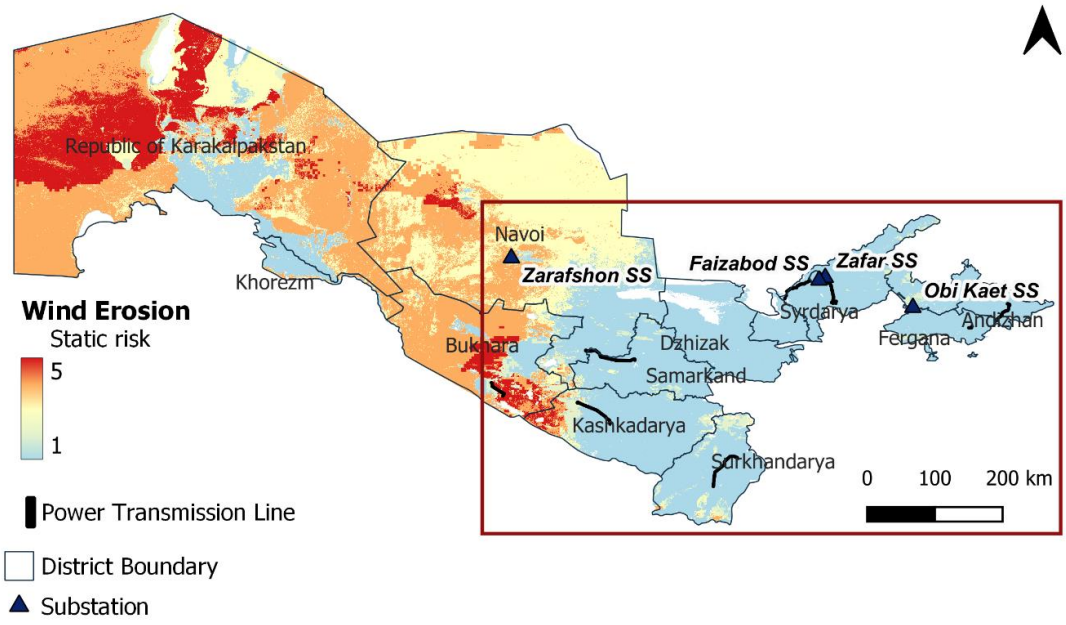

Figure 27. Wind Erosion risk (Low-1 to High-5) for Uzbekistan, based on historical wind records, land cover and soil texture.

5.3.4 Landslides, water-related erosion, and mudflows

More than 3,300 mudflows of which 85% are associated with storm activity has been registered in Uzbekistan between 1900-2013. Approximately 83% of the mudflow occurred in the months between March to July.[1] Fergana valley alone has experience more than 44% of such mudflow events in the past. More than 90 % of all recorded mudflows were associated with extreme precipitation events, hail and sleet, whereas 6 % of mudflow episodes were observed during intensive snowmelt events induced by respective temperature and precipitation changes.[2]

Climate model projections (CMIP5-based) revealed that mudflow generating large-scale circulation flows will increase by up to 5% to the end of the century for Uzbekistan (Mamadjanova & Leckebusch, 2022). Moreover, third UNFCCC national report of Uzbekistan[3] have also confirmed the increase of precipitation induced natural hazards such as mudflows to be 4 times more in the country by 2080. Two significant mudslide events have been reported, one in the Ferghana Valley in the Namagan Region in 2021 and the other earlier this year in Samarkand, Navoi and Qashgadarya regions.

As shown in Figure 28, most of the transmission lines and substations are situated in either none or low rainfall-induced landslide hazard zones. The spatial pattern for this landslide dataset resembles very much the spatial pattern of the recorded mudflow events in Uzbekistan (Mamadjanova et al., 2018). However, the transmission lines in the region Fergana, Andizhan, Samarkand and Surkhadarya could potentially be impacted by landslides in the future – depending on the extent and magnitude of landslide. Projected increases in temperature are likely to increase the liquid fraction of precipitation; given the high mountainous region in the northeast and southeast part of the country, there is a **medium to high** rainfall-induced landslide hazard.

[1] Mamadjanova, Gavkhar, et al. "The role of synoptic processes in mudflow formation in the piedmont areas of Uzbekistan." Natural Hazards and Earth System Sciences 18.11 (2018): 2893-2919.
[2] Ibis
[3] https://unfccc.int/sites/default/files/resource/TNC%20of%20Uzbekistan%20under%20UNFCCC_english_n.pdf

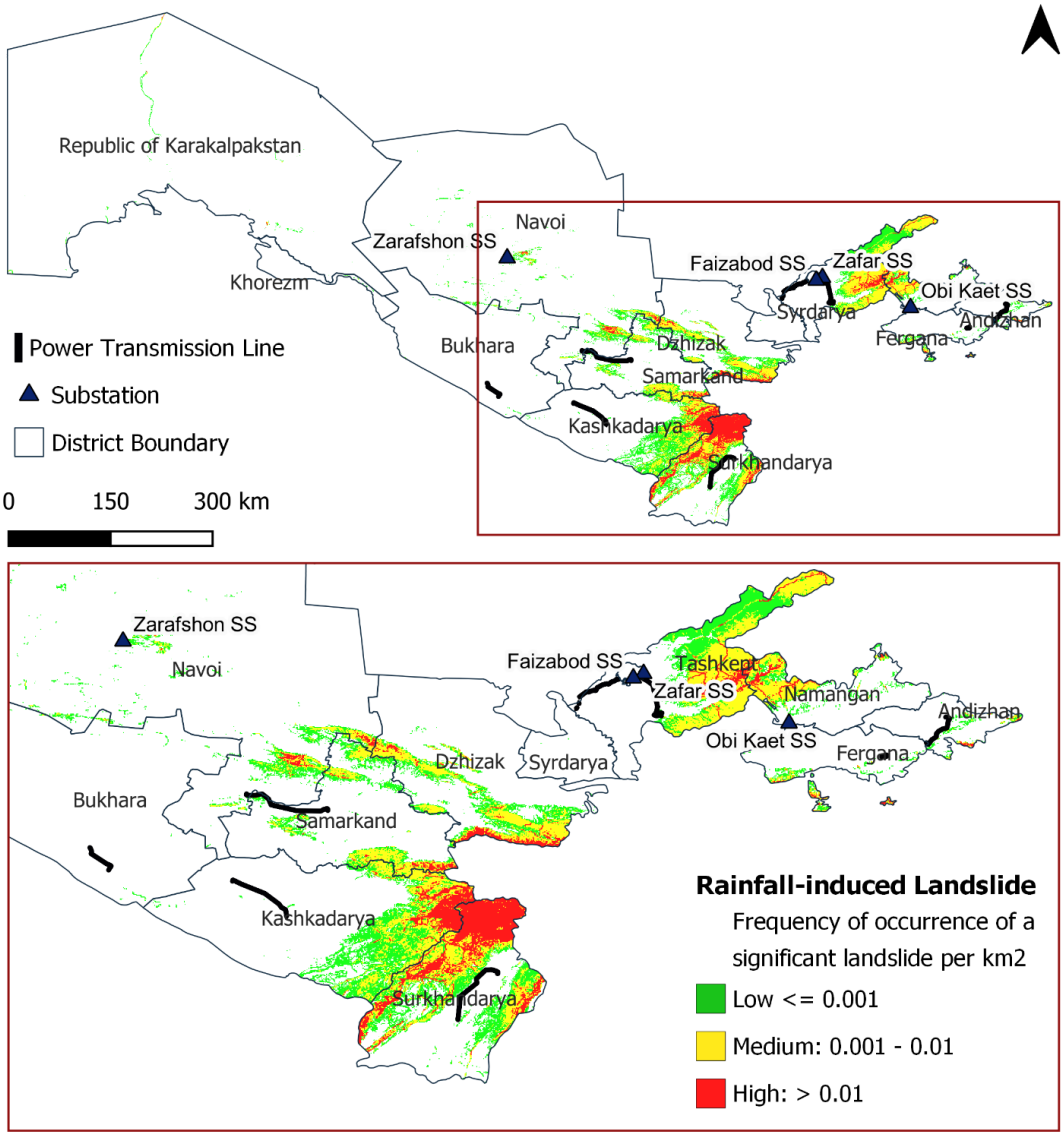

Figure 28. Rainfall-induced landslide hazard across Uzbekistan (Source: Global Landslide Hazard Map: Rainfall trigger, The World Bank).

5.3.5 Wildfire

The wildfire hazard across Uzbekistan is classified as **high**, indicating that there is a greater than 50% probability of weather conditions causing a significant wildfire[1]. The extent of the wildfire hazard zone is also likely to increase in the future, posing a serious risk for major infrastructure developments.

Like the map depicting heat wave hazard across the country (Figure 25), the wildfire hazard (Figure 29) is also categorized as high in areas where the transmission lines and substations are located. The highest hazard is in the regions of Samarkand and Kashkadarya followed by Andizhan. Therefore, extra protection measures need to be in place to minimize damage caused by wildfires.

[1] https://thinkhazard.org/en/report/261-uzbekistan/WF

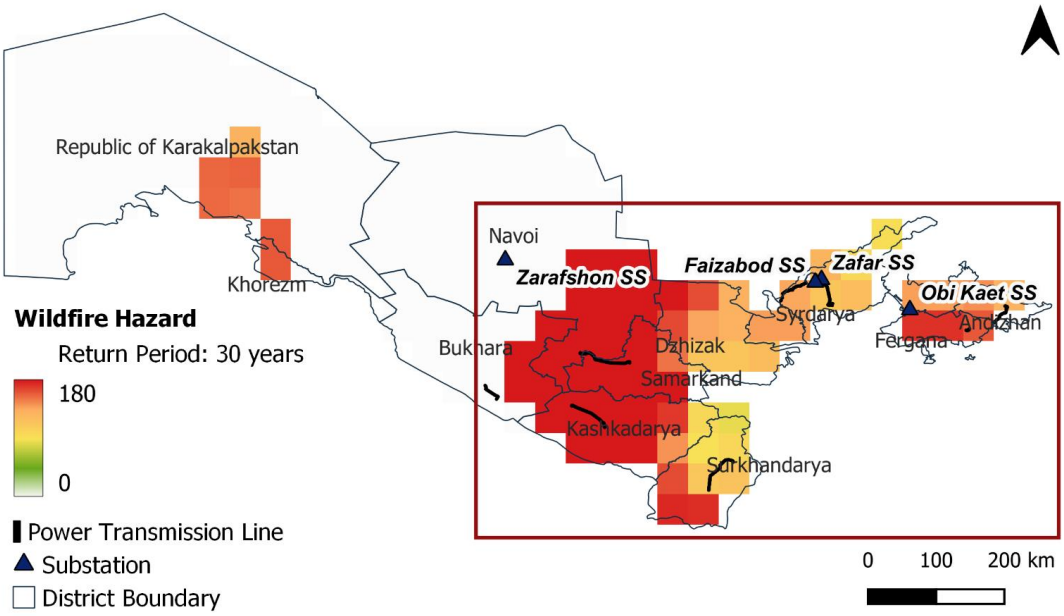

Figure 29. Wildfire hazard across Uzbekistan (Source: Global Facility for Disaster Reduction and Recovery, GeoNode).

5.4 Risk summary table

The climate vulnerability and risk analysis process has gathered several datasets in the public domain, together with local information, associated with each risk to determine the most important risks associated with the project area. Table 14 summarizes this and provides an expert judgement of the risk for the project components.

Table 14. Climate risk assessment of the project outputs.

Hazard	Expected Change in related climate indices	Exposed Project Output	Risk	Detailed comments
Floods	Increase in maximum 5-day rainfall and precipitation intensity predicted by climate model ensemble	Transmission lines and substations (Output 1 and Output 2) *FerAnd* *Tasken* *Surkha* *BuSaKa* *Navoi*	**M to H** M H M H H	The transmission lines (output 1) and the substations (output2) in the boxes Tasken, BuSaKa and Navoi face the highest risk (>30% of RX5 day) of floods in the future (see Table 12). For these infrastructures, heavy rains and flooding can undermine tower structures through erosion, as well damage underground cables and infrastructure when moisture comes into contact with the equipment and leads to short circuiting.
Droughts and heatwaves	Moderate increase in CDD and high increase in extreme temperature predicted by climate model ensemble	Transmission lines and substations (Output 1 and Output 2) *FerAnd* *Tasken* *Surkha* *BuSaKa* *Navoi*	H H H H M H	The transmission lines (output 1) and the substations (output2) in all the are at high risk of droughts and heatwaves in the future. This is mainly due to large increase in the average temperature and TXx (~7%) in the future for all the boxes (see section 4.2 and Table 12). The increase in temperature related extremes will significantly increase the energy loss from the transmission lines. High temperatures can damage control systems through loss of information and communications technology service or reduce quality of service. Drought may also cause additional risk for damage from dust.
Dust storms and wind erosion	Increase in maximum temperature predicted by climate model ensemble	Transmission lines and substations (Output 1 and Output 2) *FerAnd* *Tasken* *Surkha* *BuSaKa* *Navoi*	**M to H** M M M H H	The transmission lines (output 1) and the substations (output2) in the BuSaKa and Navoi are at high risk of dust storms and wind erosion hazards in the future. The consistent increase in average temperature and TXx (~7%) in the future will likely increase the frequency and magnitude of wind related hazards (see section 4.2 and Table 12). The increased hazard level may adversely affect energy transmission performance, as dust storms are known to cause corrosion and transmission losses from overhead power lines and can cause damage to pole mounted transformers and energy distribution systems.

Landslides, water-related erosion, and mudflows	Increase in maximum 1-day and 5-day precipitation predicted by climate model ensemble	Transmission lines and substations (Output 1 and Output 2) *FerAnd* *Tasken* *Surkha* *BuSaKa* *Navoi*	**Medium** **H** **M** **M** **M** **L**	The consistent increase in the precipitation related extremes RX1 and RX5 in the future will likely increase the risk of landslide and erosion activity in the region. Moreover, the mountainous part in the east and south are highly vulnerable to landslide hazard.
Wildfire	Increase in maximum temperature predicted by climate model ensemble	Transmission lines and substations (Output 1 and Output 2) *FerAnd* *Tasken* *Surkha* *BuSaKa* *Navoi*	**Low** **L** **L** **L** **L** **L**	The project has a low exposure to wildfires, and thus a low risk level

6 Climate Adaptation Options

The climate risks assessed in the previous chapter urge for the adoption of effective adaptation measures to ensure that the project development objectives are not compromised by climatic changes. This chapter presents potential adaptation measures that address both medium (next decades) and long-term (second half of the century) impacts of climate change.

In general, robust design specifications could allow structures to withstand more extreme conditions (such as floods and dust storms). In some circumstances, it may also be necessary to consider redesigning extremely vulnerable existing infrastructure. The proposed adaptation measures address the following climate risks that were classified as “medium” or “high” in the climate risk assessment. These are:

- **Floods:** Due to increased frequency and magnitude of rainfall, there is a higher probability of flooding in the region. Therefore, flood-prone areas should be avoided for project implementation and infrastructure solutions or Nature-based solutions should be adopted to further mitigate flood risk.

- **Droughts and heatwaves:** Higher temperatures and increased frequency and duration of heat waves can reduce the electricity carrying capacity of the transmission lines and damage control systems.

- **Dust storms and wind erosion:** Strong winds and erosion have already increased the occurrence of dust storms in parts of Uzbekistan. High speed winds can weaken the stability of transmission pylons; thus, the design should be able to endure extreme weather conditions.

- **Landslides and mudflows:** In areas of higher elevation, there is an increased risk of water-related erosion, landslides and mudflows which can tamper the power grid infrastructure. Therefore, added protection measures need to be in place to minimize damage and ensure uninterrupted transmission.

- **Wildfire:** Given the increasing number of days with high temperatures, the risk of wildfires erupting during the summer period will likely increase. Transmission lines crossing through these areas will be susceptible to fires; therefore, it is crucial to implement mitigation and adaptation strategies to prevent such incidents.

6.1 Options for resilient design

The following adaptation measures comprise of both engineering and non-engineering measures for all four components of the project. Since Output 3 and 4 relate to improved project management and institutional development of JSC-NEGU, they are identified as least sensitive to the above-mentioned climate risks.

Optional adaptation measures for including in the project design have been identified in Table 15 along with the relative cost estimates derived from the relative change in the related climate index. This cost estimate is based on a combination of expert-judgement and the projected changes in the climate indices as presented in Table 12. The absolute estimates of the costs, and the total adaptation cost can be

estimated from these relative figures as soon as the project design with component-specific cost estimates is available.

Table 15. Potential adaptation options for enhanced climate resilience.

Climate Risk	Adaptation Options	Initial estimate of costs[1]	Justification for adaptation finance
Floods	**Output 1:** Prepare an inventory with substitute T&D equipment to ensure quick recovery of power supply in case of disaster Use underground cables in flood-prone areas and use materials such as cross-linked polyethylene (XLPE) cables as they are waterproof Avoid construction of power lines near dikes Ensure pile foundation for the transmission towers in flood prone areas **Output 2:** Design and construct flood protection measures such as high retaining walls to keep the equipment that is mounted at ground level in substations safe Increase the plinth height of the substation as well as the equipment installed in the substation **Output 1 & 2:** Expand hydrological monitoring to identify level of risk and develop an early warning system Develop contingency funds for post disaster rehabilitation and restoration Transmission lines and substation footings should be located above the highest recorded flood levels Increase drainage facilities in both capacity and number	35%	Implementation of these adaptation options would reduce potential infrastructure damage as well as assist the JSC NEGU to forecast climate-induced disasters and better manage the impacts to ensure quick recovery.
Drought and heatwaves	**Output 1:** Construct additional transmission circuits to re-route power in case existing circuit is damaged Selection of more temperature-resilient insulating and conducting material for transmission lines **Output 2:** Install more efficient cooling systems for substations	10%	Design and material modifications can enhance the tolerance of the system to high temperatures. Investments should be directed towards installing cooling systems to prevent the substations from malfunctioning due to excessive heat.

[1] The percentage is assigned in accordance with the level of risk, the type of proposed adaptation activity, and the relative changes estimated in the related climate extreme indices (Table 12).

	<u>Output 1 & 2</u>: Recruit and train staff on fire early response to prevent infrastructure damage Ensure that ICT components and electricity metering systems are certified for higher temperatures		
Dust storms and Erosion	**<u>Output 1</u>:** Consider underground infrastructure for transmission in areas with high wind speed Design more robust transmission towers that can withstand strong winds Reduce the distance between two towers to maintain energy conservation and avoid sag **<u>Output 1 & 2:</u>** Ensure that the area in the proximity of the transmission and substation infrastructure is free of trees to avoid damages caused by uprooting of trees	10%	Effective planning with respect to the location of transmission lines and substations can significantly minimize the exposure of the infrastructure to high-speed winds.
Landslides and mudflows	**<u>Output 1</u>:** Conduct a slope protection study to shift the transmission poles (if need be) Ensure proper drainage from the tower base to prevent the foundation from becoming unstable **<u>Output 2</u>:** Build retaining walls to protect the substation infrastructure	35%	In-depth assessment of parameters such as slope, and drainage can strengthen the stability of the structures.
Wildfire	**<u>Output 1</u>:** Use either underground cables in forested/vegetated areas or ensure the transmission lines are at a safe distance from forested zones where there is a higher likelihood of wildfires **<u>Output 2</u>:** Ensure the area is clear of trees and vegetation to minimize the risk of wildfires reaching the substation infrastructure **<u>Output 1 & 2</u>:** Recruit and train staff on fire early response to prevent infrastructure damage	<10%	No/low cost assuming these adaptations are not implemented, given wildfire risk level is low

All risks	**<u>Output 1 & 2:</u>** Adopt digital solutions and capacity building measures (described in the following section) Expand the meteorological monitoring network to gain a better understanding of variations in climatic conditions and climate-induced disasters	Digital solutions: TBD Installation of 2 automatic weather stations: 20,000 US$	Through a dense hydrometeorological monitoring network, the JSC NEGU can develop a comprehensive database consisting of measurements for different climate variables. These ground observations, in combination with modern tools and technology can enable JSC NEGU to conduct quantitative assessments of climate risks and forecast disasters. Such analyses can lead to the design and implementation of robust adaptation strategies.

The adaptation costs were derived from the mean percentage change calculated over three time-horizons and two emission scenarios for all project locations (Table 16). The weightage was assigned based on expert judgement as the impact of a higher percentage change in temperature is more severe than change in precipitation. Therefore, taking into account both the percentage change as well as the weightage, the relative contribution was determined for events related to extreme temperatures and precipitation, respectively.

Table 16. Relative share of the adaptation costs based on climate risks' assessment.

Region	Rx1day	Rx5day	CDD	TXX
Related hazard	*Floods, landslides, erosion, mudflows*		*Droughts, dust storms, wildfire*	
FerAnd	48,3	28,1	11,4	6,6
BuSaKa	61,5	43,1	0,6	6,5
Navoi	73,6	59	0,9	6,5
Surkha	45,6	20,9	1,8	7,4
Tasken	61,2	31,5	2,9	6,5
Average (% change)	47,28		5,11	
Weightage	0,2		0,8	
Relative contribution (%)	70%		30%	

The relative contribution was then equally divided among the related climate hazards (Table 17). The proposed adaptation budget, based on relative investment costs, was distributed accordingly.

Table 17. Budget division as per weightage of each climate hazard.

Hazards	Weightage	Component	Budget in millions
Floods	0,35	Output 1	10,5
		Output 2	10,5
Droughts and heat wave	0,10	Output 1	3,0
		Output 2	3,0
Dust storms and erosion	0,10	Output 1	3,0
		Output 2	3,0

Landslide and mudflows	0,35	Output 1	10,5
		Output 2	10,5
Wildfire	0,10	Output 1	3,0
		Output 2	3,0

**Output 1: Transmission lines efficiency, Output 2: Improvement in substations*

In addition to considering the relative percentage contribution, the adaptation costs were also in line with previously established accounts[1] where design and infrastructure made up 70% of the costs and capacity building activities amounted to 10%. The remaining 20% i.e. (12 million of the 60 million budget) was dedicated for the use and adoption of modern tools and technologies.

6.2 Digital solutions

In addition to the adaptation options above, supervisory control and data acquisition (SCADA) system should be installed in the substations to avoid regional blackouts. Such digital protection relays improve the transmission operation reliability. In particular, SCADA enables the operation dispatch center to gain remote access to real-time data and historical data. Therefore, the use of modern tools would allow JSC NEGU to effectively manage critical situations and support the contribution of renewable energy to the national grid.

Moreover, as per United Nations Office for Disaster Risk Reduction (UNDRR) early warning system (EWS) is an integrated part of hazard monitoring forecasting, prediction, assessment, and communication (Meechaiya et al., 2019). Dissemination and communication of flood risk, landslide and dust storms information and early warnings to the operators and managers of JSC NEGU could help in improved risk management and adaptation.

6.3 Capacity building measures

Adaptation measures are not limited to engineering interventions but also include capacity building. Output 3 and 4 of the project focus on establishing a risk management unit and enhancing JSC NEGU's project management expertise, respectively. A designated risk management unit will enable JSC NEGU to effectively analyse and manage climate risks. The unit can also be responsible for the timely implementation of the abovementioned adaptation options to minimize the electric system's vulnerability. Without a specialized institution and a well-defined strategy, implementation of adaptation measures becomes a challenge. Additionally, through improved project management skills, JSC NEGU can increase the scope, impact, and reach of their activities. Capacity building should enable JSC NEGU's staff to analyze climate data, forecast disasters such as floods, explore more climate resilient materials for substation and transmission operations, and design mitigation and adaptation plans accordingly.

It is equally important for the JSC NEGU staff to track the reliability of the electric grid through indices such as System Average Interruption Duration Index (SAIDI) and System Average Interruption Frequency Index (SAIFI)[2]. Through this, JSC NEGU can measure its performance and identify areas for improvement.

6.4 Strengthening meteorological monitoring capacity

A universal methodology for sensor network design is not available and this is mainly attributed to the diversity of cases, criteria, assumptions, and limitations. The scale of the processes to be monitored and

[1] UZB: Northwest Region Power Transmission Line project - Technical Due Diligence Report, March 2015, Asian Development Bank.
[2] https://www.ensto.com/company/newsroom/articles/saidi-and-saifi-indices-guiding-towards-more-reliable-distribution-network/

the objectives to be addressed drive the design of meteorological sensors (Chacon-Hurtado et al., 2017). According to the information available for this study, which taken from the website of the Uzbekistan Hydrometeorological Service[1], the existing meteorological monitoring network consists of one weather station per province, as shown in Figure 30. The density of meteorological sensors in Uzbekistan is about 32,000 Km^2 per station. This number is significantly higher compared to the WMO recommendation as shown in Table 18. Almost 21% (96000 Km^2) of the area of Uzbekistan is covered by the mountains. This number suggests almost 38 stations (based on recording type precipitation stations in Table 18) in the mountain and 61 stations in the interior plain regions of Uzbekistan.

Table 18. Recommended minimum densities of stations (area in km^2 per station) as per WMO[2].

Physiographic unit	*Precipitation*		*Evaporation*	*Streamflow*	*Sediments*	*Water quality*
	Non-recording	*Recording*				
Coastal	900	9000	50000	2750	18300	55000
Mountains	250	2500	50000	1000	6700	20000
Interior plains	575	5750	5000	1875	12500	37500
Hilly/undulating	575	5750	50000	1875	12500	47500
Small islands	25	250	50000	300	2000	6000
Urban areas	–	10–20	–	–	–	–
Polar/arid	10000	100000	100000	20000	200000	200000

Figure 30. Meteorological monitoring network of Uzbekistan (Source: Uzhydromet).

Given the topographic variation in Uzbekistan, shown in Figure 31, the existing network does not spatially capture the local weather and climatic conditions adequately. The elevation reaches up to 4,400 meters in northeastern and southeastern provinces, namely Tashkent, Namangan, Surkhdarya and Kashkadarya. The location of the stations in these provinces does not account for weather conditions in the mountainous regions which makes glacial/snow monitoring a challenge. This is crucial to analyse trends and forecast risks relevant to the energy transmission project, especially to monitor temperature and better anticipate heatwaves. Also, extreme rainfall leading to flood risk to the project can be monitored better with a denser network around the project infrastructure. Therefore, it is strongly

[1] https://hydromet.uz/
[2] Guide to Hydrological Practices, Volume I: Hydrology – From Measurement to Hydrological Information,WMO

recommended to install additional hydrometeorological stations in the mountainous regions of these provinces.

Moreover, with respect to historic trends, climate projections and the areal extents of the provinces, the coverage of the existing hydrometeorological monitoring network is considered sparse. As summarized in Table 12, the average percentage change in climate extremes compared to historic extremes is quite significant. Therefore, the density of the network needs to be increased to better monitor the climatic variations and enhance climate preparedness of the vulnerable regions.

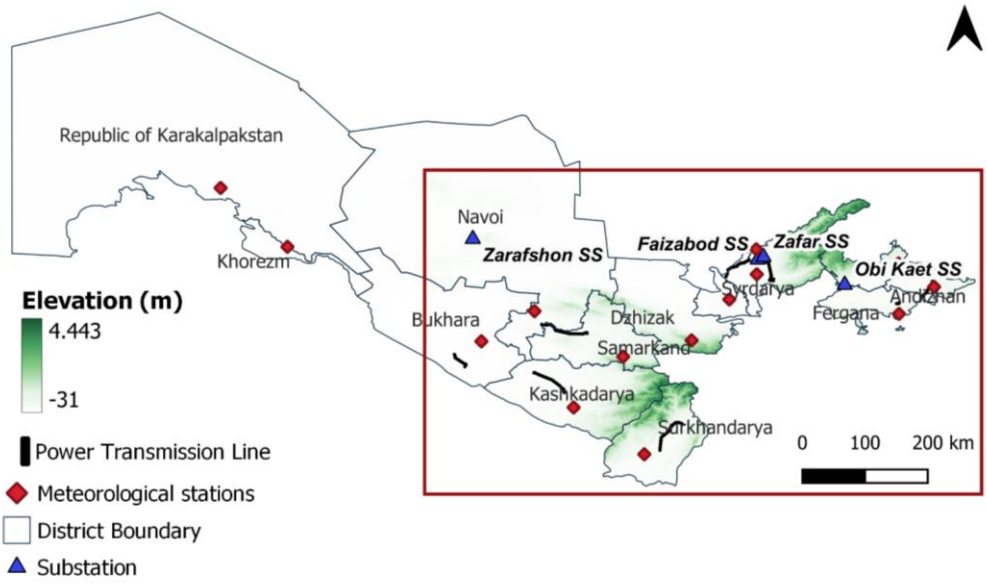

Figure 31. Location of meteorological stations with respect to transmission lines and substations.

As shown in Table 19, the largest distance identified between a substation and the nearest meteorological station is approximately 167.5 kilometers in Navoi. Assessing climate risks as well as forecasting climate-induced disasters can become a challenge when the monitoring network is limited. Similarly, adaptation options for increasing the climate resilience of project infrastructure can only be effective when the climate risk assessment is data driven. Through a larger number of hydrometeorological stations, more ground observations can enhance the reliability and accuracy of such analyses.

Table 19. Shortest approximate distance to the nearest meteorological station.

Project components	Type of infrastructure	Shortest distance (km)
L_Yu_L_MM (Andizhan)	Transmission line	6.0
L-7-F-1 (Fergana)	Transmission line	20.7
Obi Kaet (Namangan)	Sub-station	91.0
L_D_W (Surkhandarya)	Transmission line	25.5
L-Hamza (Bukhara)	Transmission line	50.3
L-H-K (Samarkand)	Transmission line	71.7
L-32-K (Kashkadarya)	Transmission line	63.8
L-32-M (Kashkadarya)	Transmission line	89.3

L_K_K_MM (Kashkadarya)	Transmission line	31.6
L-A-F (Tashkent)	Transmission line	20.3
L_Kc_A_MM (Tashkent)	Transmission line	29.8
L-19-D (Tashkent)	Transmission line	24.0
L-19-23 (Tashkent)	Transmission line	29.4
L-22-23 (Tashkent)	Transmission line	33.8
L-F-CH (Tashkent)	Transmission line	45.8
Zafar (Tashkent)	Sub-station	18.8
Faizabod (Tashkent)	Sub-station	20.3
Zarafshon (Navoi)	Sub-station	167.5

More generally, beyond this specific project, the map showing the population density by province (Figure 32) also indicates that majority of the population is concentrated in eastern parts of Uzbekistan, starting from the province of Bukhara. This means that the large population in these areas is vulnerable to risks associated with high elevation such as landslides and floods. Thus, for improved climate-induced disaster mitigation and preparedness, improved surveillance is required in this region.

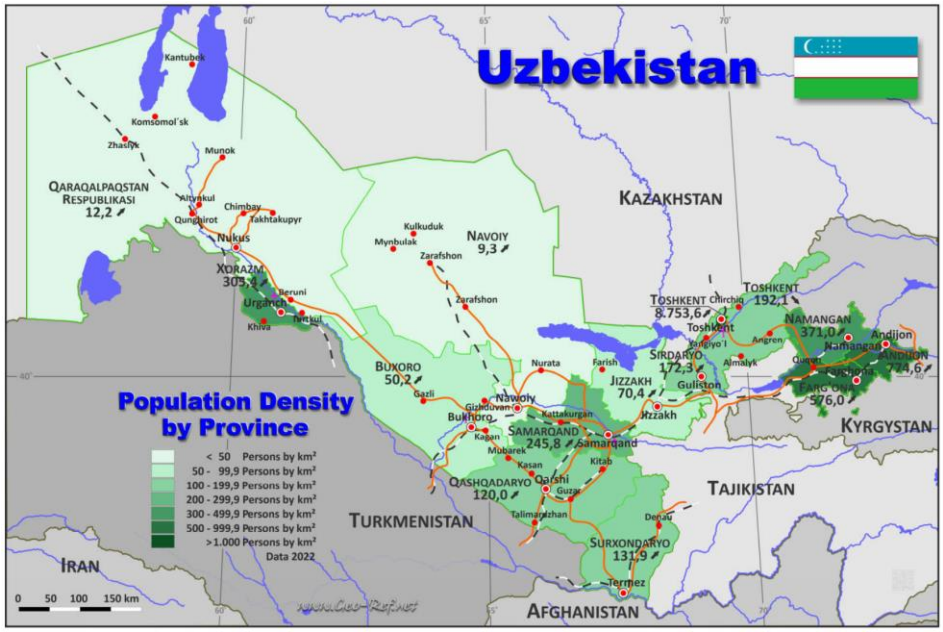

Figure 32. Population density by province (Source: Geo-ref.net).

7 Climate Mitigation

This CRA focuses on climate change risks to the projects and possible adaptation measures to be included in the project to respond and reduce those risks to an acceptable level. Projects however may also have the potential to contribute to climate mitigation, i.e. have a positive impact through the reduction of greenhouse gas (GHG) emissions. Due to increasing annual emission rates of carbon dioxide and methane (Smith et al., 2015), global temperature is rising rapidly, but even more in some areas of the world, as also in Uzbekistan. Since the early 1950s, the average rate of increase in air temperature in Uzbekistan has been 0.29°C for every ten years[1], which is twice the rate of global warming.

Despite being relatively minimal contributors to the overall greenhouse gas emissions, developing countries can have a crucial role to play in order to limit their emissions. As per Uzbekistan's revised Nationally Determined Contribution (NDC, 2021), the country has committed to reducing its specific greenhouse gas emissions per unit of GDP by 35% (compared to the level in 2010), by the year 2030. The previously intended goal was set at 10%. This means that Uzbekistan must accelerate its efforts on multiple fronts in order to fulfil its commitment. Higher energy efficiency and a diverse energy mix are essential to significantly reduce GHG emissions as this sector currently accounts for approximately 76% of the national GHG emissions[2] (Figure 33).

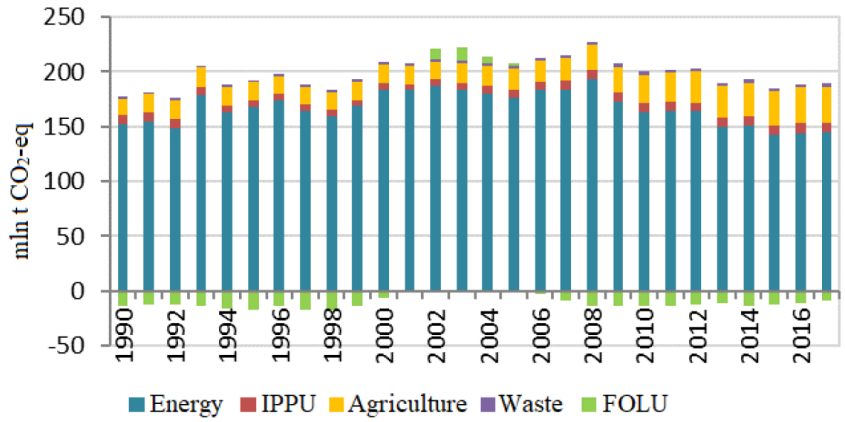

Figure 33. Dynamics of greenhouse gas emissions for 1990-2017 by sectors (Source: Updated NDC, 2021).

Uzbekistan is one of the world's largest producers of natural gas, annually producing approximately 60 billion cubic metres[3]. As shown in Table 15, extraction, processing, transportation of natural gas accounts for 22.6 percent of the total GHG emissions, followed by combustion of fuels for power generation (15.2 percent). Compared to 2010, the percentage of GHGs emitted from the fuel combustion for power generation increased by almost 2 percent in 2017 despite the pledge to cut down emissions. An aging power transmission system means higher transmission and distribution losses which leads to increased combustion of fuels to meet the swelling energy demands.

[1] Updated Nationally Determined Contribution, 2021. https://unfccc.int/sites/default/files/NDC/202206/Uzbekistan_Updated%20NDC_2021_EN.pdf
[2] Nationally Determined Contribution, 2017.
[3] https://www.iea.org/reports/uzbekistan-energy-profile

Table 20. Greenhouse gas emissions and removals in 2010-2017 (Source: Updated NDC, 2021).

Sector	IPCC category	2010 GHG emissions / removals (Gg of CO_2-eq)	Share of the source in the total emission, %	2017 GHG emissions / removals (Gg of CO_2-eq)	Share of the source in the total emission, %
		A	B	C	D
Energy	Extraction, processing, transportation of natural gas	63,783.31	27.1	47,370.58	22.6
	Fuel combustion. Residential sector	32,170.63	13.7	19,627.03	9.4
	Fuel combustion. Power generation	31,611.01	13.4	31,933.28	15.2
	Fuel combustion. Commercial sector	10,519.01	4.5	6,113.32	2.9
	Fuel combustion. Processing industry and construction	7,580.12	3.2	21,214.68	10.1
	Road transport	7,465.28	3.2	11,900.08	5.7
	Other means of transport	5,375.21	2.3	3,781.49	1.8
	Oil production and refining	2,732.12	1.2	1,872.12	1.7
	Fuel combustion. Agriculture	1,435.73	0.6	54.72	0.0
	Railway transport	498.63	0.2	354.26	0.2
	Solid fuels	109.24	<0.1	127.66	0.1
	Civil aviation	100.62	<0.1	58.46	<0.1
	Total for sector	**163,380.91**		**144,407.83**	

Therefore, it is critical to not only upgrade the existing infrastructure to minimize losses but also diversify the energy mix and promote the development of renewable energy to sustainably meet the growing demands. The updated NDC (2021) recognizes the importance of structural reforms and prioritizes energy efficiency measures and expansion of renewable energy sources. However, such development agendas require investment. As part of this project, ADB has agreed to fund the implementation of climate mitigation and adaptation measures. To secure climate financing, it is important to provide an estimate of the GHG emission reduction attributable to the proposed project interventions. Therefore, ADB has developed two harmonized guidance documents on GHG accounting: one for energy efficient projects and another for renewable energy projects (ADB, 2017).

7.1 Methods

The GHG emission is calculated as per the methodology outlined in the guidelines for *Energy Efficiency Projects (Improvement of Existing Electricity Transmission and Distribution System)*[1] specifically. This methodology is applicable for projects that aim to reduce electricity losses by improving the existing transmission system by either reconductoring, controlling power flow, optimizing transformer locations etc. The key components are:

Emission Reduction (*ER*)

Emission reduction is the difference between baseline and project emissions when the T&D system delivers the same amount of electrical power or energy.

$ER = BE - PE$

where:
BE = baseline emission
PE = project emission

Baseline Emission (*BE*)

[1] Guidelines for Estimating Greenhouse Gas Emissions of ADB project, April 2017. http://dx.doi.org/10.22617/TIM178659-2

BE is the amount of emissions generated by the existing T&D when delivering the same amount of electricity as the project.

BEe = ECb × EFgrid/(1-%Lb)

where:
BEe = Baseline emission for the T&D system, tCO_2/year
ECb = annual electricity delivered by the existing T&D system, MWh/year
%Lb = baseline T&D losses expressed as decimal equivalent (i.e. 20% loss is expressed as 0.20)
EFgrid = combined emission factor for the grid, tCO_2/MWh

Project emission (*PE*)
Project emission is the amount of emissions generated by the project activity.

PEe = ECp × EFgrid/(1-%Lp)

where:
PEe = Project emission from the project activity, tCO_2/year
ECp = annual electricity delivered by the project activity, MWh/year;
%*Lp* = project T&D losses expressed as decimal equivalent (i.e. 20% loss is expressed as 0.20)
EFgrid = combined emission factor for the grid, tCO_2/MWh

7.2 Results

The GHG emission reductions were calculated for two project interventions:

7.2.1 Intervention A: Efficiency of transmission lines is improved by 0.5%

Baseline T&D Efficiency: 83.28% (%*Lb* = 0.1672)

Assumptions:

- Desired T&D Efficiency: 83.78% (%*Lp* = 0.1622)
- Electricity Generated (*ECb*) and carried by the 12 transmission lines: 15,820,546 MWh/yr[1]
- Baseline grid emission factor (*EFgrid*): 0.533 tCO_2/MWh (For Uzbekistan based on Append C of ADB, (2017) report)

Table 21. Carbon emission calculation for Intervention A.

Emission	Equation	Value	Units
Baseline Emission (BE)	*BEe = ECb × EFgrid/(1-%Lb)*	10,125,301	tCO_2/yr
Project Emission (PE)	*PEe = ECp × EFgrid/(1-%Lp)*	10,064,873	tCO_2/yr
Emission Reduction (ER)	*BE - PE*	60,428	tCO_2/yr

The above emission reduction is calculated based on several assumptions. The foremost being the target efficiency of the transmission lines. Currently, it is reported that the transmission and distribution lines suffer from 16.72% losses, with the transmission losses amounting to 2.72%. Therefore, the target

[1] Information received by Transmission Expert at ADB

efficiency of the transmission lines in this case is assumed to increase by 0.5%, leading to only 2.22% losses through the transmission lines and an overall efficiency of the T&D system to be 83.78%. Next, the amount of power that is being supplied through these transmission lines annually is assumed to be 15,820,546 MWh[1].

As per these assumptions and methodology, an increase of 0.5% in transmission efficiency will result in the reduction of 60,428 tCO_2 per year.

7.2.2 Intervention B: Power demands of the substations' auxiliary services are partially met by solar power

Assumptions:

- Power demand for auxiliary services per substation: 50,000 kWh/month[1]
- Power generated by 100 kW solar panels at a substation: 16,000 kWh/month
- Solar power contribution: 32%
- Power plant contribution: 68% (0.68)
- Annual Electricity Generation (EG) by fossil fuels for entirely (100%) fulfilling the substations' auxiliary services' power demands: 2,400 MWh
- Annual Electricity Generation (EG) by fossil fuels for partially (68%) fulfilling the substations' auxiliary services' power demands: 1,632 MWh
- For RE projects, PE is considered zero (Eq. 26 of ADB (2017) report)
- Baseline grid emission factor (EFgrid): 0.533 tCO_2/MWh (For Uzbekistan based on Append C of ADB, (2017) report)

Table 22. Carbon emission calculation for Intervention B.

Emission	Equation	Value	Units
Baseline Emission (BE) – 100% provision	*BE = EG × EFgrid*	1,279	tCO_2/yr
Baseline Emission (BE) – 68% provision	*BE = EG x EFgrid*	870	tCO_2/yr
Emission Reduction (ER)	*BE - PE*	409	tCO_2/yr

To estimate reduction in GHG emissions for the second project intervention, which aims to fulfil the power demand of the auxiliary services by solar energy, the demand per substation is assumed to be 50,000 kWh per month i.e. 600 MWh per year. Of this demand, it is assumed that 30% will be met by the solar panels fitted on the roofs while the rest (70%) will be delivered by the electric grid powered by thermal power plants. This 30% was based on the assumption that 285 solar panels are required to generate 100 kWp, and depending on the location of the substation, they will produce around 16,000 kWh per month on average. Therefore, electricity generation by fossil fuels for meeting the demands of the four substations is calculated to be 1,632 MWh per year.

Based on this, the reduction in GHG emissions is estimated as 409 tCO_2/yr. It is important to highlight that this estimate is derived from a number of assumptions since the exact power demand of the auxiliary services is unknown. The power demand may vary per substation. Moreover, the reduction would be higher if the entire demand is fully supplied by solar power – making this a conservative estimate in that case.

[1] Information received by consultation with the 'Transmission Expert' at ADB

In addition, the project also aims to promote the use of alternatives for sulfur-hexflouride (SF6) in gas-insulated switchgear substations as SF6 has a global warming potential of 23,900 – the highest noted by the Intergovernmental Panel on Climate Change. Certain climate extreme events which lead to increased levels of humidity and corrosion can enhance the risk of SF6 leakages. On average, the SF6 capacity for a 500kV substation circuit breaker is 49.6 kg (Acton, 2020). The substations subject to upgradation under this project are 220 kV which means the SF6 capacity is approximately 21.8 kg per substation. This is equivalent to 2,086 tCO_2 for all four substations. Therefore, the use of SF6-free switchgear and circuit breakers will significantly reduce the potential GHG emissions which are presently estimated at 2,086 tCO_2 and support the country in its efforts towards achieving its greener economy development agenda.

7.3 Summary table

Mitigation Activity	**Estimated GHG Emissions Reduction** (tCO_2e/year)	**Estimated Mitigation Costs** ($ million)	**Mitigation Finance Justification**
Improved transmission efficiency	60,428	35	By reducing losses through the transmission lines, less fossil-fuelled power needs to be produced, leading to a net emission reduction.
Solar panels installed on substations' rooftops	409	5	Substituting part of the power demand by a renewable power source will lead to emission reductions.
Use of alternatives for sulfur-hexflouride in gas-insulated switchgear substations	2,806	10	Substituting SF6, which has the highest global warming potential, will significantly reduce GHG emissions.

Note: - The estimated mitigation costs require detailed cost estimates of all the project components which are not available at this moment.

Overall, the adaptation costs are estimated at 60 million while mitigation costs are estimated to be 49.4 million[1]. Adaptation includes strengthening the climate resilience of the transmission lines and substations as well as expanding the hydrometeorological network while mitigation efforts are focused on measures that will reduce GHG emissions. These include improving the energy efficiency of the power transmission lines, installing solar panels on the roofs of substations and substituting the use of SF6 in substations. The projected costs for upgrading the 12 transmission lines are estimated as 56.9 million, and 36.5 million for the four substations[2]. Improving the efficiency of the transmission lines and fitting solar panels on substations are identified as mitigation costs.

In line with previously established accounts[3], the mitigation costs were assigned based on the relative investment costs. 70% is allocated for improving transmission efficiency while 20% costs are designated for substituting SF6 in substations. The remaining 10% is assigned for installing solar panels on rooftops of substations. Since the cost of improving the transmission efficiency (56.9 million) exceeds 35 million, the remainder can be met by the project costs (58.4 million) as well as the adaptation cost (60 million).

[1] Concept paper: Proposed Loan - Republic of Uzbekistan: Digitize to Decarbonize – Power Transmission Grid Enhancement Project, October 2022, Asian Development Bank.
[2] Cost estimates shared by ADB expert.
[3] UZB: Northwest Region Power Transmission Line project - Technical Due Diligence Report, March 2015, Asian Development Bank.

8 References

ADB. (2012). *Climate Risk and Adaptation in the Electric Power Sector*. Manila, Philippines.

ADB. (2013). *Guidelines for climate proofing investment in the energy sector*. Manila, Philippines.

ADB. (2014). *Climate Risk Management in ADB projects*. Manila.

ADB. (2016). *Guidelines for Climate Proofing Investment in the Water Sector - Water Supply and Sanitation*. Manila.

Chacon-Hurtado, J. C., Alfonso, L., & Solomatine, D. P. (2017). Rainfall and streamflow sensor network design: A review of applications, classification, and a proposed framework. *Hydrology and Earth System Sciences*, *21*(6), 3071–3091. https://doi.org/10.5194/hess-21-3071-2017

FutureWater. (2020). Draft Final Report for the Detailed Risk and Vulnerability Assessment for preparing ADB's Climate Adaptive Water Resources Management in the Aral Sea Basin Project, (August).

Immerzeel, W.W., Wanders, N., Lutz, A. F., Shea, J. M., & Bierkens, M. F. P. (2015). Reconciling high altitude precipitation with glacier mass balances and runoff. *Hydrology and Earth System Sciences*, *12*, 4755–4784. https://doi.org/10.5194/hessd-12-4755-2015

Immerzeel, W W, Wanders, N., Lutz, A. F., Shea, J. M., & Bierkens, M. F. P. (2015). Reconciling high-altitude precipitation in the upper Indus basin with glacier mass balances and runoff. *Hydrology and Earth System Sciences*, *19*(11), 4673–4687. https://doi.org/10.5194/hess-19-4673-2015

Immerzeel, Walter Willem, Pellicciotti, F., & Shrestha, A. B. (2012). Glaciers as a Proxy to Quantify the Spatial Distribution of Precipitation in the Hunza Basin. *Mountain Research and Development*, *32*(1), 30–38. https://doi.org/10.1659/MRD-JOURNAL-D-11-00097.1

Khanal, S., Lutz, A. F., Kraaijenbrink, P. D. A., van den Hurk, B., Yao, T., & Immerzeel, W. W. (2021). Variable 21st Century Climate Change Response for Rivers in High Mountain Asia at Seasonal to Decadal Time Scales. *Water Resources Research*, *57*(5), e2020WR029266. https://doi.org/10.1029/2020wr029266

Lange, S., Volkholz, J., Geiger, T., Zhao, F., Vega, I., Veldkamp, T., et al. (2020). Projecting Exposure to Extreme Climate Impact Events Across Six Event Categories and Three Spatial Scales. *Earth's Future*, *8*(12), 1–22. https://doi.org/10.1029/2020EF001616

Mamadjanova, G., & Leckebusch, G. C. (2022). Assessment of mudflow risk in Uzbekistan using CMIP5 models. *Weather and Climate Extremes*, *35*(March), 100403. https://doi.org/10.1016/j.wace.2021.100403

Meechaiya, C., Wilkinson, E., Lovell, E., Brown, S., & Budimir, M. (2019). the Governance of Warning System Opportunities Under Federalism, 48.

Thrasher, B., Wang, W., Michaelis, A., Melton, F., Lee, T., & Nemani, R. (2022). NASA Global Daily Downscaled Projections, CMIP6. *Scientific Data 2022 9:1*, *9*(1), 1–6. https://doi.org/10.1038/s41597-022-01393-4

Ward, P. J., Winsemius, H. C., Kuzma, S., Bierkens, M. F. P., Bouwman, A., Moel, H. DE, et al. (2020). Aqueduct Floods Methodology. *World Resources Institute*, (January), 1–28. Retrieved from www.wri.org/publication/aqueduct-floods-methodology

WB, & ADB. (2020). Climate risk country profile - Uzbekistan, 32. Retrieved from www.worldbank.org

Appendix A: Figure

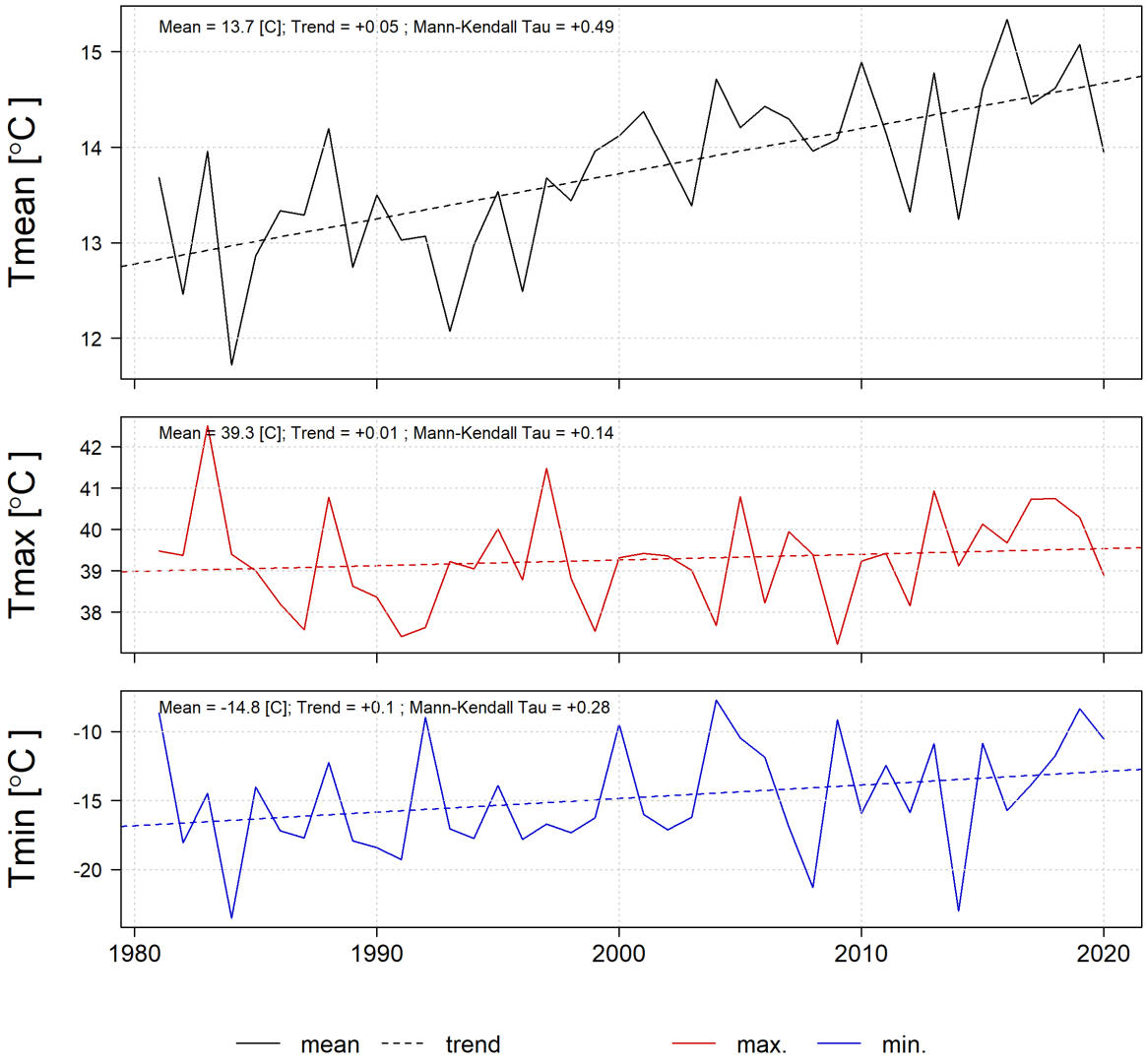

Figure A1: Average, maximum and minimum yearly temperatures from ERA-5 dataset with trendline for box Tasken as shown in Figure 5.

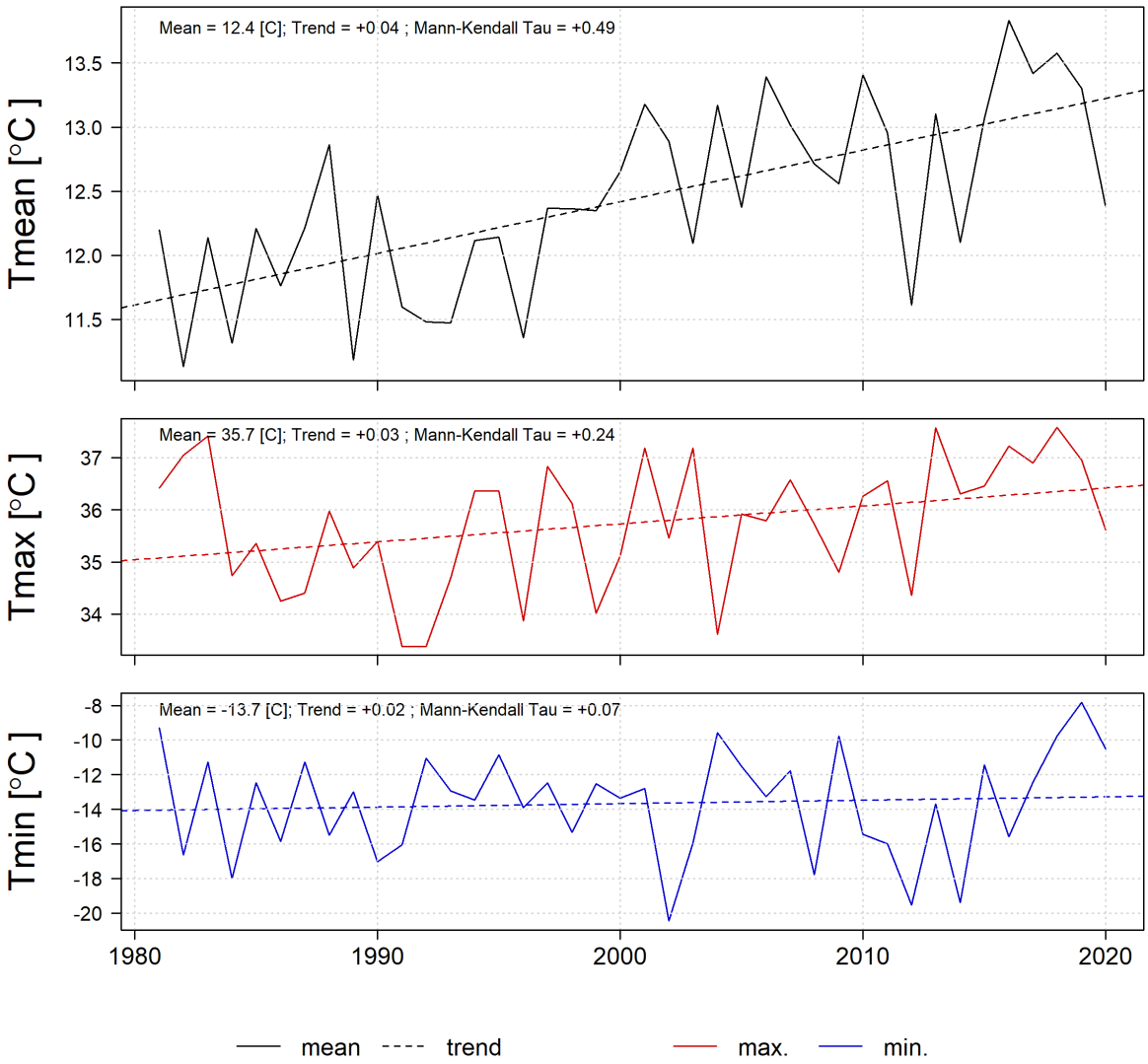

Figure A2: Average, maximum and minimum yearly temperatures from ERA-5 dataset with trendline for box Surkha as shown in Figure 5.

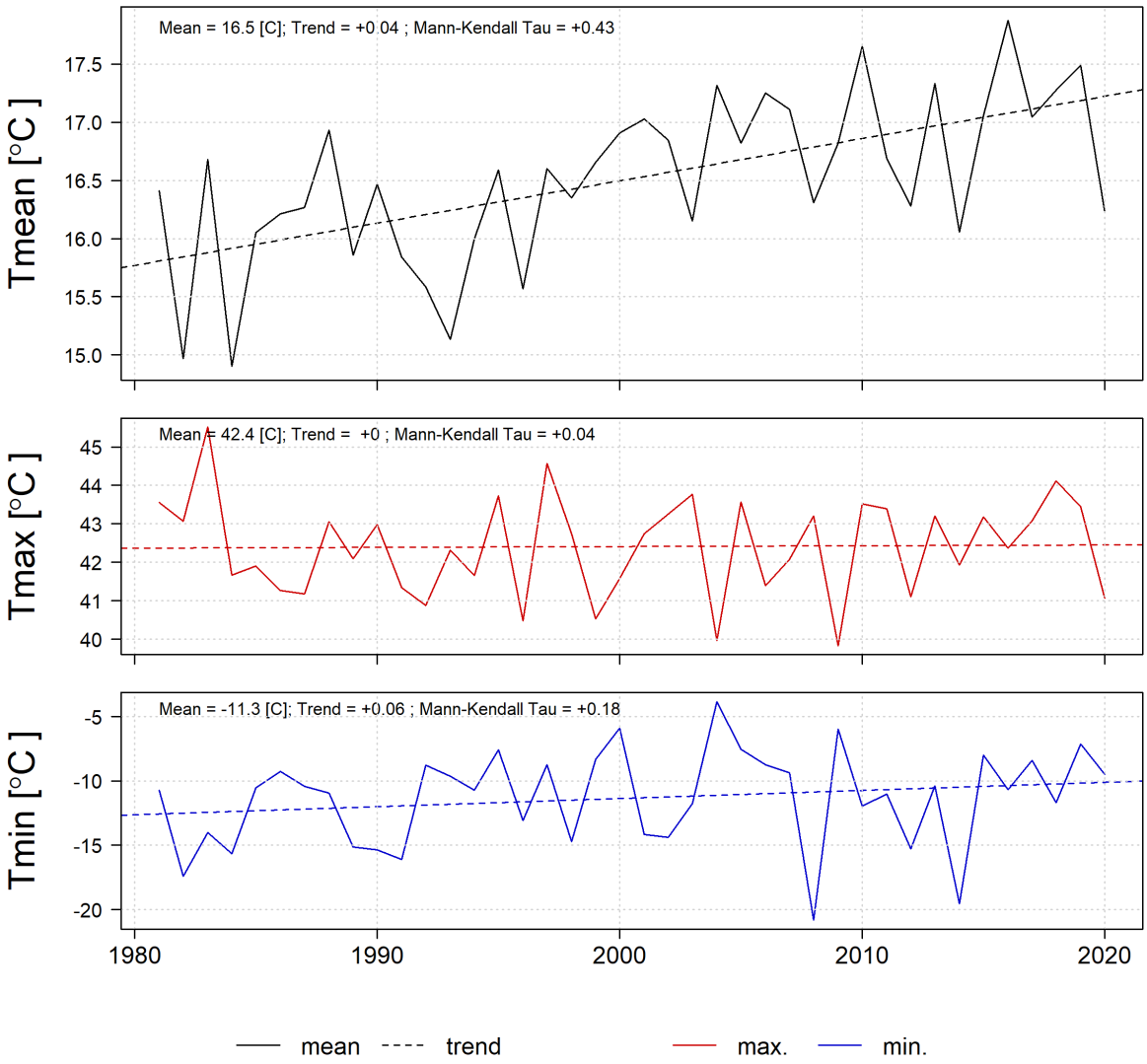

Figure A3: Average, maximum and minimum yearly temperatures from ERA-5 dataset with trendline for box BuSaKa as shown in Figure 5.

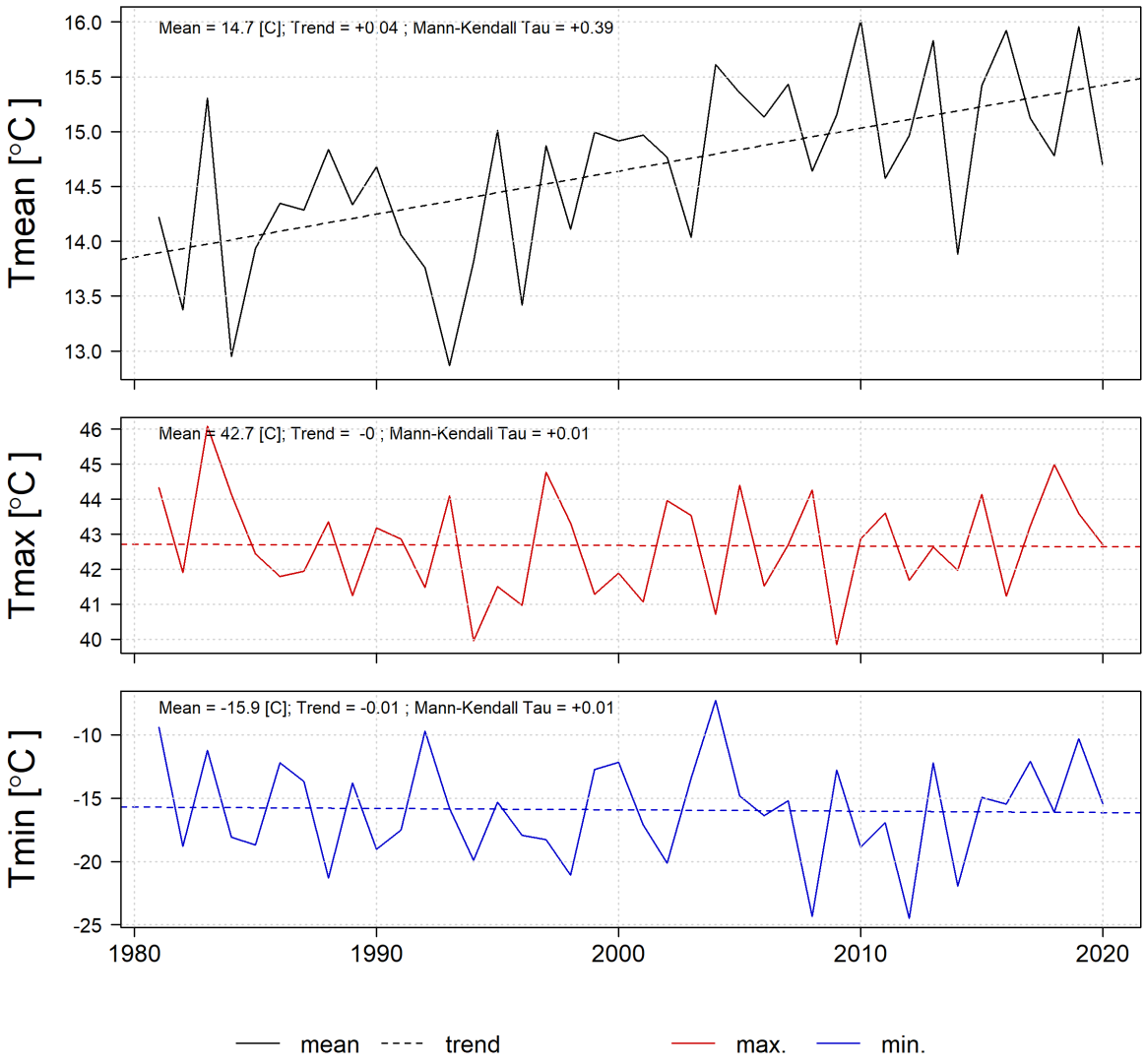

Figure A4: Average, maximum and minimum yearly temperatures from ERA-5 dataset with trendline for box Navoi as shown in Figure 5.

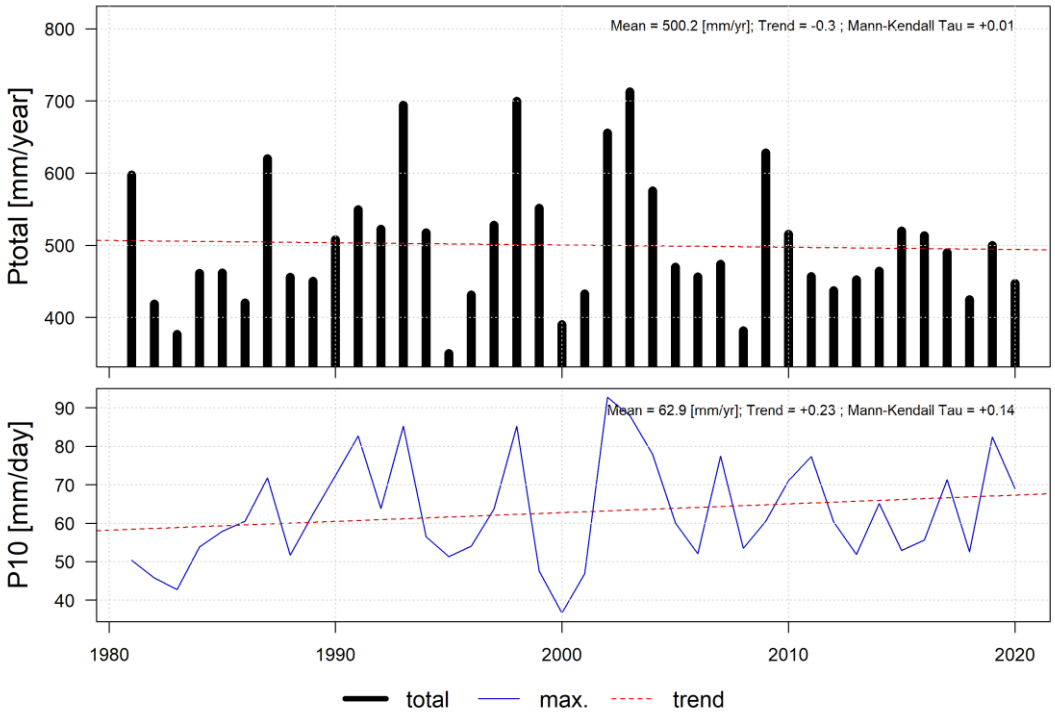

Figure A5: Total yearly and maximum 10-day precipitation with a trendline for box Tasken as shown in Figure 5. Mann Kendall Tau value indicates the strength of the monotonic trend of increase or decrease in a time series, with a value of 1 indicating a strong significant trend and -1 indicating no trend.

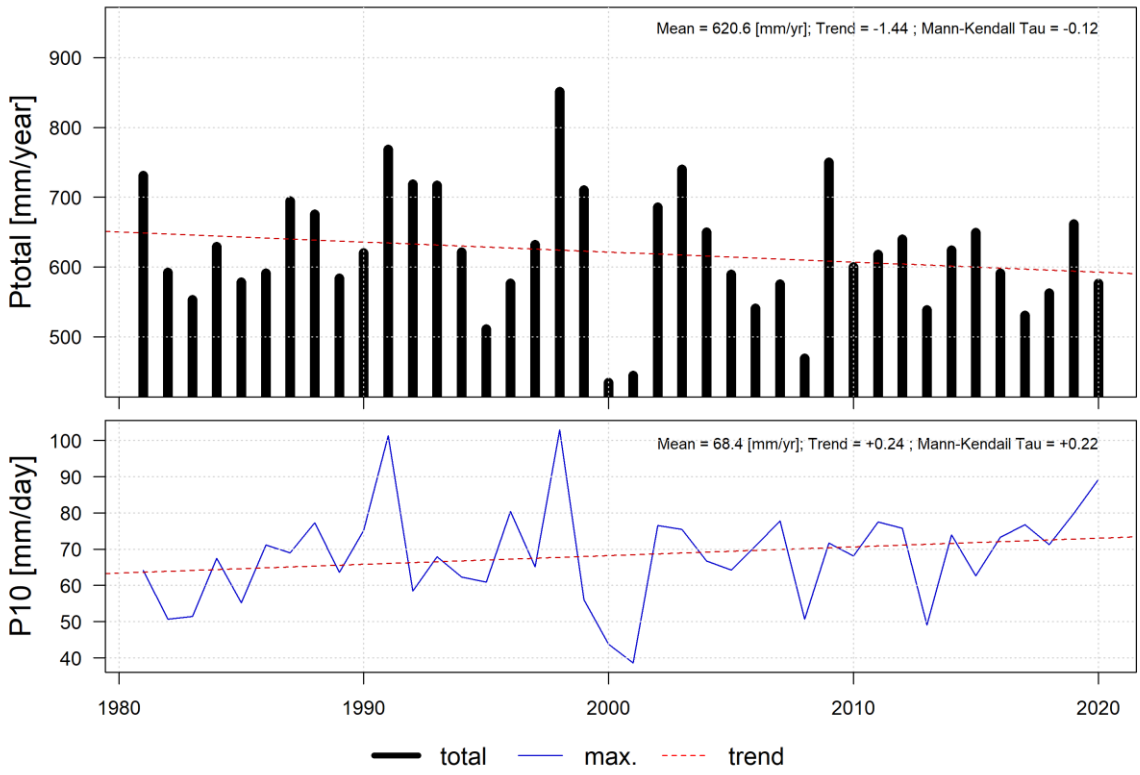

Figure A6: Total yearly and maximum 10-day precipitation with a trendline for box Surkha as shown in Figure 5. Mann Kendall Tau value indicates the strength of the monotonic trend of increase or decrease in a time series, with a value of 1 indicating a strong significant trend and -1 indicating no trend.

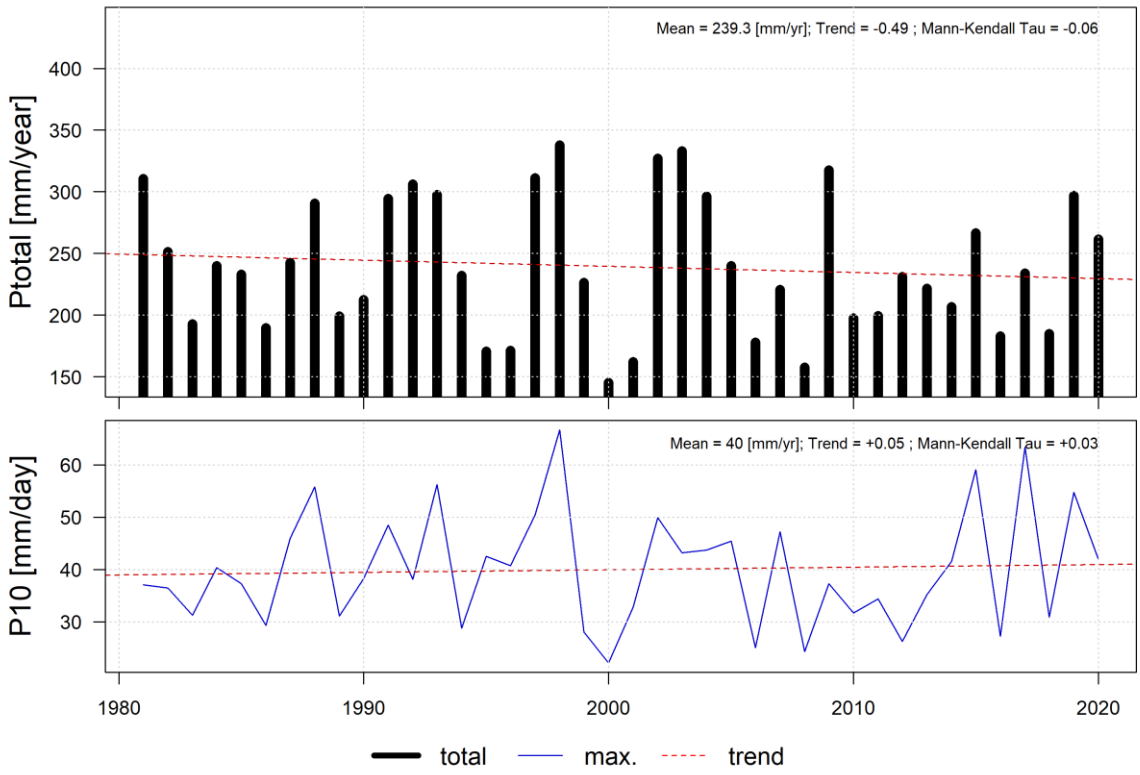

Figure A7: Total yearly and maximum 10-day precipitation with a trendline for box BuSaKa as shown in Figure 5. Mann Kendall Tau value indicates the strength of the monotonic trend of increase or decrease in a time series, with a value of 1 indicating a strong significant trend and -1 indicating no trend.

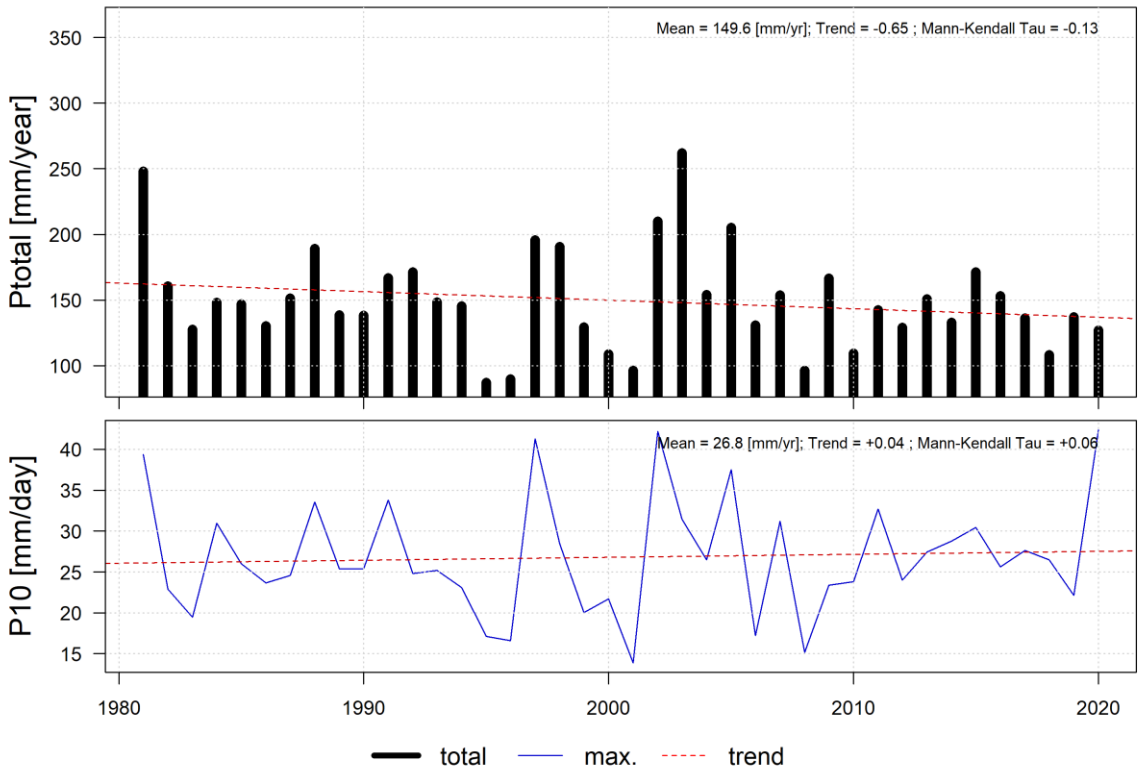

Figure A8: Total yearly and maximum one-day precipitation with a trendline for box Navoi as shown in Figure 5. Mann Kendall Tau value indicates the strength of the monotonic trend of increase or decrease in a time series, with a value of 1 indicating a strong significant trend and -1 indicating no trend.

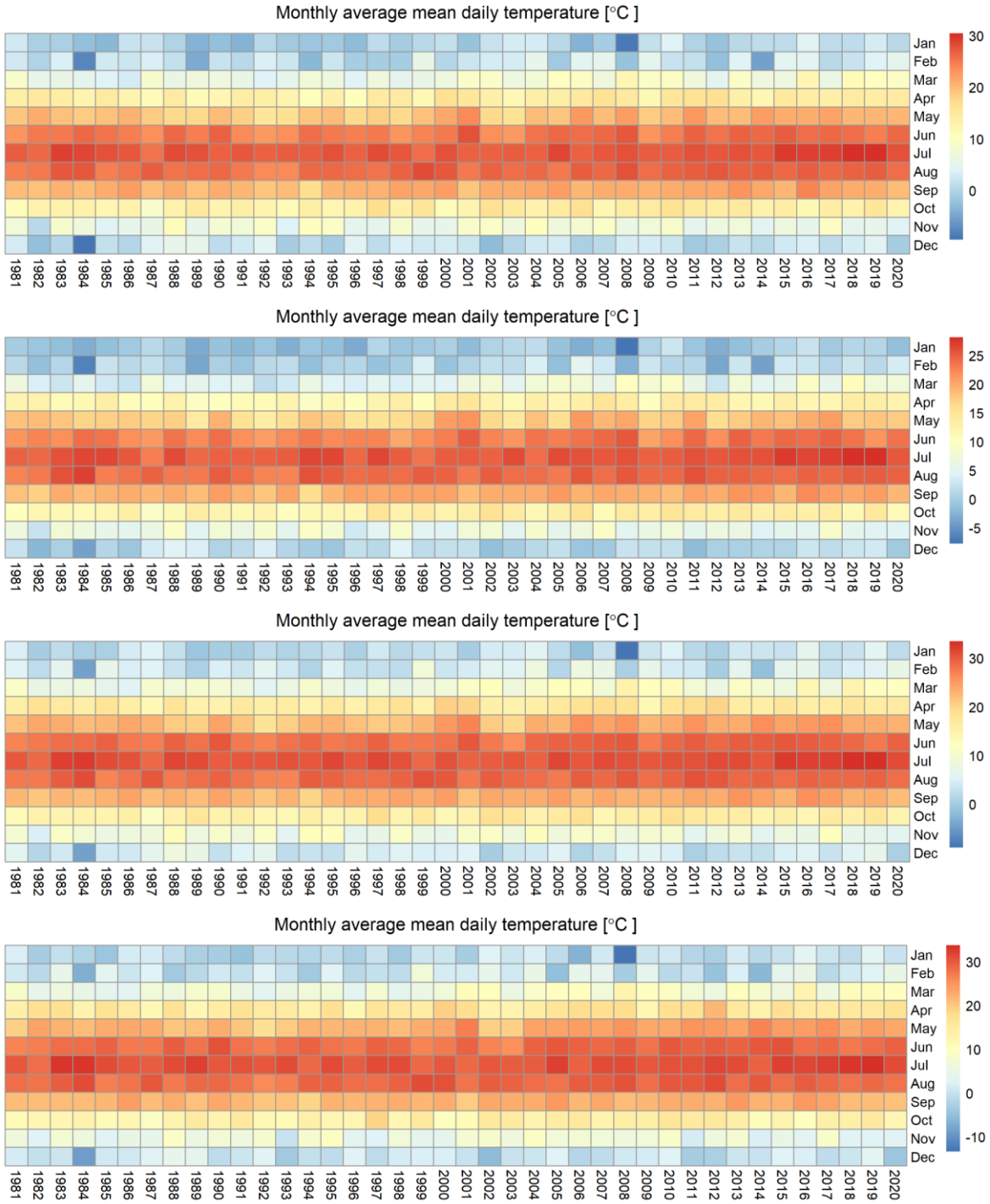

Figure A9: Seasonality in mean temperature from ERA-5 dataset for box Tasken, Surkha, BuSaKa and Navoi as shown in Figure 5.

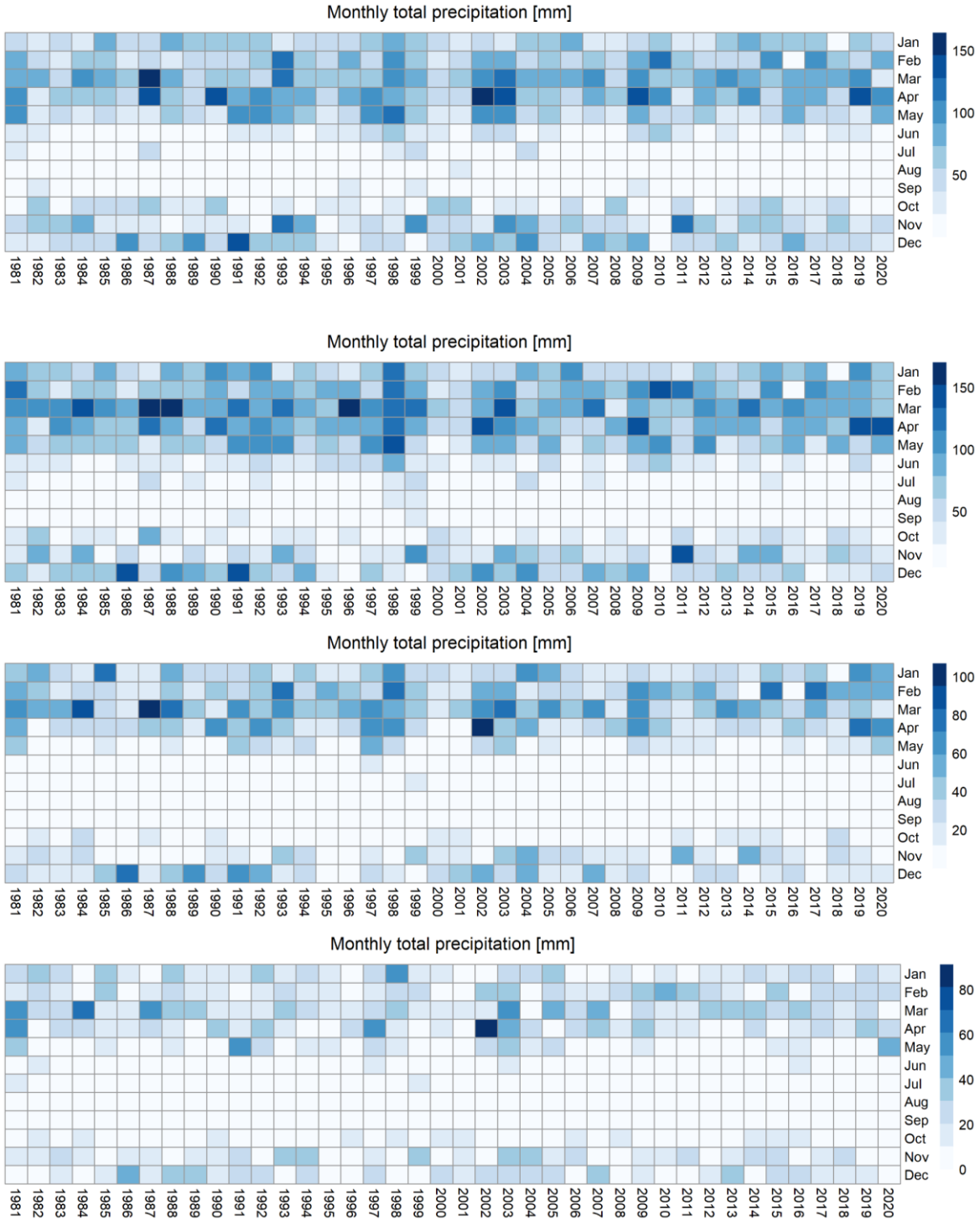

Figure A10: Seasonality in annual precipitation from ERA-5 dataset for box Tasken, Surkha, BuSaKa and Navoi as shown in Figure 5.

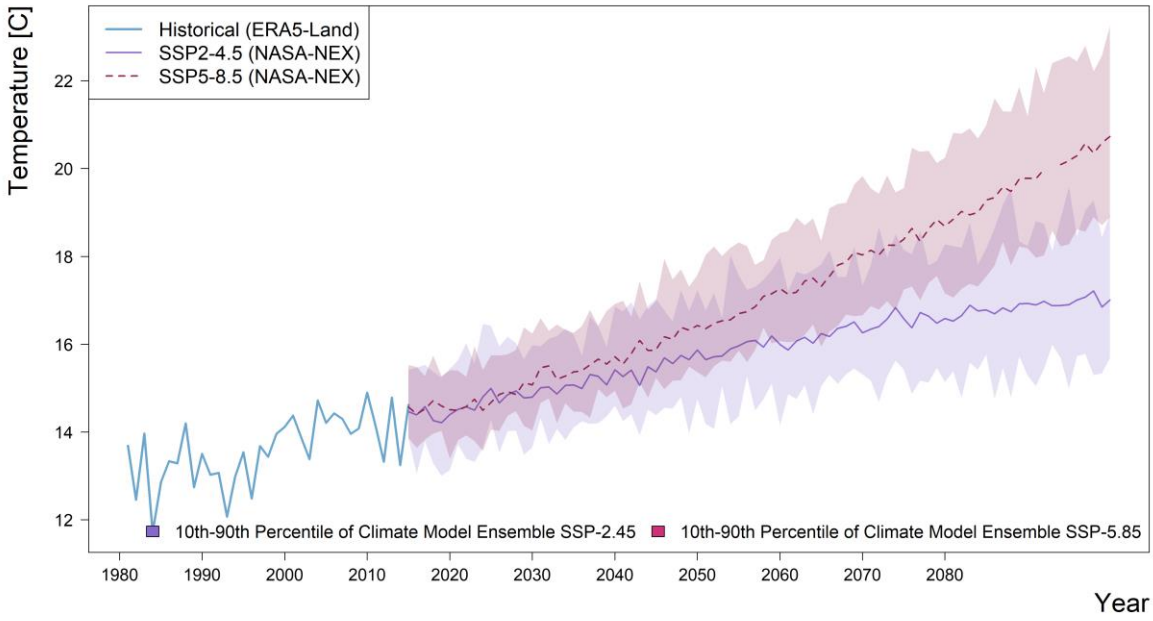

Figure A11: Time series of mean yearly ERA5 temperature for the box Tasken for the historical period (1981-2020), and NASA NEX (per model bias corrected) for the future period. Shaded areas show the 10th and 90th percentiles in the spread of model predictions

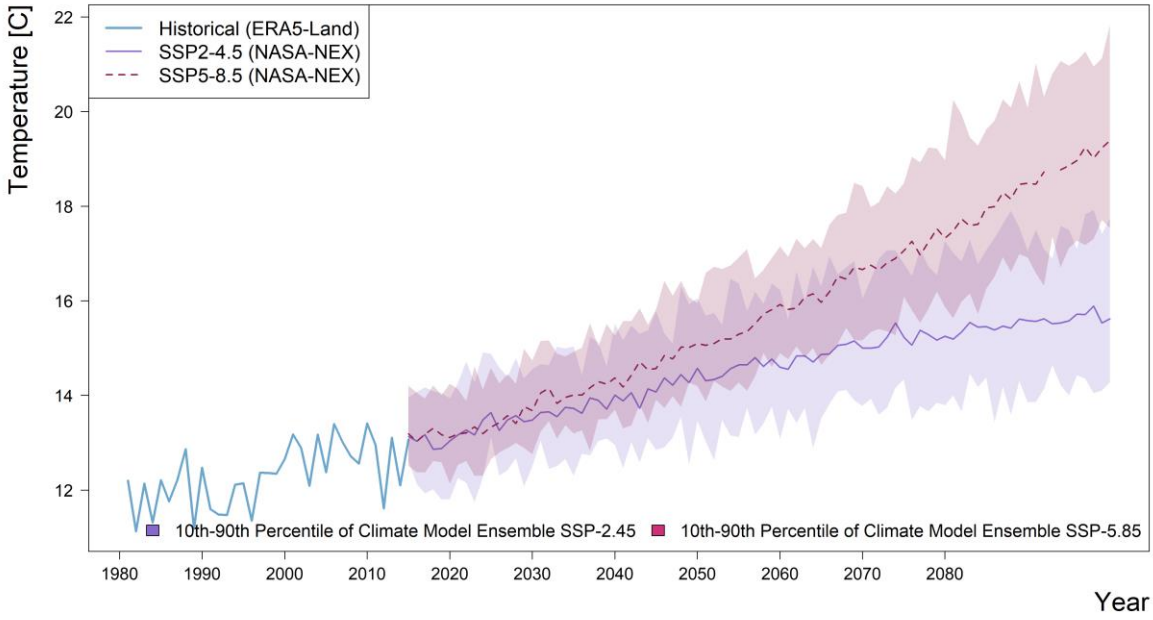

Figure A12: Time series of mean yearly ERA5 temperature for the box Surkha for the historical period (1981-2020), and NASA NEX (per model bias corrected) for the future period. Shaded areas show the 10th and 90th percentiles in the spread of model predictions.

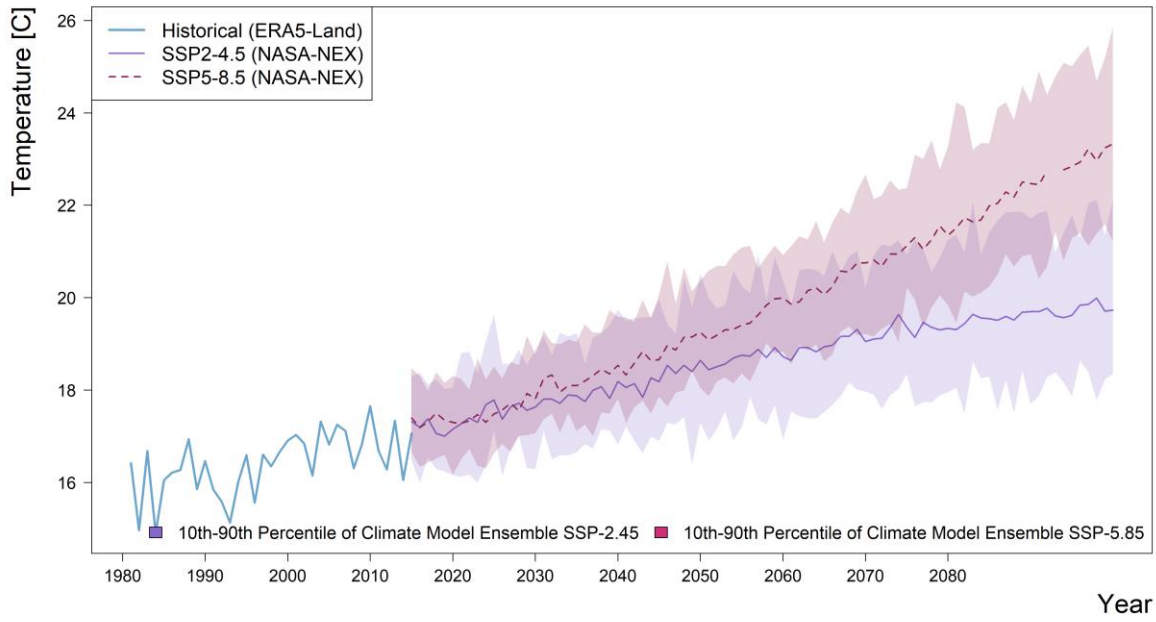

Figure A13: Time series of mean yearly ERA5 temperature for the box BuSaKa for the historical period (1981-2020), and NASA NEX (per model bias corrected) for the future period. Shaded areas show the 10th and 90th percentiles in the spread of model predictions.

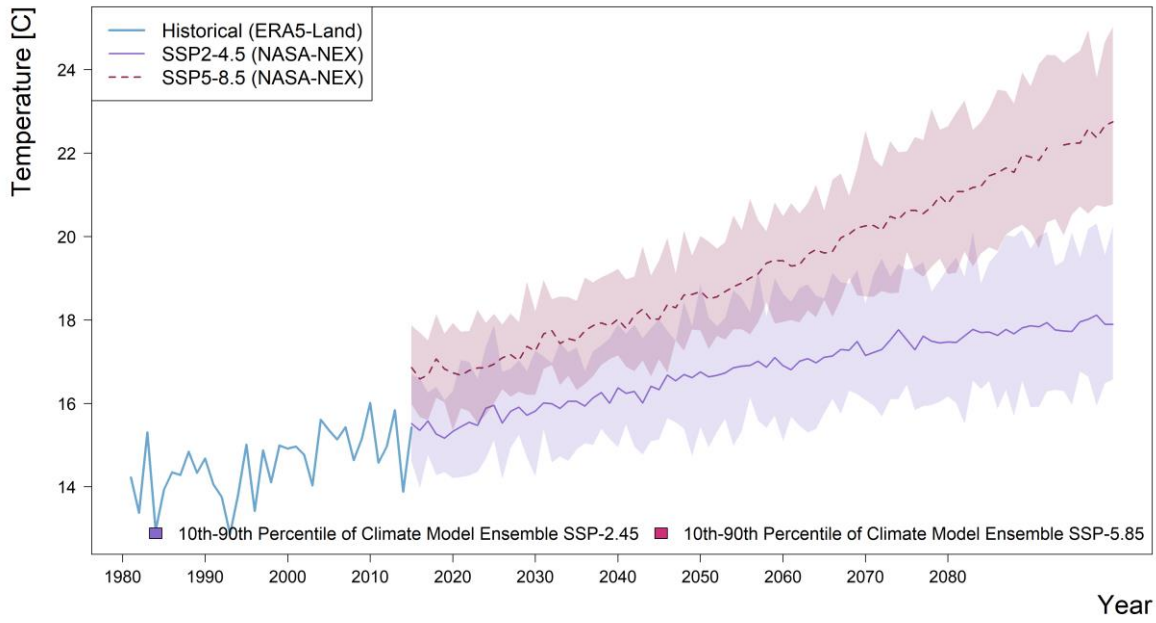

Figure A14: Time series of mean yearly ERA5 temperature for the box Navoi for the historical period (1981-2020), and NASA NEX (per model bias corrected) for the future period. Shaded areas show the 10th and 90th percentiles in the spread of model predictions.

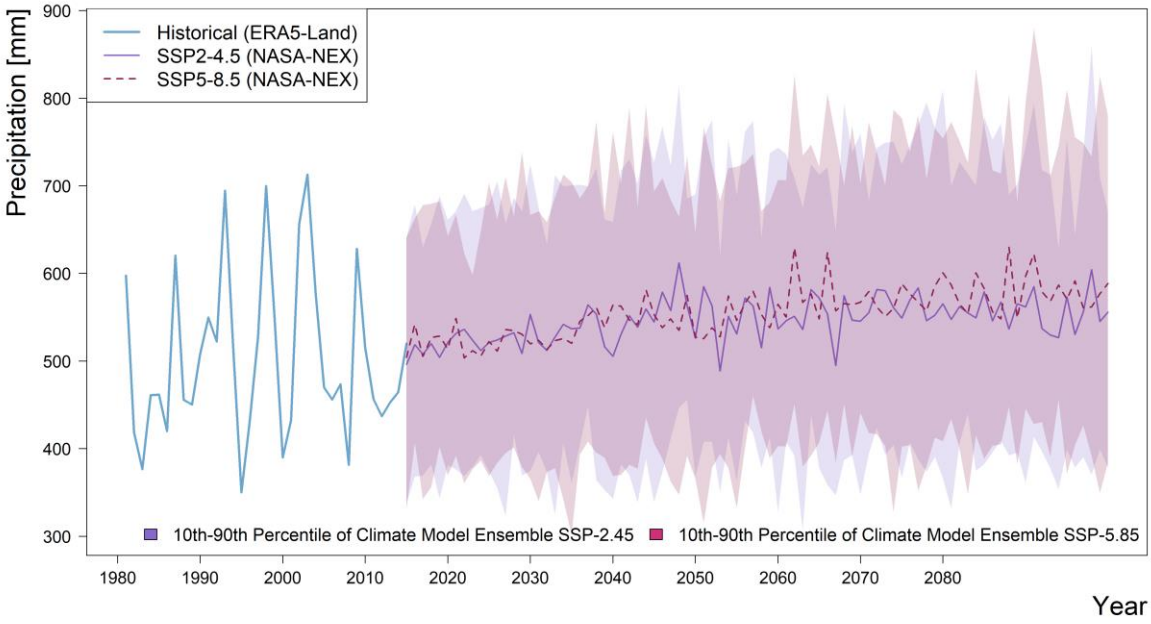

Figure A15: Time series of yearly ERA5 precipitation for the box Tasken for the historical period (1981-2020), and NASA NEX (per model bias corrected) for the future period. Shaded areas show the 10th and 90th percentiles in the spread of model predictions.

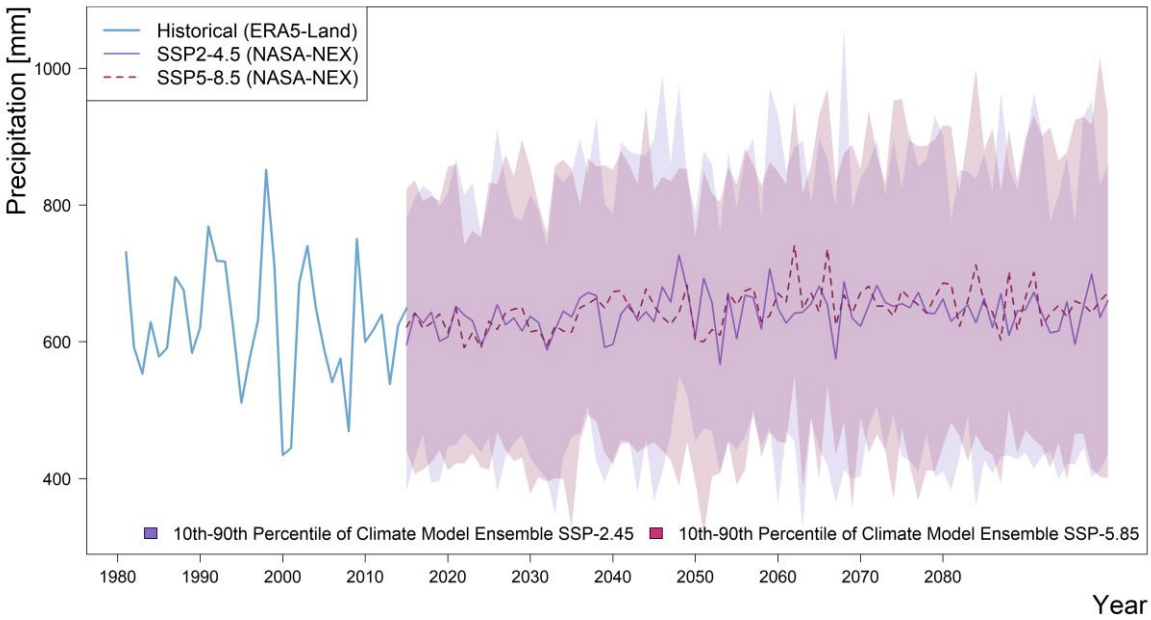

Figure A16: Time series of yearly ERA5 precipitation for the box Surkha for the historical period (1981-2020), and NASA NEX (per model bias corrected) for the future period. Shaded areas show the 10th and 90th percentiles in the spread of model predictions.

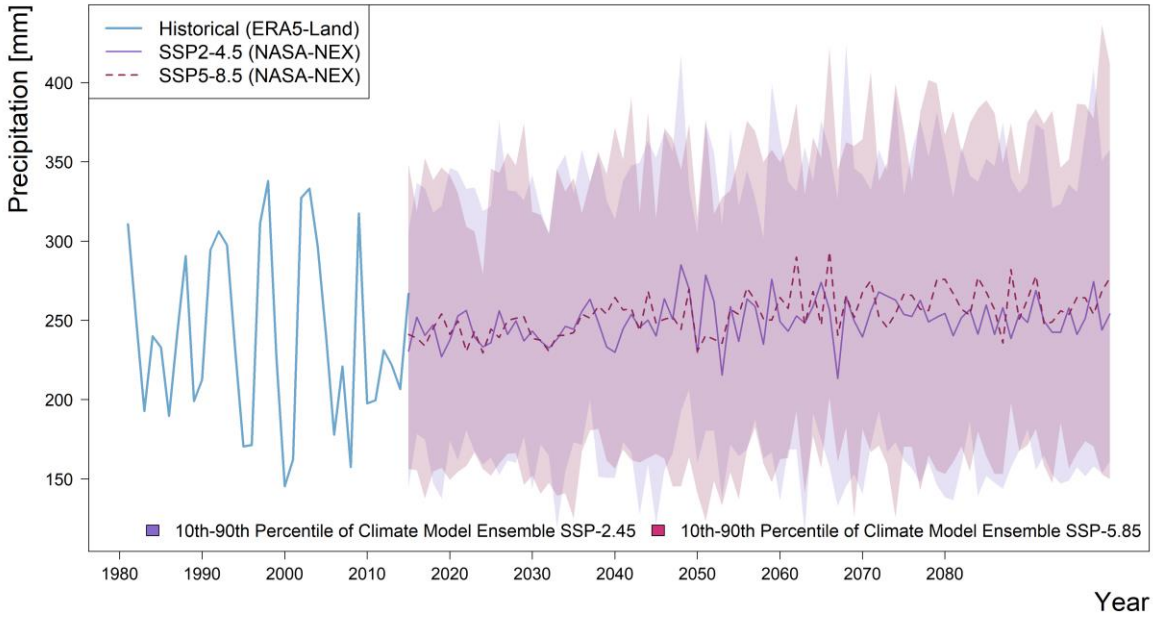

Figure A17: Time series of yearly ERA5 precipitation for the box BuSaKa for the historical period (1981-2020), and NASA NEX (per model bias corrected) for the future period. Shaded areas show the 10th and 90th percentiles in the spread of model predictions.

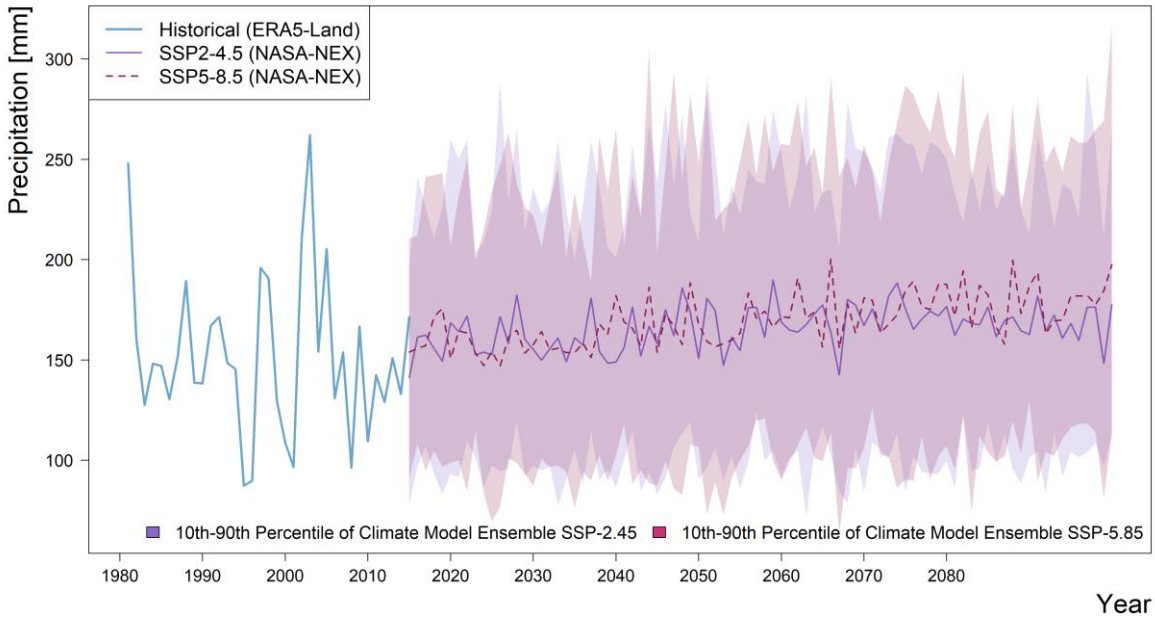

Figure A18: Time series of yearly ERA5 precipitation for the box Navoi for the historical period (1981-2020), and NASA NEX (per model bias corrected) for the future period. Shaded areas show the 10th and 90th percentiles in the spread of model predictions.

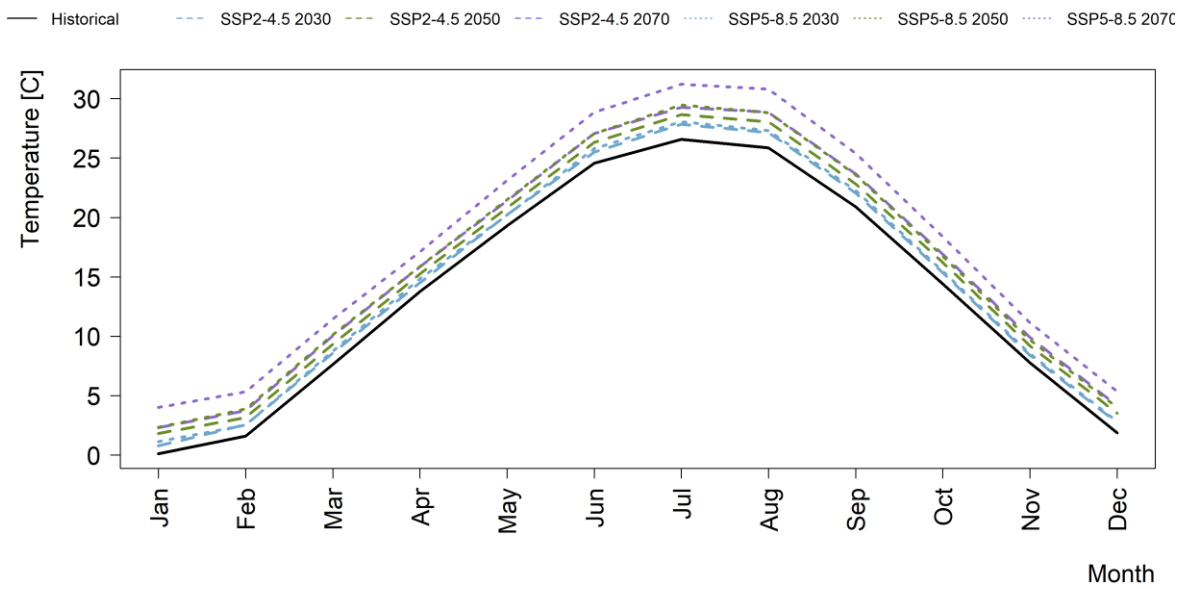

Figure A19: Average monthly temperature for historical (1995-2014) and future (time horizons under the two SSP scenarios for the box Tasken.

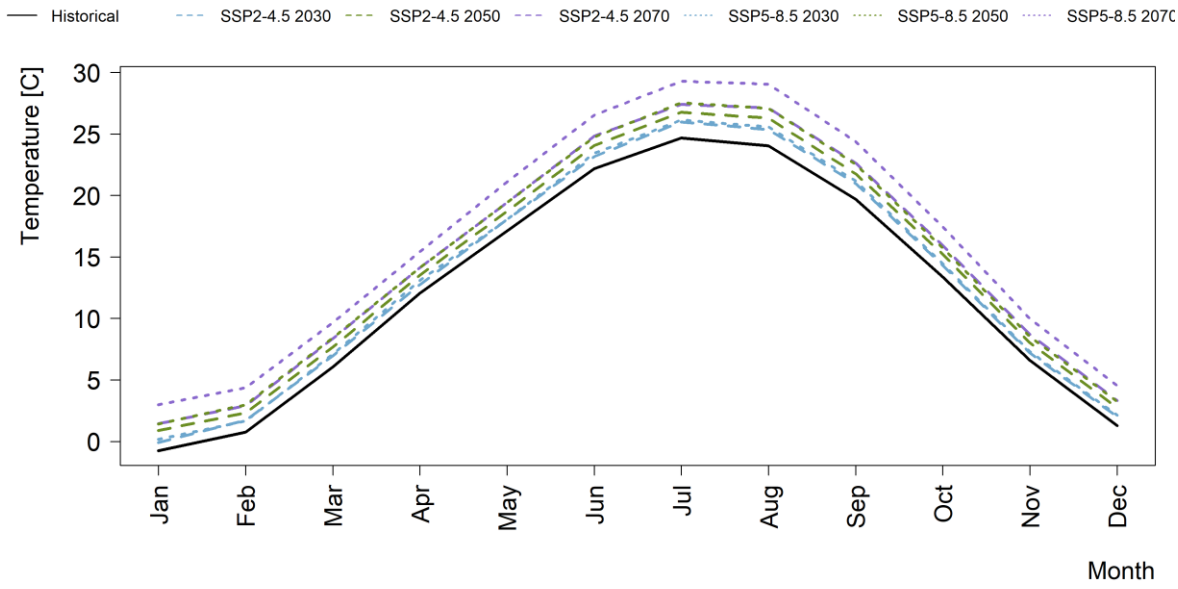

Figure A20: Average monthly temperature for historical (1995-2014) and future (time horizons under the two SSP scenarios for the box Surkha.

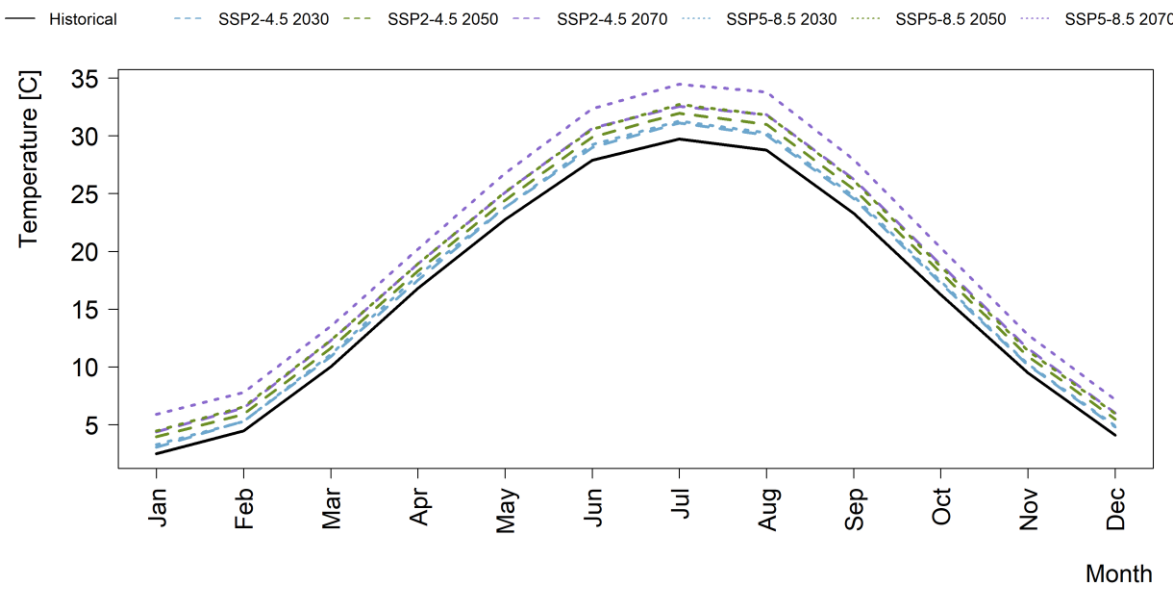

Figure A21: Average monthly temperature for historical (1995-2014) and future (time horizons under the two SSP scenarios for the box BuSaKa.

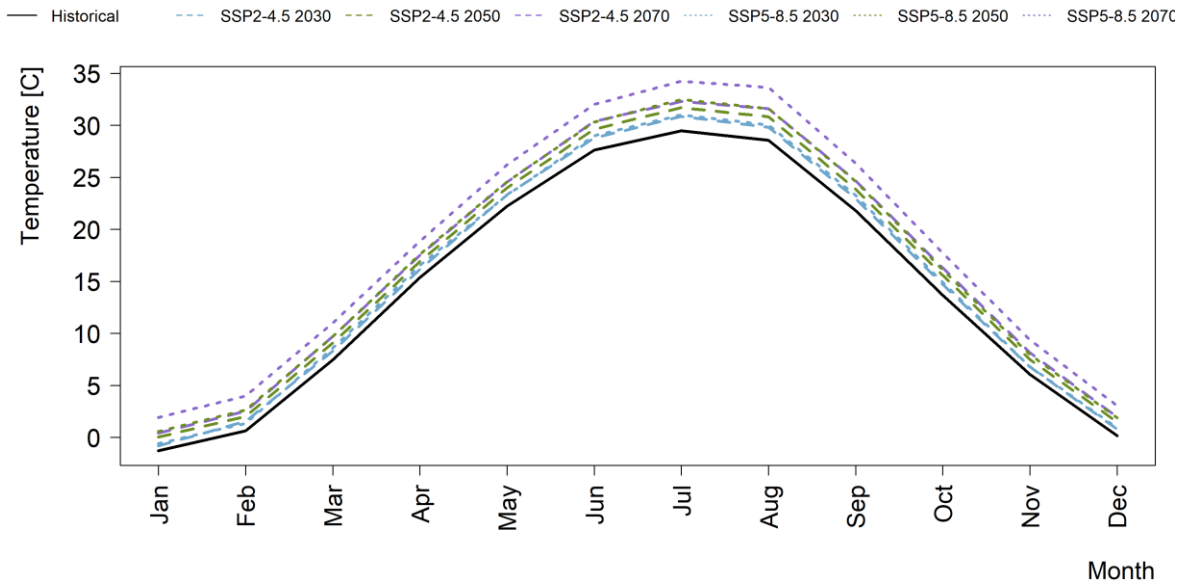

Figure A22: Average monthly temperature for historical (1995-2014) and future (time horizons under the two SSP scenarios for the box Navoi.

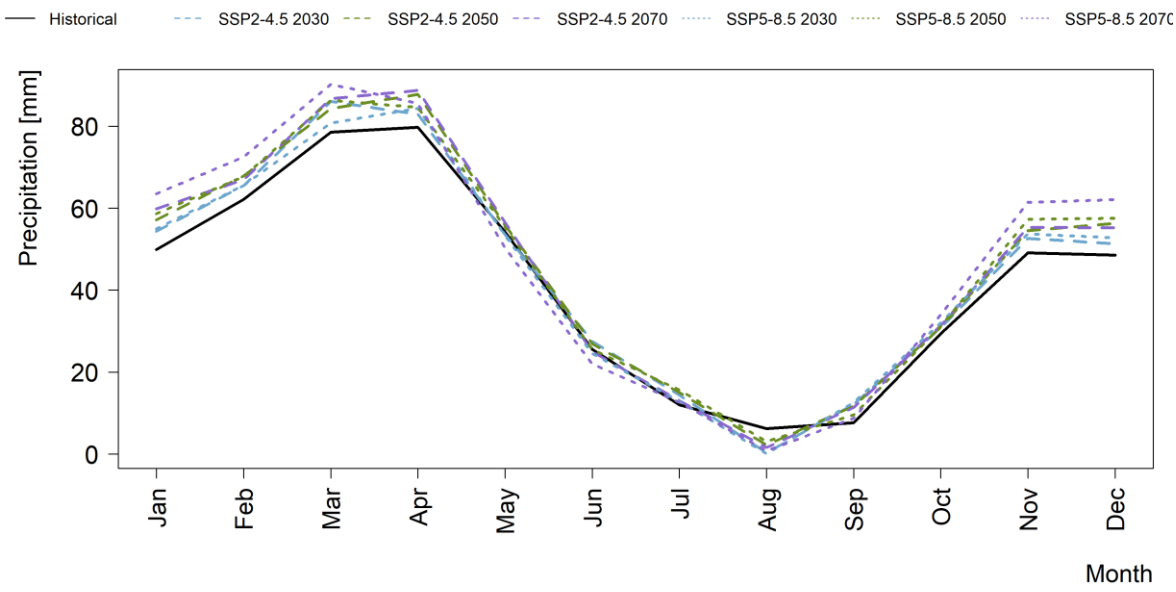

Figure A23: Average monthly precipitation for historical (1995-2014) and future (time horizons under the two SSP scenarios for the box Tasken.

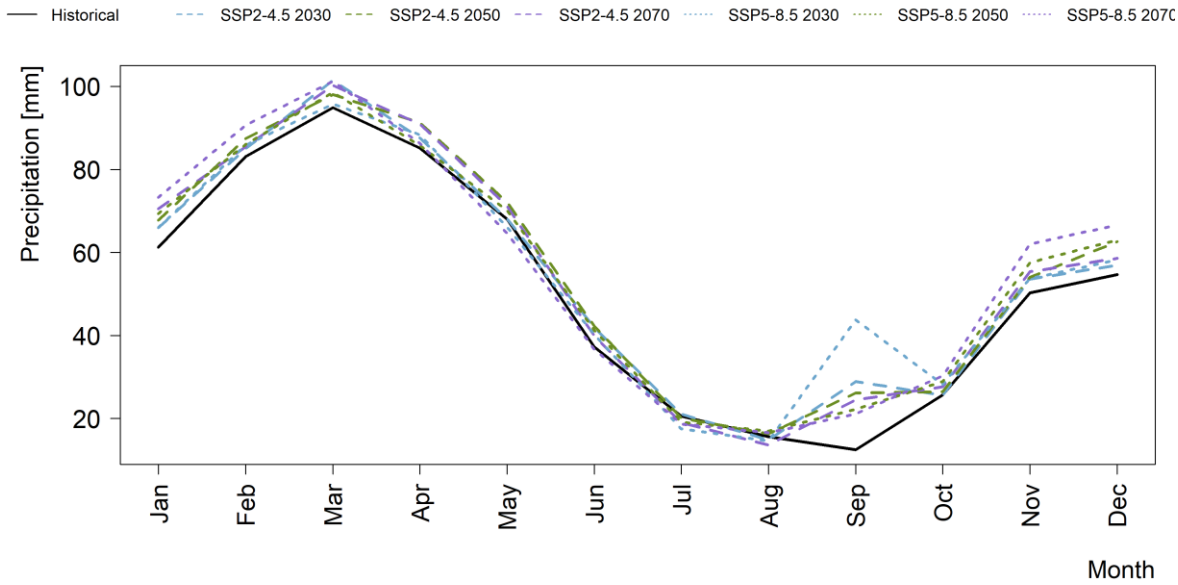

Figure A24: Average monthly precipitation for historical (1995-2014) and future (time horizons under the two SSP scenarios for the box Surkha.

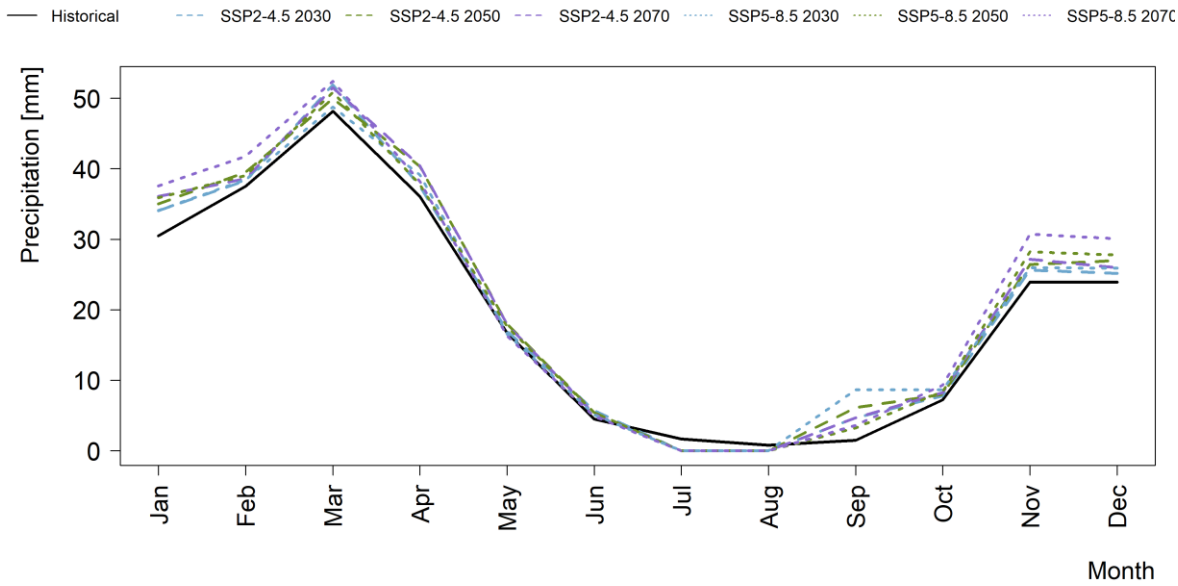

Figure A25: Average monthly precipitation for historical (1995-2014) and future (time horizons under the two SSP scenarios for the box BuSaKa.

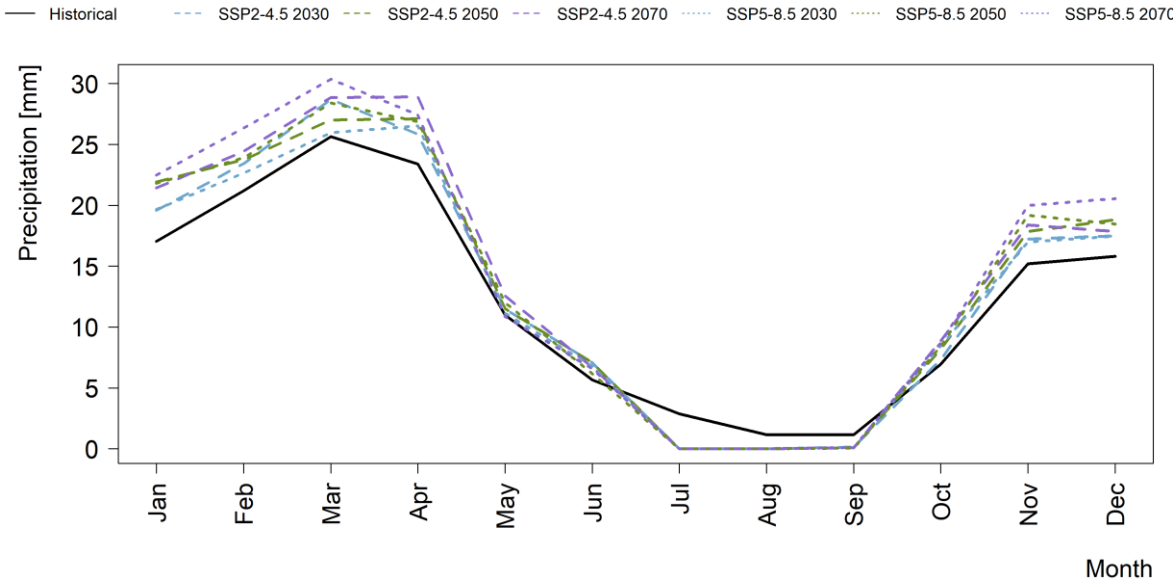

Figure A26: Average monthly precipitation for historical (1995-2014) and future (time horizons under the two SSP scenarios for the box Navoi

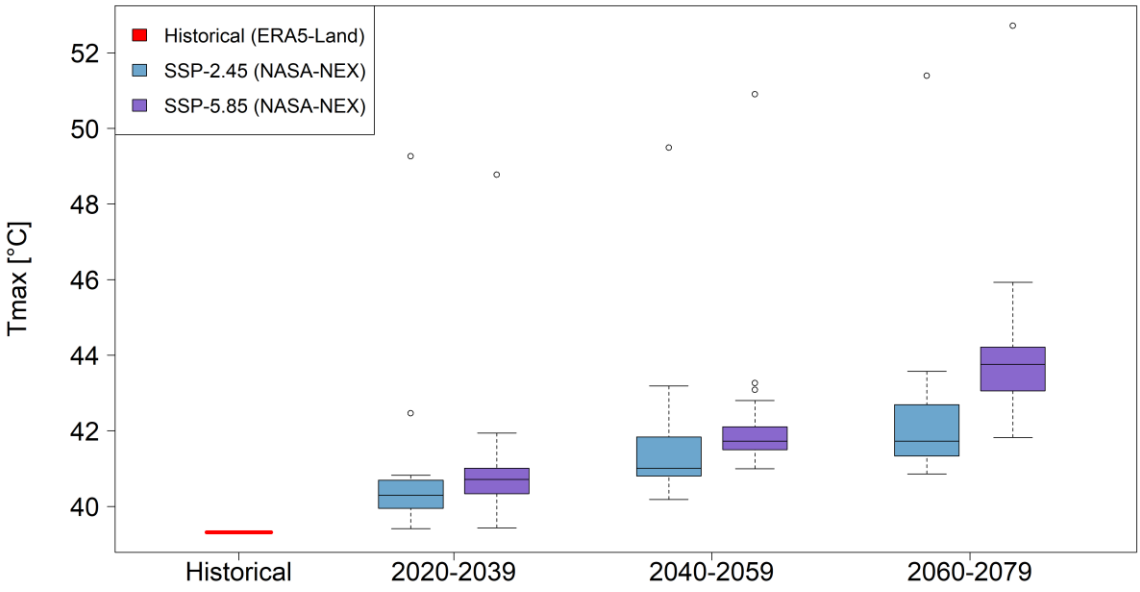

Figure A27: Boxplots indicating the spread in climate model predictions of maximum daily temperature per year (TXx) for the historical (1995-2014) and future time horizons under the two SSP scenarios for the box Tasken.

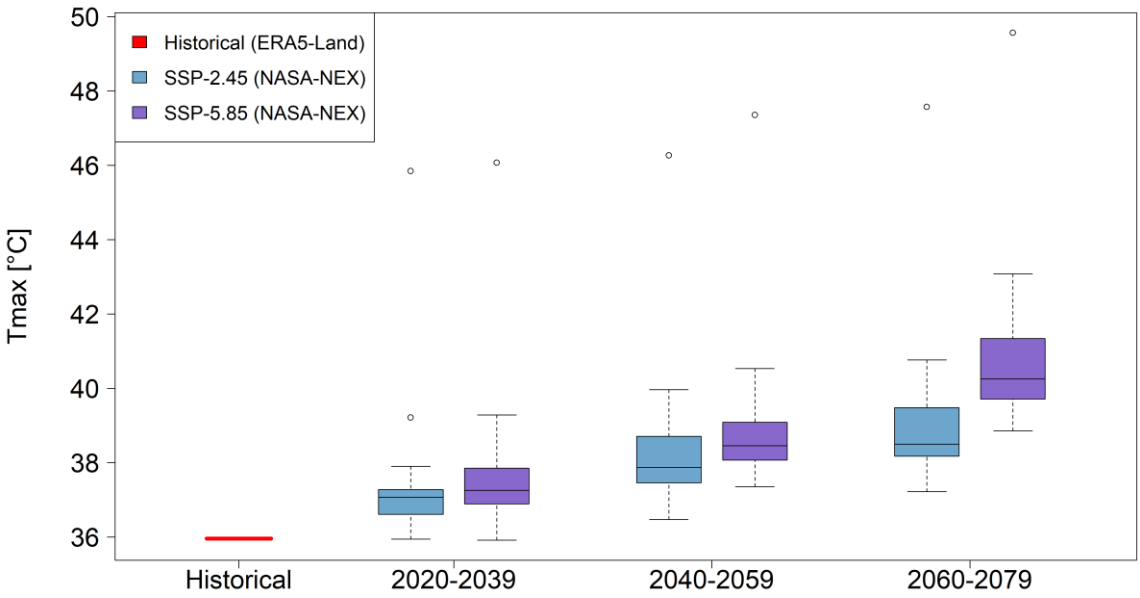

Figure A28: Boxplots indicating the spread in climate model predictions of maximum daily temperature per year (TXx) for the historical (1995-2014) and future time horizons under the two SSP scenarios for the box Surkha

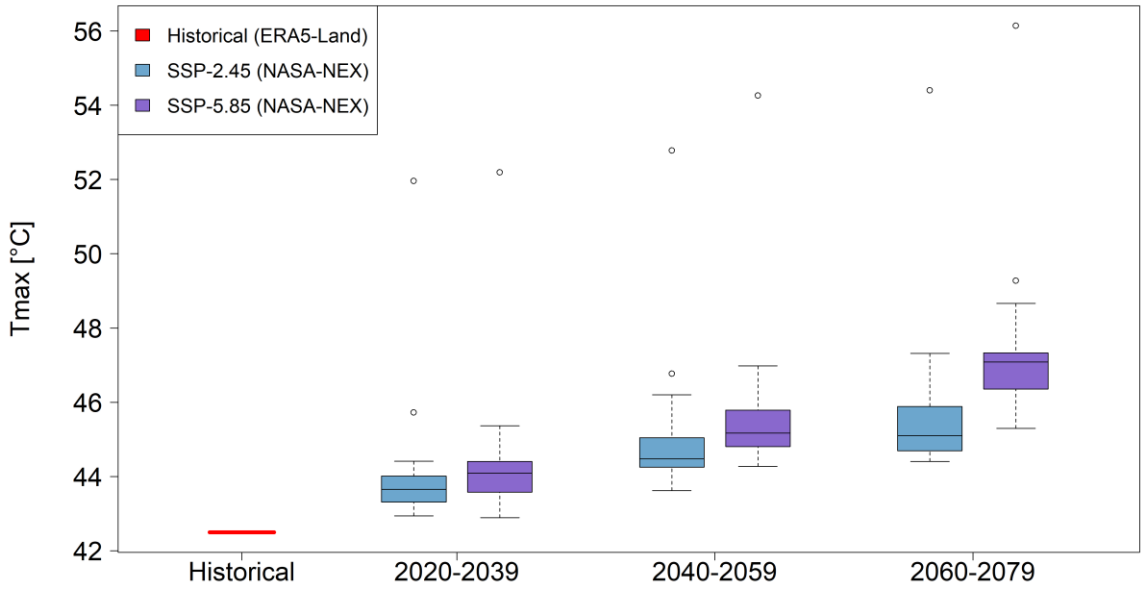

Figure A29: Boxplots indicating the spread in climate model predictions of maximum daily temperature per year (TXx) for the historical (1995-2014) and future time horizons under the two SSP scenarios for the box BuSaKa

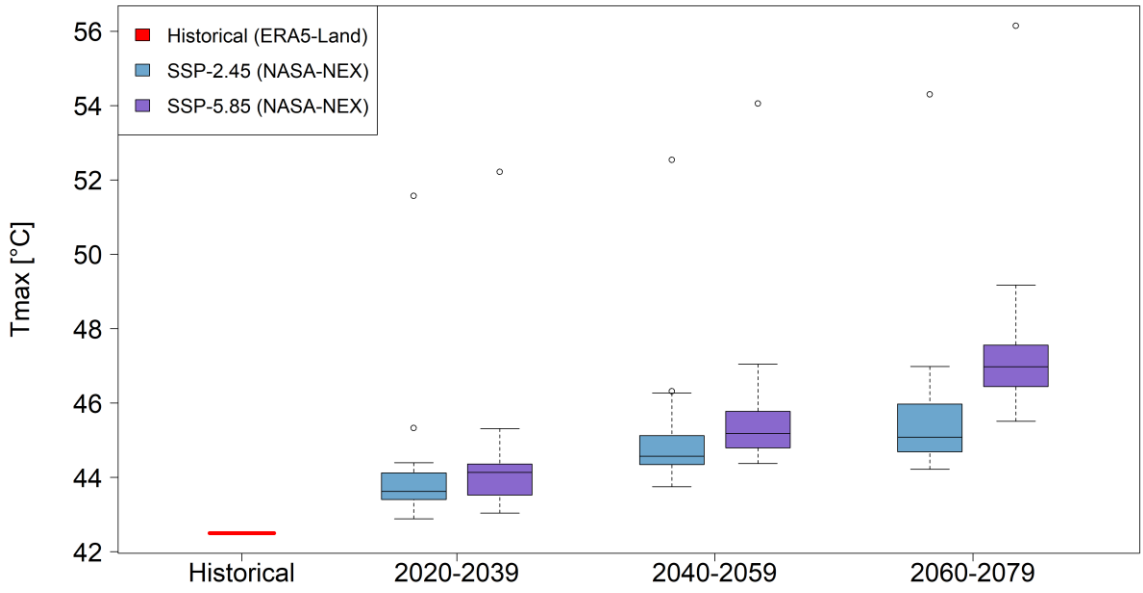

Figure A30: Boxplots indicating the spread in climate model predictions of maximum daily temperature per year (TXx) for the historical (1995-2014) and future time horizons under the two SSP scenarios for the box Navoi

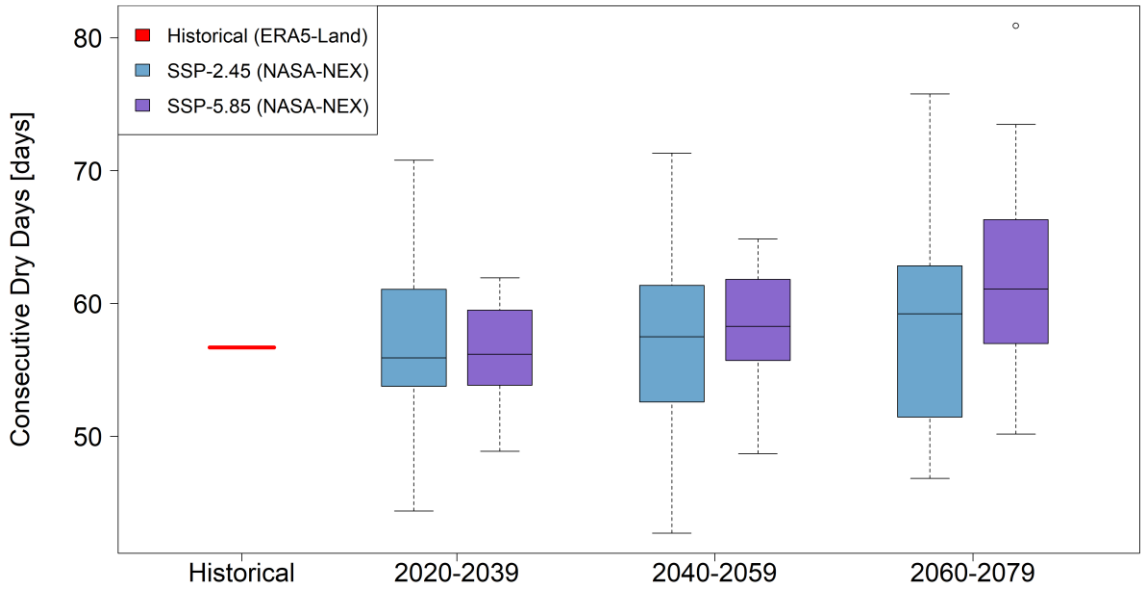

Figure A31: Boxplots indicating the spread in climate model predictions of average consecutive dry days per year (CDD) for the historical (1995-2014) and future time horizons under the two SSP scenarios for the box Tasken.

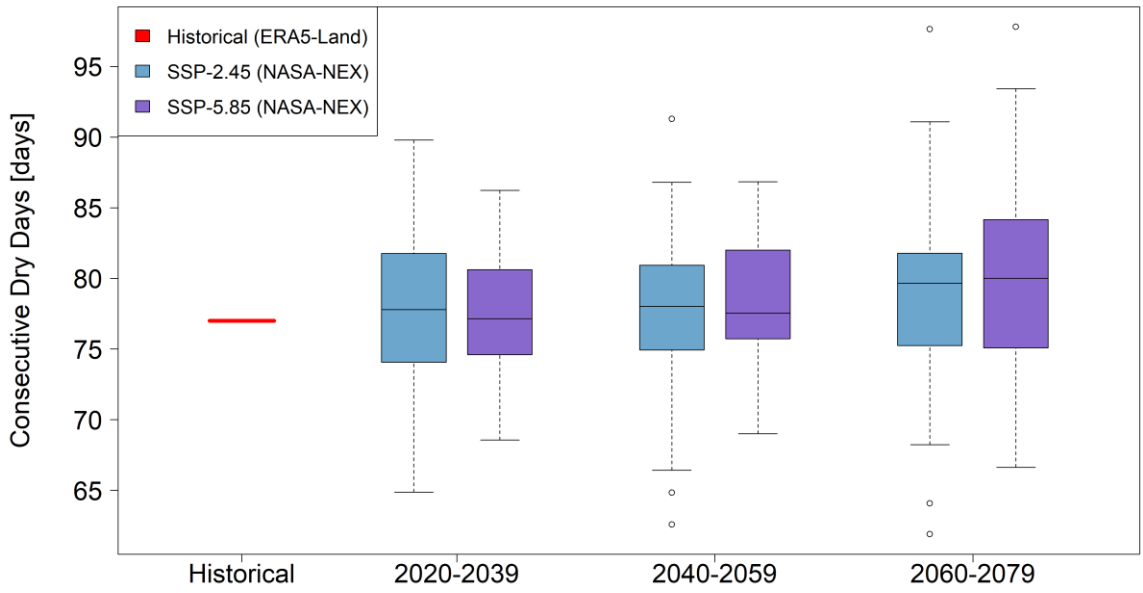

Figure A32: Boxplots indicating the spread in climate model predictions of average consecutive dry days per year (CDD) for the historical (1995-2014) and future time horizons under the two SSP scenarios for the box Surkha.

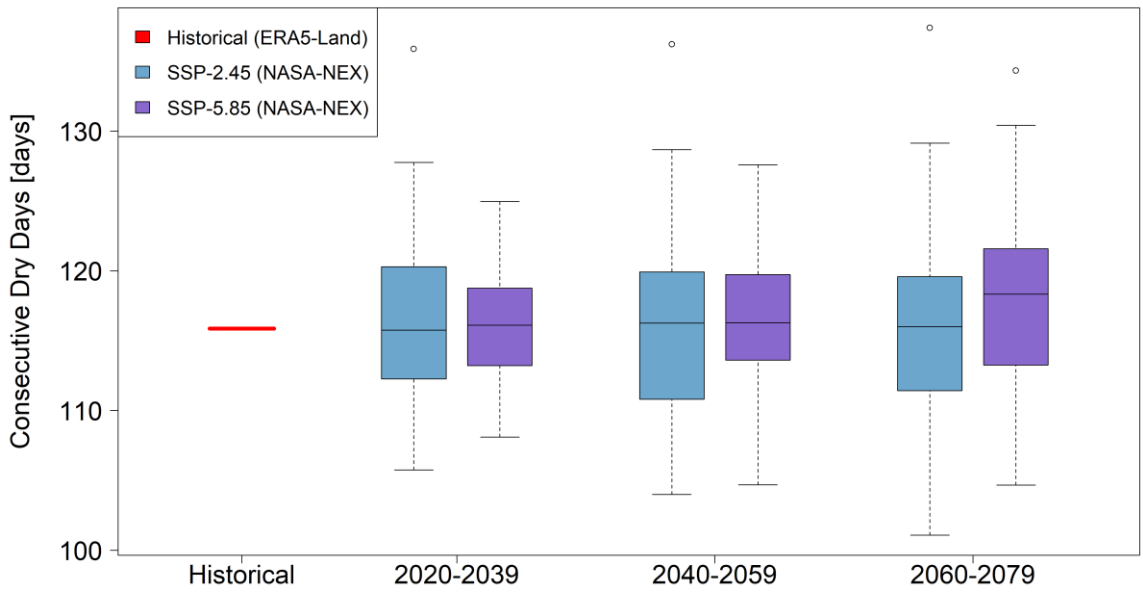

Figure A33: Boxplots indicating the spread in climate model predictions of average consecutive dry days per year (CDD) for the historical (1995-2014) and future time horizons under the two SSP scenarios for the box BuSaKa.

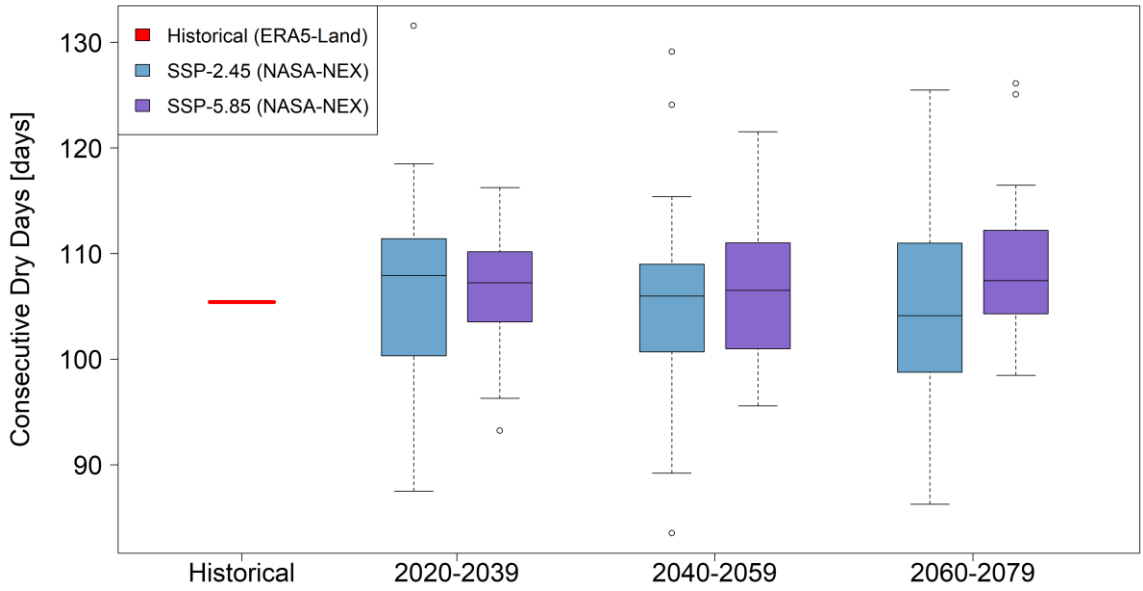

Figure A34: Boxplots indicating the spread in climate model predictions of average consecutive dry days per year (CDD) for the historical (1995-2014) and future time horizons under the two SSP scenarios for the box Navoi.

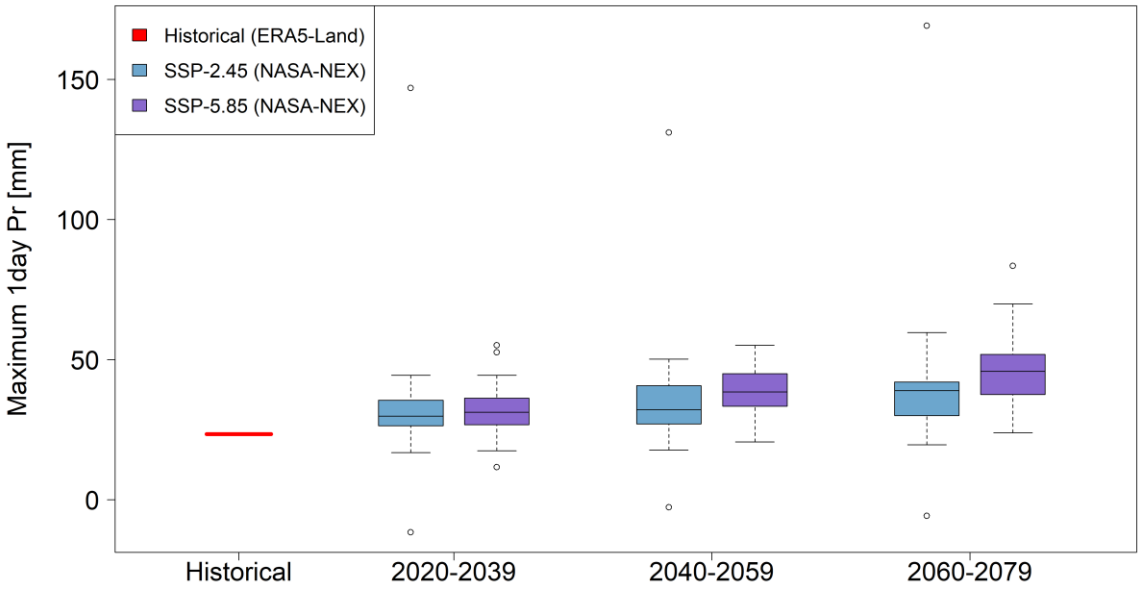

Figure A35: Boxplots indicating the spread in climate model predictions of yearly maximum 1-day precipitation sum (Rx1day, in mm/day) for the historical and future time periods under two SSP scenarios for the box Tasken.

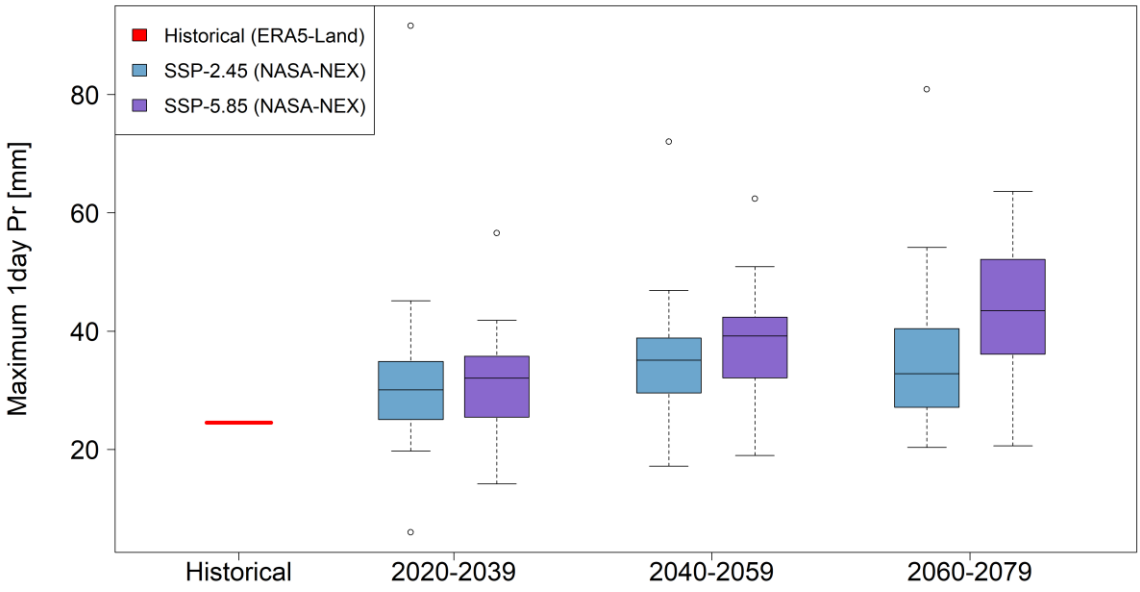

Figure A36: Boxplots indicating the spread in climate model predictions of yearly maximum 1-day precipitation sum (Rx1day, in mm/day) for the historical and future time periods under two SSP scenarios for the box Surkha.

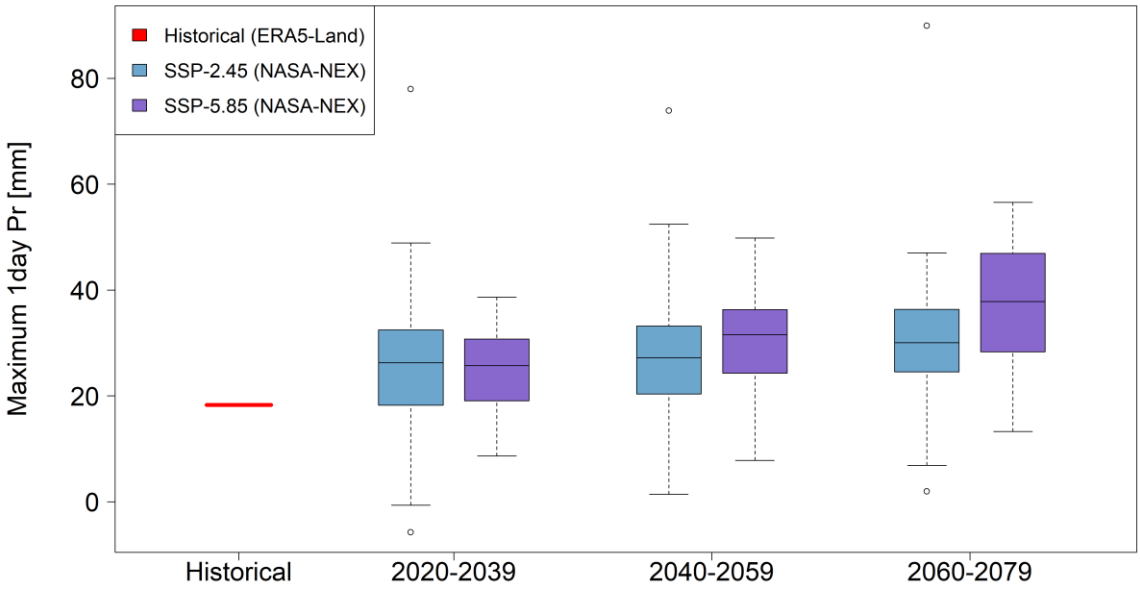

Figure A37: Boxplots indicating the spread in climate model predictions of yearly maximum 1-day precipitation sum (Rx1day, in mm/day) for the historical and future time periods under two SSP scenarios for the box BuSaKa.

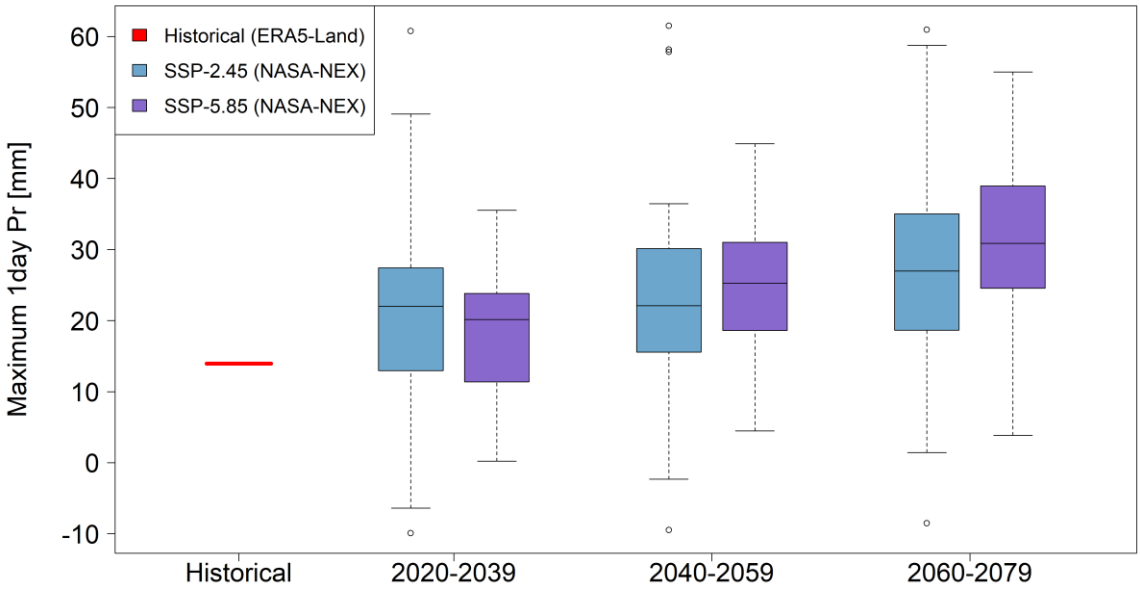

Figure A38: Boxplots indicating the spread in climate model predictions of yearly maximum 1-day precipitation sum (Rx1day, in mm/day) for the historical and future time periods under two SSP scenarios for the box Navoi.

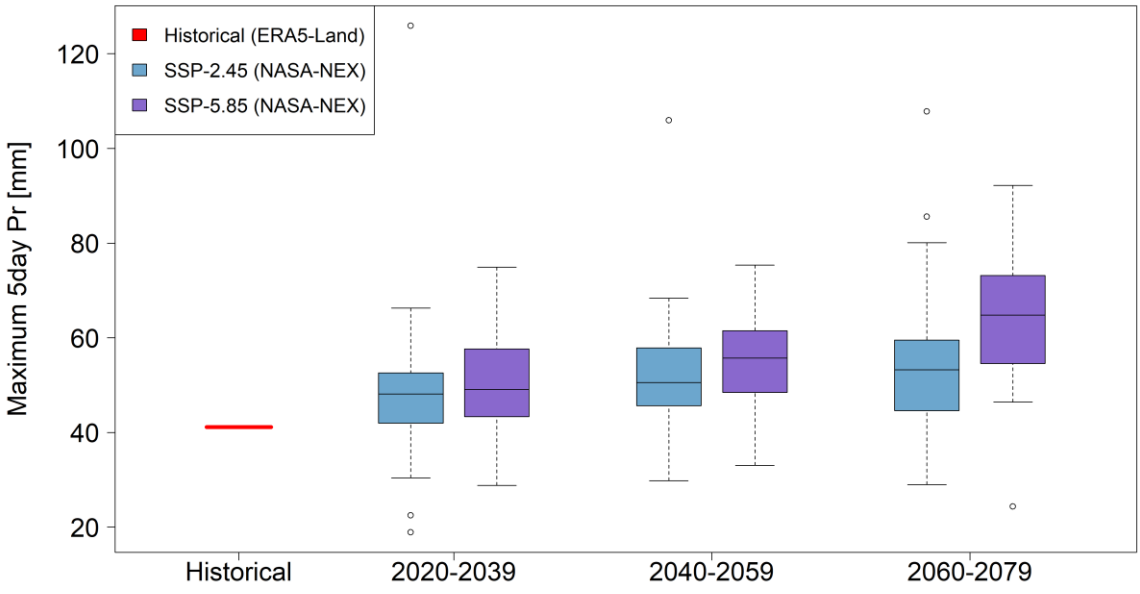

Figure A39: Boxplots indicating the spread in climate model predictions of yearly maximum 5-day precipitation sum (Rx5day, in mm/day) for the historical and future time periods under two SSP scenarios for the box Tasken.

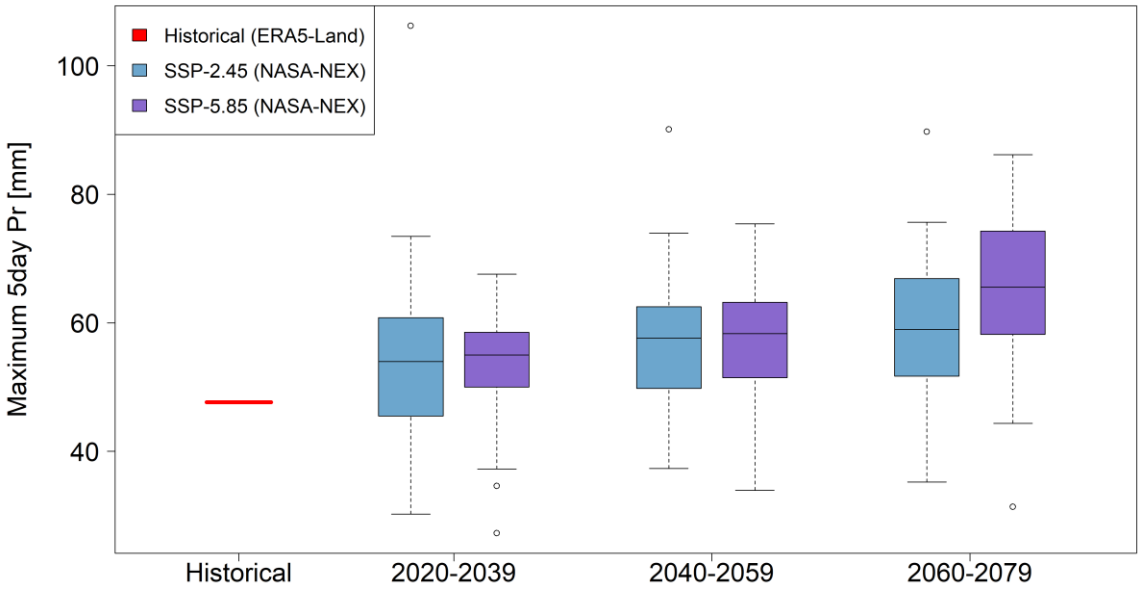

Figure A40: Boxplots indicating the spread in climate model predictions of yearly maximum 5-day precipitation sum (Rx5day, in mm/day) for the historical and future time periods under two SSP scenarios for the box Surkha.

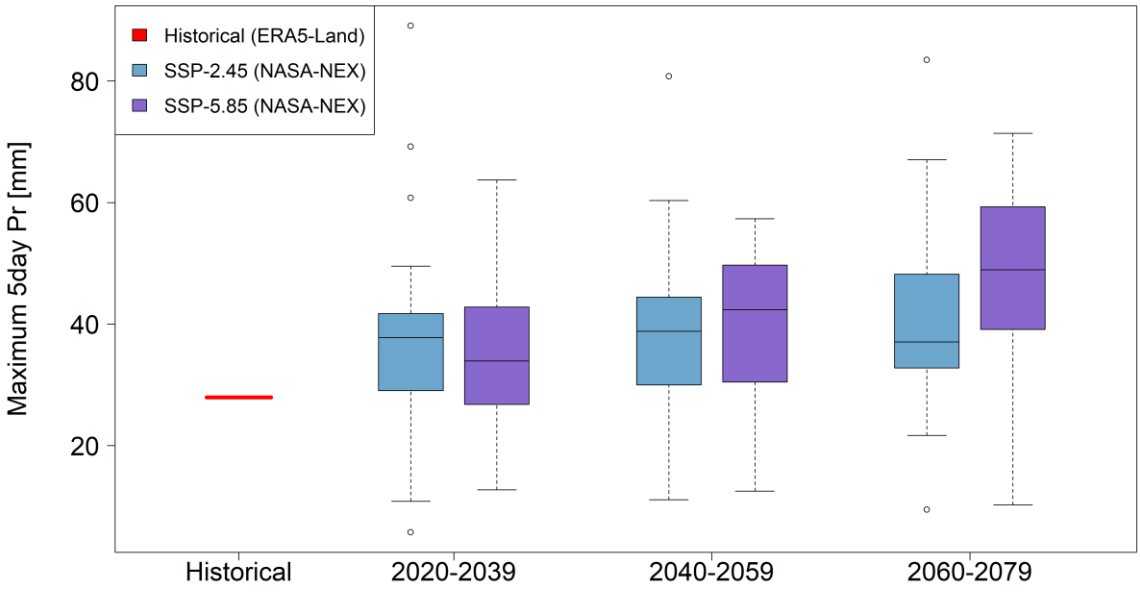

Figure A41: Boxplots indicating the spread in climate model predictions of yearly maximum 5-day precipitation sum (Rx5day, in mm/day) for the historical and future time periods under two SSP scenarios for the box BuSaKa.

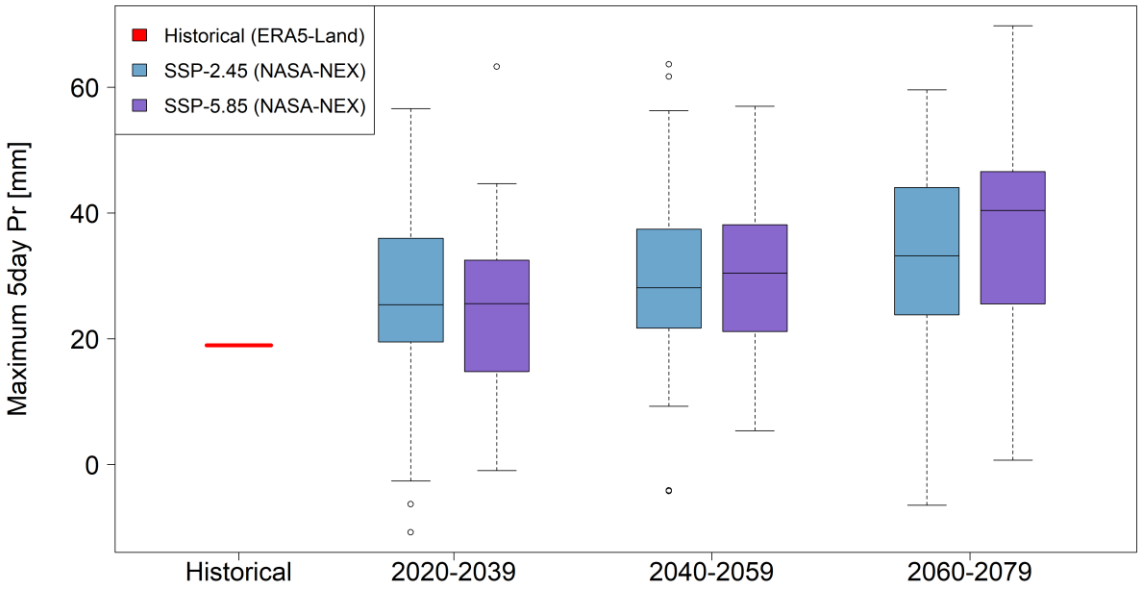

Figure A42: Boxplots indicating the spread in climate model predictions of yearly maximum 5-day precipitation sum (Rx5day, in mm/day) for the historical and future time periods under two SSP scenarios for the box Navoi.

Table A1: Summary table showing statistics regarding spread in CMIP6 ensemble predictions for future changes in annual precipitation for the box Tasken.

Scenarios	*Average (%)*	*25th Perc. (%)*	*75th Perc. (%)*	*GCMs Dryer*	*GCMs Wetter*
2030_SSP245	*5%*	*-3%*	*12%*	*9*	*25*
2050_SSP245	*9%*	*1%*	*17%*	*6*	*28*
2070_SSP245	*10%*	*4%*	*4%*	*6*	*28*
2030_SSP585	*5%*	*-1%*	*-1%*	*12*	*23*
2050_SSP585	*10%*	*2%*	*2%*	*7*	*28*
2070_SSP585	*14%*	*7%*	*21%*	*7*	*28*

Table A2: Summary table showing statistics regarding spread in CMIP6 ensemble predictions for future changes in mean temperature for the box Tasken.

Scenarios	*Average (%)*	*25th Perc. (%)*	*75th Perc. (%)*	*GCMs >2°C*	*GCMs >4°C*
2030_SSP245	*+1.0*	*+0.8*	*+1.2*	*1*	*0*
2050_SSP245	*+1.7*	*+1.5*	*+2.1*	*11*	*0*
2070_SSP245	*+2.4*	*+2.4*	*+2.4*	*25*	*25*
2030_SSP585	*+1.1*	*+1.1*	*+1.1*	*2*	*2*
2050_SSP585	*+2.4*	*+2.4*	*+2.4*	*25*	*25*
2070_SSP585	*+4.0*	*+4.0*	*+4.0*	*31*	*31*

Table A3: Summary table showing statistics regarding spread in CMIP6 ensemble predictions for future changes in annual precipitation for the box Surkha.

Scenarios	*Average (%)*	*25th Perc. (%)*	*75th Perc. (%)*	*GCMs Dryer*	*GCMs Wetter*
2030_SSP245	*4%*	*-1%*	*11%*	*11*	*23*
2050_SSP245	*6%*	*-2%*	*14%*	*13*	*21*
2070_SSP245	*6%*	*0%*	*0%*	*8*	*26*
2030_SSP585	*3%*	*-4%*	*-4%*	*12*	*23*
2050_SSP585	*6%*	*-2%*	*-2%*	*9*	*26*
2070_SSP585	*9%*	*-1%*	*21%*	*10*	*25*

Table A4: Summary table showing statistics regarding spread in CMIP6 ensemble predictions for future changes in mean temperature for the box Surkha.

Scenarios	*Average (%)*	*25th Perc. (%)*	*75th Perc. (%)*	*GCMs >2°C*	*GCMs >4°C*
2030_SSP245	*+1.0*	*+0.8*	*+1.2*	*1*	*0*
2050_SSP245	*+1.7*	*+1.5*	*+2.1*	*12*	*0*
2070_SSP245	*+2.4*	*+2.4*	*+2.4*	*24*	*24*
2030_SSP585	*+1.1*	*+1.1*	*+1.1*	*2*	*2*
2050_SSP585	*+2.4*	*+2.4*	*+2.4*	*25*	*25*
2070_SSP585	*+4.0*	*+4.0*	*+4.0*	*31*	*31*

Table A5: Summary table showing statistics regarding spread in CMIP6 ensemble predictions for future changes in annual precipitation for the box BuSaKa.

Scenarios	*Average (%)*	*25th Perc. (%)*	*75th Perc. (%)*	*GCMs Dryer*	*GCMs Wetter*
2030_SSP245	*5%*	*-3%*	*14%*	*12*	*22*
2050_SSP245	*8%*	*-3%*	*19%*	*9*	*25*
2070_SSP245	*9%*	*2%*	*2%*	*6*	*28*
2030_SSP585	*5%*	*-3%*	*-3%*	*12*	*23*
2050_SSP585	*8%*	*-4%*	*-4%*	*11*	*24*
2070_SSP585	*12%*	*-2%*	*24%*	*10*	*25*

Table A6: Summary table showing statistics regarding spread in CMIP6 ensemble predictions for future changes in mean temperature for the box Tasken.

Scenarios	*Average (%)*	*25th Perc. (%)*	*75th Perc. (%)*	*GCMs >2°C*	*GCMs >4°C*
2030_SSP245	*+1.0*	*+0.8*	*+1.2*	*1*	*0*
2050_SSP245	*+1.7*	*+1.4*	*+2.1*	*11*	*0*
2070_SSP245	*+2.4*	*+2.4*	*+2.4*	*23*	*23*
2030_SSP585	*+1.1*	*+1.1*	*+1.1*	*2*	*2*
2050_SSP585	*+2.4*	*+2.4*	*+2.4*	*22*	*22*
2070_SSP585	*+3.9*	*+3.9*	*+3.9*	*31*	*31*

Table A7: Summary table showing statistics regarding spread in CMIP6 ensemble predictions for future changes in annual precipitation for the box Navoi.

Scenarios	*Average (%)*	*25th Perc. (%)*	*75th Perc. (%)*	*GCMs Dryer*	*GCMs Wetter*
2030_SSP245	*9%*	*0%*	*17%*	*8*	*26*
2050_SSP245	*13%*	*4%*	*18%*	*5*	*29*
2070_SSP245	*16%*	*4%*	*4%*	*7*	*27*
2030_SSP585	*7%*	*-3%*	*-3%*	*12*	*23*
2050_SSP585	*14%*	*0%*	*0%*	*6*	*29*
2070_SSP585	*19%*	*7%*	*28%*	*3*	*32*

Table A8: Summary table showing statistics regarding spread in CMIP6 ensemble predictions for future changes in mean temperature for the box Navoi.

Scenarios	*Average (%)*	*25th Perc. (%)*	*75th Perc. (%)*	*GCMs >2°C*	*GCMs >4°C*
2030_SSP245	*+1.0*	*+0.8*	*+1.2*	*0*	*0*
2050_SSP245	*+1.7*	*+1.3*	*+2.2*	*8*	*0*
2070_SSP245	*+2.4*	*+2.3*	*+2.3*	*21*	*21*
2030_SSP585	*+1.1*	*+1.1*	*+1.1*	*1*	*1*
2050_SSP585	*+2.3*	*+2.3*	*+2.3*	*21*	*21*
2070_SSP585	*+3.9*	*+3.8*	*+3.8*	*31*	*31*

Appendix B: Detailed task and deliverables

The Specialist's tasks are expected to include but not be limited to:

- Prepare Climate Risk and Adaptation assessment (CRA) and summarize its results in the Climate Change Assessment (CCA). CCA preparation shall follow ADB guidance note on Climate Change Assessments for CWRD projects.
- Analyze climate model projections for the regions of interest.
- Leading the detailed climate risk and adaptation assessment. The study is expected to assess the change and variability of key climate related parameters over the project lifetime to be used as inputs to the feasibility study among others.
- Identify the uncertainties associated with the projections and provide guidance on how the results
- should be interpreted.
- Review the existing meteorological monitoring network and propose additional weather stations and associated capacity requirements for proper monitoring and surveillance in the project areas.
- Prepare GHG emissions reductions calculation.
- Identify climate adaptation activities, calculate adaptation cost, and provide justification for the climate financing.

Deliverables:

- Climate Change Assessment Linked Document [using ADB Board Template]
- Detailed Climate Risk and Adaptation assessment Supplementary Document